A mass cytometry receptor occupancy study of natalizumab therapy in multiple sclerosis

Gerd Haga Bringeland

Thesis for the degree of Philosophiae Doctor (PhD)
University of Bergen, Norway
2020

UNIVERSITY OF BERGEN

A mass cytometry receptor occupancy study of natalizumab therapy in multiple sclerosis

Gerd Haga Bringeland

Thesis for the degree of Philosophiae Doctor (PhD)
at the University of Bergen

Date of defense: 05.06.2020

Year: 2020

Title: A mass cytometry receptor occupancy study of natalizumab therapy in multiple sclerosis

Name: Gerd Haga Bringeland

Print: Skipnes Kommunikasjon / University of Bergen

Content

1. Scientific enviroment

This work was carried out at the National Multiple Sclerosis Competence centre and Neuro-SysMed at the Department of Neurology, Haukeland University Hospital, Bergen, and the Department of Clinical Medicine, University of Bergen. Neuro-SysMed is jointly hosted by Haukeland University Hospital and the University of Bergen, and supported as a Centre for Clinical Treatment Research (FKB) by grants from The Research Council of Norway.

Main supervisor: Dr. Sonia Gavasso

Co-supervisors: Prof. Christian Vedeler and Prof. Kjell-Morten Myhr

Patients were included at the Department of Neurology. Sample preparation and laboratory work were performed at the Neurological research laboratory headed by Prof. Christian Vedeler and mass cytometry experiments were performed at the Flow Cytometry Core Facility, Department of Clinical Science, University of Bergen. The Helios Mass Cytometer was funded by the Bergen Research Foundation. Nello Blaser at the Department of Informatics, University of Bergen contributed with bioinformatic analyses and training. Vinko Tosevski at the University of Zürich contributed with cytometry and bioinformatics training.

The study was funded by Helse Vest. Laboratory reagents and mass cytometry analysis was financed by the Neurological research laboratory and by research grants from Novartis and *Fritz og Ingrid Nielssens legat for forskning av multippel sclerose*.

2. Acknowledgements

Firstly, I want to express my gratitude to my super-visors Sonia, Christian and Kjell-Morten for your guidance and encouragement, especially in moments of doubt. Each of you has offered indispensable knowledge necessary for the initiation and completion of this project. You have always made time for me and given me fair and honest feedback, and I have never had to pretend that things were going better than they were. Christian and Kjell-Morten – it is funny to think about that I am now working so closely with the most famous neurologists from medical school in Bergen. Sonia – this project would never have left the starting pit of technical issues if it wasn't for your exceptional efforts to make contacts and gather knowledge from all corners of the world to overcome problems. We've traveled to many of these corners together and I enjoy your friendship, pro-activeness, and humorous mood.

This project was made possible by the extra efforts from all participating patients, support from the funders of the study, and my research environment. I especially thank Hanne Linda at the Neurological research laboratory for her assistance, the Flow Cytometry Core Facility for training, technical support, and fruitful discussions, and Nello for bioinformatics support which was crucial for understanding and communicating our results.

I also want to thank my research microenvironment: my exquisite office roomies at the Archive of Neurology – Anna, Aurora and Andrej – with whom I've shared the good days and the bad through the research period. You have been a great inspiration and I'm grateful for your excitement about my research breakthroughs even though you more often than not had no idea what they were about.

Two persons have been especially important for my choice of profession: my secondary school naturfag teacher Øyvind Andreassen, who grabbed a hold of me when I was a chaotic and slightly gangsterous teenager and gave me a resolute push in the right direction, and my exceptionally generous and patient high school chemistry teacher Ivar Helgesen, who knew all the right tricks for helping even the slowest reader to succeed.

I'm surrounded by a lot of incredible people who motivate me; my family, dear friends, and inspiring colleagues. Those who know me know that I tend to have good luck, and I believe the ballast I got from home has made me able to catch opportunities when they've turned up. I want to thank mamma and pappa for not raising me like a little princess and for teaching me to finish what I started, even when it gets boring. Also thanks to my brothers Sjur, Lars, and Bård (who have *definitely* not treated me like a little princess) for various happy distractions to divert me from work, reminding me that research isn't the most important thing in the world.

I want to thank my home crew. Our nine sheep and two cats always cheer me up, despite occasionally jumping the fence and dragging mutilated mice into the living room, respectively. Finally, thanks to my best friend and co-adventurer Einar. You encourage me with your strength of mind and stamina. Thank you for your unconditional support and for making my life happier.

3. Abbrevations

ABC - antibody binding capacity

ARR - annualized relapse rate

BBB - blood-brain-barrier

CD - cluster of differentiation

CITRUS - cluster identification, characterization, and regression

CNS - central nervous system

cDCs - classical dendritic cells

CSF - cerebrospinal fluid

DMT - disease modifying therapy

EDSS - expanded disability status scale

EID - extended interval dosing

FCS file - Flow Cytometry Standard file

FSS - fatigue severity scale

HSCT - hematopoietic stem cell transplantation

ICP - inductively coupled plasma

IgG - immunoglobulin G

JCV - John Cunningham virus

MRI - magnetic resonance imaging

MS - multiple sclerosis

NEDA - no evidence of disease activity

NF-L - neurofilament light chain

NK cell - natural killer cell

PBL - peripheral blood leukocyte

PBMC - peripheral blood mononuclear cell

PML - progressive multifocal leukoencephalopathy

PPMS - primary progressive multiple sclerosis

RCT - randomized controlled trial

RO - receptor occupancy

RRMS - relapsing remitting multiple sclerosis

SDMT - symbol digit modalities test

SID - standard interval dosing

Simoa - single molecule array

SPMS - secondary progressive multiple sclerosis

T_{CM} - central memory T cell

T_{EM} - effector memory T cell

T_{EMRA} - effector memory RA T cell

tSNE - t-distributed stochastic neighbor embedding

VCAM-1 - vascular-cell adhesion molecule 1

QSC beads - quantum simply cellular beads

4. Abstract

Background: Natalizumab is a therapeutic antibody that effectively reduces disease activity in relapsing remitting multiple sclerosis (RRMS) by binding α4 integrin on leukocytes and preventing leukocyte migration into the central nervous system (CNS). Natalizumab is administered intravenously at a standard dose of 300 mg every 4 weeks. Approximately half of treated patients report subjective wearing-off symptoms at the end of the dosing interval. This phenomenon is sparsely investigated, and it is not known whether it has a biological cause or is associated with poor therapeutic efficacy. Accumulating evidence suggests that extending the dosing interval to up to 8 weeks maintains therapeutic efficacy in many patients while reducing the risk of progressive multifocal leukoencephalopathy (PML), a rare but potentially lethal complication of therapy. This has prompted efforts to personalize dosing intervals. Natalizumab receptor occupancy (RO) correlates with therapeutic response and has been suggested as a biomarker to navigate individual dosing. RO is traditionally measured by flow cytometry, but spectral overlap limits the number of markers that can be measured simultaneously. This restricts RO assays to the analysis of major cell types, although rare cell populations are of potential therapeutic relevance. Mass cytometry is a cutting-edge technology that allows simultaneous analysis of more than 40 parameters on single cells, facilitating measurement of RO in a broader array of cell types together with more biomarkers of interest than possible by conventional flow cytometry. Although RO assays are widely used in flow cytometry, no RO assay utilizing mass cytometry has been published prior to this study.

Objective: We aimed to develop a method for reliable RO measurement with high-parameter mass cytometry, and to study natalizumab RO and clinical characteristics in RRMS patients treated with natalizumab.

Methods: We developed a novel method to measure RO with mass cytometry, allowing simultaneous in-depth immune monitoring and reliable measurement of natalizumab RO on multiple peripheral blood leukocyte subtypes. This was achieved

by adapting antibody-binding beads from flow cytometry to standardize the varying detection sensitivity in mass cytometry, generating accurate and reproducible RO results. We applied the natalizumab RO assay in a cross-sectional study of 40 RRMS patients treated with natalizumab at the Department of Neurology, Haukeland University Hospital. Clinical and radiological signs of disease activity were recorded, and fatigue, cognitive function and wearing-off symptoms were evaluated. We followed the patients prospectively for one year.

Results: In the cross-sectional study, we found that patients who reported wearing-off symptoms regularly (at the end of every 4-week dosing interval) had lower natalizumab RO in several leukocyte subtypes. Body mass index (BMI) was higher in patients who regularly had wearing-off symptoms, and high BMI was associated with low RO. After 1-year follow-up none of the patients displayed clinical or radiological signs of disease activity, but patients reporting wearing-off symptoms regularly had more severe fatigue and cognitive dysfunction.

Conclusions: Low natalizumab RO may contribute to the wearing-off phenomenon and high BMI may be the underlying cause. Patients with wearing-off symptoms showed no increased short-term risk of RRMS disease activity, but they may be more vulnerable to therapeutic failure if dosing intervals are extended than patients with higher RO levels. This work provides new tools for future exploration of natalizumab and other therapeutic antibodies in the era of personalized medicine.

5. List of Publications

The thesis is based on the following papers

I. Bringeland GH, Bade L, Blaser N, Budzinski L, Schulz AR, Mei HE, Myhr KM, Vedeler CA, Gavasso S. **Optimization of Receptor Occupancy Assays in Mass Cytometry: Standardization Across Channels with QSC Beads.** Cytometry A. 2019 Mar;95(3):314-322

II. Bringeland GH, Blaser N, Myhr KM, Vedeler CA, Gavasso S. **Wearing-off at the end of natalizumab dosing intervals is associated with low receptor occupancy.** Neurol Neuroimmunol Neuroinflamm. 2020 Feb 4;7(3)

III. Bringeland GH, Myhr KM, Vedeler CA, Gavasso S. **Wearing-off at the end of natalizumab dosing interval and risk of MS disease activity: a prospective 1-year follow-up study.** 2020 *Submitted*

6. Introduction

6.1 Multiple sclerosis

Multiple sclerosis (MS) is characterized by inflammation, demyelination and neurodegeneration in the central nervous system (CNS), leading to disruption of neuronal signaling and subsequent neurological symptoms.[1] MS affects over 2 million individuals worldwide with an average age of disease onset of 30 years and is one of the most common causes of neurological disability in young adults.[2, 3] Prevalence of the disease is higher in women than in men, and shows considerable geographical variation.[4] Norway has amongst the highest prevalence in the world with 208 cases per 100 000.[5]

6.1.1 Pathogenesis

The disease was first defined in 1868 by the French neurologist Jean-Martin Charcot (1825-1893), who described disseminated sclerotic plaques ("sclerose en plaque disseminees") in the CNS with loss of the myelin sheet surrounding the axons of neurons.[6] More than 150 years later, the exact pathogenesis and etiology of MS remains unknown.

Etiology and pathology

The disease is thought to arise in genetically susceptible individuals, with environmental factors influencing disease penetrance.[7-9] Genetic risk factors account for approximately 30% of the overall disease risk, and environmental risk factors including low vitamin D levels, Epstein-Barr virus infection, smoking, and obesity can interact with MS risk genes.[9-12]

In the healthy CNS, axons of neurons are wrapped in myelin sheaths made from layers of the oligodendrocyte cell membrane. The pathological hallmark of MS is lesions with inflammation, demyelination, activation of glial cells, and axonal degeneration which can be widespread throughout the CNS.[1, 13]

Immunology

Whether the disease is initially triggered in the periphery or inside the CNS is under debate:[14, 15] MS has traditionally been considered an autoimmune inflammatory disorder, where an abnormal peripheral immune response targets the CNS (the outside-in model). According to this model, autoreactive immune cells are activated at peripheral sites and traffic over the blood-brain-barrier (BBB) into the CNS. The resulting inflammatory response and production of reactive oxygen species causes demyelination, axonal loss, neuronal damage, and eventual brain atrophy.[8, 16] The alternative hypothesis is that neurodegeneration precedes inflammation, and that exposure of highly immunogenic myelin antigens causes a secondary immune response (the inside-out model).[15] However, exposure of antigenic debris in other degenerative neurological diseases does not lead to MS and the majority of MS risk genes are associated with immune pathways, indicating that an immune predilection is necessary for the development of the disease.[11]

Whatever the initial trigger, inflammation is present at all stages of MS, although more pronounced in acute phases than in chronic phases. Both the adaptive and innate immune system play an integral role, and MS lesions contain both activated CNS-resident glial cells, including microglia and astrocytes, and infiltrates from peripheral immune cells, including macrophages, T and B lymphocytes.[8, 17] T and B lymphocytes are adaptive immune cells which specifically recognize distinct antigens and can generate memory cells that respond faster and more vigorously to repeated exposures to the same antigen.[17] T lymphocytes are classified into major subsets of cytotoxic (CD8+) and helper (CD4+) T cells, and naïve T cells can generate memory subsets with various functional properties after encountering their antigen. Central memory (T_{CM}) cells home to secondary lymphoid tissues whereas effector memory (T_{EM} and T_{EMRA}) subtypes execute effector functions such as secretion of pro-inflammatory cytokines and cytotoxicity at the site of inflammation.[18, 19] In MS, autoreactive T lymphocytes are activated in the periphery, possibly in cervical lymph nodes draining CNS lymphatics, and re-activated locally by antigen presenting cells after having entered the CNS. Invading autoreactive B lymphocytes produce

oligoclonal antibodies that are detectable in the CSF and are of diagnostic value, however the specificity of these antibodies is largely unknown. Other B cell functions such as antigen presentation to helper T cells and cytokine production may therefore play a more central role in MS pathogenesis.[20] Innate immune cells including granulocytes, natural killer (NK) cells, monocytes, and dendritic cells provide nonspecific reactions to foreign substances and debris and have specialized roles at various stages of inflammation including phagocytosis, antigen presentation to adaptive immune cells, and tissue repair. Invasion of peripheral immune cells and BBB disruption is especially pronounced in early MS lesions. Later, activation of CNS-resident microglia and astrocytes become more pronounced, forming multiple sclerotic scars which have given the disease its name.[8]

6.1.2 Diagnosis

Symptomatology

The symptoms and disease course of MS are heterogeneous. Development of new demyelinating lesions or expansion of prior lesions can be asymptomatic or lead to clinical relapses, defined as monophasic episodes of subacute neurological symptoms with a duration of at least 24 hours.[21] Symptoms depend on lesion location in the CNS, and can include visual, sensory, and motor impairment, cognitive deficits, fatigue, and autonomic disturbances often involving the urogenital system.[22] In around half of relapses the recovery is incomplete, leading to persisting residual disability.

Patients can present with one of two general MS disease patterns.[8] Relapsing-remitting MS (RRMS) is the most common form, affecting around 85% of newly diagnosed patients. This disease course is characterized by relapses followed by full or partial recovery, and patients are generally stable between relapses. The majority of patients with RRMS eventually enter a phase of secondary progressive MS (SPMS) characterized by progressively increasing neurological disability in the absence of relapses. The less common presentation is primary progressive MS

(PPMS), characterized by steadily increasing neurological disability independent of relapses from disease onset.

Diagnostic criteria

The diagnosis of MS relies on evidence of demyelinating lesions with dissemination in space and time, meaning lesions in two or more parts of the CNS that have occurred at different timepoints.[21] Patients presenting with symptoms suggestive of MS routinely undergo clinical neurological examination, magnetic resonance imaging (MRI) of the brain and spinal cord with intravenous gadolinium contrast, and lumbar puncture for examination of the cerebrospinal fluid (CSF). MRI with contrast enhancement is often sufficient to confirm dissemination in space and time, but in some patients evidence of dissemination in time is obtained from oligoclonal immunoglobulin G (IgG) in the CSF.[21] Demyelinating lesions are visible as hyperintense areas on T2-weighted MRI scans, and active inflammatory lesions with BBB disruption show gadolinium contrast enhancement because the contrast is able to pass from the blood into the CNS parenchyma.[1] Since not all CNS lesions are symptomatic, patients who have experienced only one clinical relapse may have numerous lesions on MRI. Signs of CNS inflammation in the CSF include increased number of leukocytes and CSF-specific oligoclonal IgG bands reflecting abnormal intrathecal antibody production by clonally expanded B-cells.[23]

An isolated clinical episode with MS symptoms without radiological evidence of dissemination in space and time is referred to as clinically isolated syndrome (CIS) and typical MS lesions on MRI not accompanied by clinical signs of MS (or a history of such) are referred to as radiologically isolated syndrome (RIS).

6.1.3 Therapy

There is still no cure that fully halts MS disease progression or reverses disability, but the long-term prognosis of RRMS has radically improved over the past three decades. This is mainly due to the introduction of disease modifying therapies (DMTs) in the

mid-1990s, which prevent development of demyelinating lesions and clinical relapses and reduce accumulation of disability.[1]

Each DMT has a distinct safety and efficacy profile, commonly inducing immune-suppression and reduction of CNS inflammation by various mechanisms of action like reducing numbers of circulating leukocytes, inhibiting trafficking over the BBB, or reducing cytokine production.[24, 25] Choice of DMT is influenced by a combination of patient-related factors including disease aggressiveness, comorbidities, patient preferences, and family planning (pregnancy) and drug-related factors including mode of action, efficacy and side-effect profile, route and frequency of administration, and price.[26] New compounds are constantly in development, and currently approved DMTs can be categorized as moderately effective (glatiramer acetate, β interferons, dimethyl fumarate, fingolimod, teriflunomide) and highly effective (natalizumab, alemtuzumab, cladribine, ocrelizumab, rituximab, and ofatumumab).[24] Highly effective DMTs are generally associated with potentially more serious safety concerns and require greater monitoring. Thus, the traditional therapeutic strategy is an escalation approach where moderately effective DMTs are used as first-line therapy and escalation to highly effective DMTs is considered in cases of treatment failure with breakthrough disease. However, most patients have already accumulated disability before escalation, and highly effective DMTs have a more pronounced effect in young patients with little neurological disability.[27] This has encouraged a paradigm shift towards early highly effective therapy to improve disease control and thus delay accumulation of disability. DMTs have been found to be effective only in RRMS with the exception of ocrelizumab, which was recently licensed for PPMS.[28]

Autologous hematopoietic stem cell transplantation (HSCT) causes a sustained reduction of inflammatory activity in RRMS through “immune resetting” by immunoablative therapy followed by reconstitution of the immune system from hematopoietic stem and progenitor cells.[29] Recently, a phase III randomized clinical trial reported HSCT to be superior to the best available DMT for a subset of RRMS patients with highly active disease.[30]

Methylprednisolone is used for relapse therapy to speed up and possibly improve recovery, and a wide range of further therapeutics and aids are available to relieve MS-related symptoms including spasticity, gait difficulties, urinary and sexual challenges, depression, fatigue, and pain.[31]

6.1.4 Therapeutic response

With the introduction of highly effective DMTs, the perception of what constitutes treatment success has become stricter. Careful monitoring for signs of disease activity is crucial for the early discovery of suboptimal response to therapy, preferably at a subclinical stage, to prevent accumulation of disability. Although DMTs are effective on a population level in RRMS, the therapeutic response and disease course in individual patients is unpredictable, and biomarkers are being sought to guide therapeutic decision-making and personalize therapy.

Evidence of disease activity

Disease activity is commonly evaluated by occurrence of clinical relapses, progression of neurological disability and MRI activity. MRI activity, often defined as new or enlarged T2 lesions or gadolinium-enhancing lesions, is more sensitive for disease activity than clinical relapses as it also captures clinically silent new lesions, thereby lowering the threshold for detecting treatment failure.[27, 32] The most widely used scoring tool for neurological disability in MS is the Expanded Disability Status Scale (EDSS), a clinician-based assessment of CNS-functions with a score ranging from 0 to 10 where higher scores indicate more severe disability.[33] An increasingly used treatment target and surrogate end point in MS clinical trials is ”no evidence of disease activity” (NEDA-3), defined as the absence of clinical relapses, disability progression (as measured by EDSS), and MRI activity.[34]

What constitutes evidence of disease activity is currently debated, and the NEDA-3 concept has been criticized for not adequately reflecting overall response to therapy.[35] Because the criteria emphasize inflammation more than degeneration, inclusion of annualized brain volume loss as a surrogate marker of neurodegeneration has been

suggested a fourth criterion (NEDA-4).[36] The criteria have also been criticized for not taking into account neuropsychological symptoms like fatigue and cognitive impairment.[37] Fatigue, a feeling of extreme mental or physical exhaustion, is a common symptom in MS which influences quality of life and working ability independently of MS-related physical disability.[38-41] Cognitive impairment, affecting approximately half of patients with MS, may be present even before the first physical signs of the disease and reduces working ability and quality of life.[42, 43] Cognitive impairment is underreported and correlates poorly with T2 lesions on MRI, and many patients have worsening of cognitive scores although fulfilling the criteria for NEDA-3.[44-46] Future NEDA definitions may include neuropsychological and working ability parameters, as well as patient reported outcomes to catch subjective symptoms of suboptimal therapeutic response that may not be perceived as important to physicians as they are to patients.[35, 37, 47, 48]

Biomarkers and individual therapeutic response

The heterogeneity of disease course and therapeutic response in MS has garnered interest for personalized therapy approaches that take into account individual variability.[49] Development of personalized therapy can be aided by identification of biomarkers that elucidate the biological basis of observed variations in clinical disease activity and response to therapy. A biomarker is defined as a characteristic that can be objectively measured and serves as an indicator of normal biological processes, pathological processes or pharmacological reactions to therapy.[50] MRI lesion activity is a well-established imaging biomarker in MS, and other MRI-based measures for regional or global cerebral atrophy are receiving increasing attention.[35, 51] Numerous molecular biomarkers, often measured in body fluids, have been proposed to aid the diagnosis of MS and allow prediction and early discovery of suboptimal therapeutic response and identification of patients at high risk for side-effects.[23] Despite extensive research, a gap remains between the numerous exploratory biomarkers proposed in studies and biomarkers that are validated and finally integrated into routine clinical practice. A body fluid biomarker for treatment response in MS should be process-specific and easily accessible (preferably in

peripheral blood), and most importantly; clinically useful, as assessed by the probability to improve patient outcome.[23] For implementation in clinical practice, the test should have high analytic validity and be simple, cost effective, safe, and non-invasive.

Neurofilament as a multiple sclerosis biomarker

Neurofilament light chain (NF-L) stands out as the most promising new molecular MS biomarker for use in routine clinical practice.[52] Neurofilaments are neuron-specific cytoskeletal components which are released into the CSF upon neuronal and axonal damage in the CNS, and have been explored as potential MS biomarkers for more than two decades since they were first reported to be elevated in patients with RRMS.[53] The light chain subunit of neurofilaments, NF-L, has proven more useful in MS than other subunits.[54] A small proportion of NF-L in CSF passes the BBB into peripheral blood and, although over 40-fold lower, serum NF-L levels strongly correlate with CSF levels.[55, 56] Recent development of sufficiently sensitive methods for detection of NF-L in serum by single molecule array (Simoa) has made the biomarker feasible for repeated measurements in peripheral blood.[57] NF-L levels are higher in MS patients than in healthy controls[58] and further increase during relapses and MRI lesion activity.[56, 59, 60] Levels decline both after initiation of DMT in treatment-naïve RRMS patients and when switching from moderately to highly effective DMTs.[55, 56, 61, 62] Accumulating evidence supports NF-L as an important biomarker in clinical follow-up of therapeutic response in RRMS patients,[52] particularly as a marker of subclinical disease activity.[56, 60] Normalization of NF-L levels has been proposed as a fifth treatment goal to be included in future NEDA definitions (NEDA-5).[35, 47]

NF-L levels increase by approximately 2% per year in healthy individuals and show substantial inter-individual variation, and an age-specific cut-off for pathological levels is necessary before taking the biomarker into clinical use.[52, 59] Using each patient as its own control has also been suggested.[52] NF-L levels are elevated in a range of other neurological diseases including ALS, Alzheimer's disease, stroke,

frontotemporal dementia, and Creutzfeldt-Jacobs disease,[63-66] and combining NF-L with other biomarkers more specific to MS may be of value.[52]

6.1.5 Prognosis

Half a century ago, the prognosis of MS was poor: 10 years after diagnosis, 25% of patients could still work, 50% were out of work, and 25% had died of the disease.[67] The introduction of increasingly effective DMTs together with improved diagnostics and a more aggressive treatment target of NEDA instead of only clinical relapse reduction have contributed to the radically improved prognosis of RRMS.[27] However, it is doubtful that RRMS can be fully arrested and that conversion to SPMS can be prevented with current therapies.[68] Patients with MS have a shorter life expectancy than the general population, but over the last decades the relative survival has increased. This started already before the introduction of DMTs, possibly due to improved care, rehabilitation and treatment of symptoms and comorbidities.[69, 70]

6.2 Natalizumab

Natalizumab (Tysabri®, Biogen) is a highly effective DMT that prevents RRMS disease activity by blocking leukocytes from entering the CNS over the BBB. Natalizumab was approved for MS therapy in 2006 and is administered intravenously at a standard dose of 300 mg every 4 weeks.[71]

6.2.1 Mode of action

Infiltration of circulating leukocytes is an early event in the formation of demyelinating CNS lesions in RRMS.[13] Leukocyte migration across the BBB in the vessels of the brain and spinal cord is facilitated by the adhesion of α4β1 integrin on leukocytes to vascular-cell adhesion molecule 1 (VCAM-1) on vascular endothelial cells (figure 1A).[72, 73] Natalizumab is a recombinant humanized monoclonal IgG4 antibody that selectively binds to the α4 subunit of α4β1 integrin and blocks binding to VCAM-1 (figure 1B). This results in the prevention of leukocyte migration over

the BBB and drastically reduces the formation of demyelinating CNS lesions, as first shown in an animal model of MS in 1992.[74]

Figure 1: Natalizumab blocks leukocyte trafficking to the central nervous system (CNS) over the blood-brain barrier (BBB). (A) *α4 integrin binds to vascular cell adhesion molecule 1 (VCAM1) on endothelial cells, giving leukocytes access to the CNS.* ***(B)*** *Natalizumab, a humanized antibody to α4 integrin, blocks binding of leukocytes to VCAM-1, thereby preventing lymphocyte entry into the CNS. Adapted and reprinted by permission from Rockefeller University Press: Journal of Cell Biology, [75] © 2012*

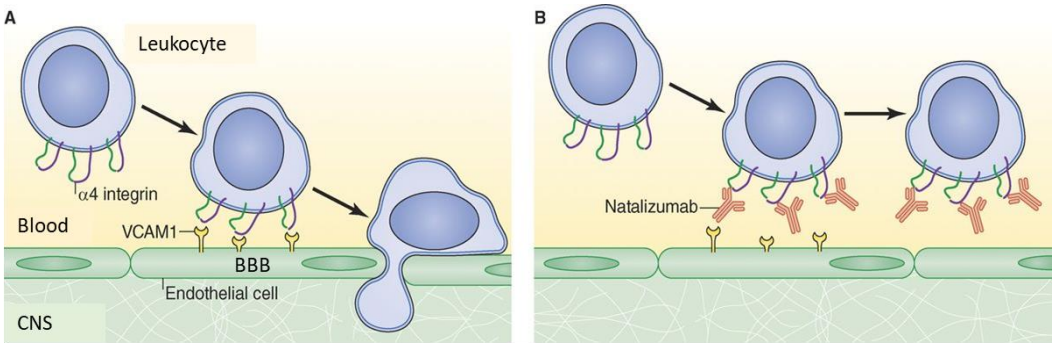

Disrupted trafficking of T lymphocytes was initially thought to be the major therapeutic effect of natalizumab,[74] however its impact on trafficking, composition and function of other leukocyte subsets including B cells[76-79] and altered levels of circulating lymphocytes[80] and CD34+ hematopoietic stem cells[81] has also been suggested to play a role. Further pharmacodynamic effects of natalizumab include downregulation of α4β1 integrin on the surface of leukocytes which contributes to their reduced migratory capacity over the BBB,[82] and reduction of lymphocytes in the CSF reflecting restricted immune surveillance of the CNS.[83] α4β1 integrin can modulate the survival, priming, and activation of leukocytes through interaction with fibronectin and osteopontin in the CNS, and natalizumab may also modulate inflammatory reactions inside the CNS by inhibiting these interactions.[72]

6.2.2 Clinical efficacy

Reduction of disease activity

Natalizumab efficiently prevents clinical relapses, formation of new CNS lesions, and accumulation of disability and in patients with RRMS, as demonstrated by randomized clinical trials, [84, 85] real-world data,[86, 87] and meta-analyses comparing natalizumab to other DMTs.[88, 89] Compared to placebo, natalizumab reduces the annualized relapse rate (ARR) by 68 % and the two-year risk of disability progression and formation of new or enlarged T2 MRI lesions by 42 and 83%, respectively.[85] The ARR on natalizumab therapy is approximately 0.3[85, 86] and 24-month proportion with NEDA-3 is 70%.[87] Natalizumab has positive effects on MS-related fatigue, cognitive dysfunction, mood, well-being, and quality of life.[84, 90-94] The high efficacy is further supported by the observed reduction of NF-L to similar levels as healthy controls after initiation of natalizumab, indicating reduced axonal damage.[62]

After natalizumab withdrawal, disease activity typically starts returning 10-12 weeks following cessation of therapy, but in some patients this occurs after only 6-8 weeks.[95, 96] Extensive rebound of MS disease activity can occur in this period.

Development of transient or persisting anti-natalizumab antibodies is seen in 6-9% of patients, often during the first 3 months of therapy. Such antibodies bind to natalizumab and reduce therapeutic efficacy due to increased natalizumab clearance and may be accompanied by infusion-related adverse events.[71, 97]

The wearing-off phenomenon

As many as 54-63% of patients who receive natalizumab report that the effect “wears off” towards the end of the 4-week dosing interval, and that subjective symptoms, most commonly fatigue, increase during the last week of the dosing interval and improve shortly after receiving their next infusion.[98-101] These patients show improved scores for fatigue, depression and quality of life after a new natalizumab infusion, while patients without wearing-off symptoms have stable scores throughout the dosing interval.[100] Although frequent, the wearing-off phenomenon has been

sparsely investigated, and it is unknown whether the symptoms have an underlying biological mechanism or are purely psychological.

6.2.3 Progressive multifocal leukoencephalopathy

Natalizumab is generally well tolerated,[85] but treatment is associated with increased risk of progressive multifocal leukoencephalopathy (PML), a rare but potentially lethal demyelinating CNS disease caused by infection of oligodendrocytes with John Cunningham (JC) virus.[71, 102] About 30-70% of healthy adults have antibodies against JC virus, but primary infection usually goes unnoticed. PML is thought to be an opportunistic infection in immunocompromised patients, and is most often reported in patients with human immunodeficiency virus (HIV) and hematological malignancies and in patients receiving immunomodulatory therapy.[103, 104] Natalizumab increases PML risk more than any other immunomodulatory therapy. This is attributed to the reduced migratory capacity of immune cells over the BBB, resulting in impaired CNS immune surveillance and risk of opportunistic CNS infections.[83, 105, 106] The incidence is highly dependent on three established risk factors: level of JC virus antibodies in serum (JCV index), use of immunosuppressant therapy prior to natalizumab, and duration of natalizumab treatment.[71] Overall, PML affects 4/1000 natalizumab treated patients, however in patients with a high JCV index who have been treated with natalizumab for more than 2 years after previously receiving other immunosuppressants, the estimated PML risk increases to 17/1000 treated patients.[104] PML causes subacute neurological symptoms and can be diagnosed by typical MRI findings and detection of JC virus DNA in the CSF. Re-establishing immune defense in the CNS by discontinuation of natalizumab (and sometimes plasmapheresis to remove drug from the circulation) is the only current treatment for natalizumab-associated PML, but the mortality is still approximately 20%.[104, 107] Starting natalizumab therapy is generally avoided in JC virus-positive RRMS patients to reduce the risk of PML. JC virus-negative patients under treatment with natalizumab are routinely screened for JC virus antibodies every 6th month, and switching to other DMTs is considered if patients convert to JCV-positive status.

6.2.4 Individualized natalizumab dosing and receptor occupancy

The clinical response to natalizumab therapy is individual. While some patients still have disease activity when natalizumab is administered at the standard dose, several observational studies of doses administered with extended intervals suggest reduced risk of PML while maintaining therapeutic efficacy. Under-dosing may induce therapy failure and relapses with potentially permanent CNS damage, and a biomarker to safely navigate natalizumab dose optimization based on the individual therapeutic response is therefore highly relevant.

Extended interval dosing

As natalizumab-associated PML is attributed to reduced CNS immune surveillance, extending the natalizumab dosing intervals from 4 to 5-8 weeks has been proposed in an effort to reduce the PML risk by restoring partial immune surveillance of the CNS. Retrospective observational studies of such off-label extended interval dosing (EID) suggest that the therapeutic efficacy is maintained compared to standard interval dosing (SID).[108-111] However, these studies are limited by non-randomized design with a possible selection bias of patients with less aggressive MS disease to the EID treatment group. A recent retrospective evaluation of over 35,000 JC virus positive patients treated with natalizumab showed substantially reduced occurrence of PML in patients treated with EID compared to those treated with SID, but the study was not randomized and did not evaluate therapeutic efficacy.[112] The first randomized prospective trial of effectiveness and safety in SID versus EID (ClinicalTrials.gov identifier NCT03689972) is ongoing.

Natalizumab receptor occupancy

Receptor occupancy (RO) assays measure the binding of therapeutic antibodies to their cellular targets and are widely used in drug development and selection of optimal therapeutic dose.[113] Natalizumab RO, defined as the proportion of α4 integrin bound by natalizumab, varies considerably between patients receiving the same dose and correlates with therapeutic efficacy and possibly with risk of natalizumab-

associated PML.[95, 96, 114-116] Therefore, natalizumab RO has been suggested as a biomarker to navigate individualized dosing, aiming to minimize natalizumab exposure to reduce the risk of PML while maintaining therapeutic efficacy.[117] The lowest RO threshold to maintain therapeutic efficacy has not been determined, but some data suggest that optimal efficacy is achieved when RO is kept over 70-80%.[118]

Natalizumab binds α4 integrin on the leukocyte surface with high avidity immediately after intravenous infusion.[118] In general, natalizumab RO correlates with the level of free natalizumab in serum, peaking after infusion and declining towards the end of the dosing interval. Natalizumab has a mean volume of distribution of 5.7 (SD ± 1.9) liters and a mean half-life of 11 (SD ± 4) days.[71] Natalizumab serum level and RO varies between patients receiving the same standard dose of 300 mg every 4 weeks, but generally decrease if dosing intervals are extended.[116, 119] Serum levels of natalizumab are influenced by body weight and the presence of anti-natalizumab antibodies; serum natalizumab is estimated to be around 40% lower in a 100-kg individual compared to a 60-kg individual, and anti-natalizumab antibodies increase the clearance of natalizumab by approximately 3-fold.[118] However, these factors alone only explain a small fraction the observed inter-individual variability in RO, and additional unknown factors apparently affect the relationship between natalizumab serum levels and RO.[118]

Measurement of natalizumab receptor occupancy

RO of therapeutic antibodies can be estimated by a variety of flow cytometry assays (figure 2).[113, 120] The number of drug molecules that can bind to a cell depends on the number of available target receptors. Therefore, isolated measurement of bound drug is insufficient and total receptor levels need to be taken into account if levels vary between individuals or over time.[113] Unknown variations in receptor levels can have disastrous consequences: in the first-in-human clinical trial of a novel anti-CD28 therapy, a life-threatening cytokine storm occurred in healthy human subjects that had never been observed in preclinical trials in monkey.[121] Follow-up studies revealed

that unexpectedly low receptor levels in humans compared to monkeys dramatically increased RO, causing a severe cytokine release syndrome.

Levels of α4 integrin vary between individuals and natalizumab therapy itself induces reduction of α4 integrin levels, necessitating simultaneous quantitation of both natalizumab and α4 integrin in a natalizumab RO assay.[122]

Figure 2: Receptor occupancy assays measure bound drug relative to total receptor level. *Bound drug can be measured either indirectly by measuring only free receptors with an anti-receptor antibody competing with bound drug* ***(A)*** *or directly by measuring occupied receptors with an anti-drug-antibody* ***(B)****. Total receptors can be measured either directly with an anti-receptor antibody that does not compete with bound drug* ***(C)*** *or indirectly by measuring occupied receptors* ***(B)*** *in an in vitro drug saturated sample aliquot. Adapted and reprinted by permission from Wiley: Cytometry part A,[123] © 2016*

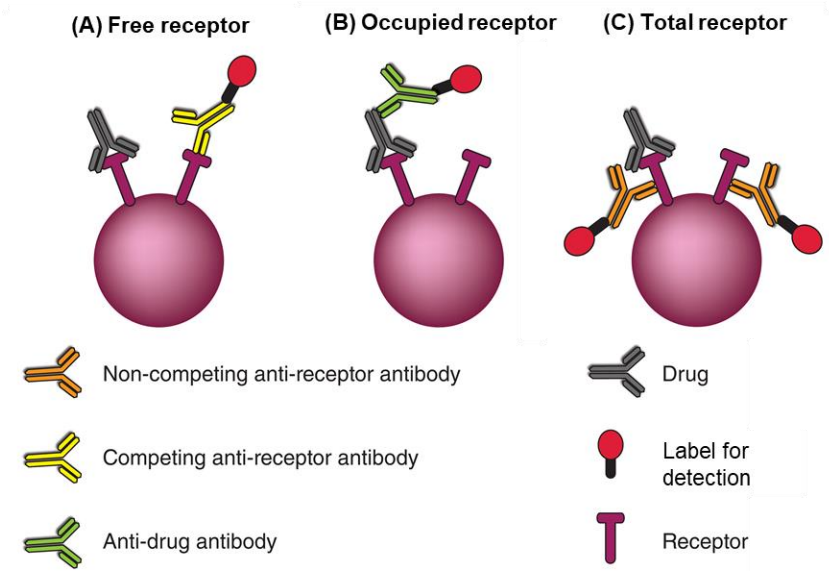

6.3 Mass cytometry

The central method in this study is the relatively novel analytical technology mass cytometry, and the following sections will provide a brief introduction to the method and associated caveats relevant to this study.

Cytometry (Greek for cell measurement) involves the detection and quantitation of features on the single-cell level, and typically employs labeled antibodies that bind specifically to these features. Since the late 1960s, flow cytometry has been the standard technique for single-cell analysis and employs antibodies conjugated to fluorescent labels to detect cellular features.[124] Technological advances in flow cytometry allowing simultaneous measurement of increasing numbers of parameters have come hand-in-hand with more detailed knowledge of the complexity of immune cell subsets and functions. Despite these advances, signal overlap between fluorescent labels, causing signals to be measured not only in the primary channel but also in other channels, restrict the number of parameters that can be measured simultaneously by conventional flow cytometry. This limitation was radically overcome by the introduction of *mass* cytometry in 2009.[125] Capable of simultaneous analysis of more than 40 cellular targets, mass cytometry allows insights into heterogeneous biological systems at a new level of complexity.[126, 127] This is accomplished by conjugating antibodies to purified non-biological metal isotopes instead of fluorescent labels, dramatically reducing signal overlap.[128]

6.3.1 The mass cytometry method

Mass cytometry, or Cytometry by Time-Of-Flight (CyTOF), combines detection of isotopes by inductively coupled plasma (ICP) mass spectrometry with single-cell analysis.[125] The methodology is outlined in figure 3.[127] Cells in suspension are stained with a cocktail of metal-conjugated antibodies and sequentially introduced into the ICP where each cell is atomized and ionized to an ion cloud. Biological atoms originating from cells are removed so that only the isotopes originating from metal-conjugated antibodies remain in the cloud. These are finally identified by their atomic mass, determined by time-of flight (TOF), and the abundance of each isotope in the cloud is determined by the signal intensity in detection channels corresponding to their atomic mass. The acquired signal from each ion cloud is recorded in Flow Cytometry Standard (FCS) files.[129]

Figure 3: Schematic of single-cell analysis with mass cytometry. *Cells stained with metal-labeled antibodies are introduced into the mass cytometer via a capillary system ending in a nebulizer that disperses the suspension into droplets mostly carrying single cells. In the inductively coupled plasma (ICP, 5000 °C), each cell is vaporized and ionized into an ion cloud, which passes a quadrupole where biological ions are removed. The remaining ion cloud is analyzed by a time-of-flight detector and its ion content is recorded in Flow Cytometry Standard (FCS) files. Reprinted by permission from Elsevier: Trends in Immunology,*[127] *© 2012*

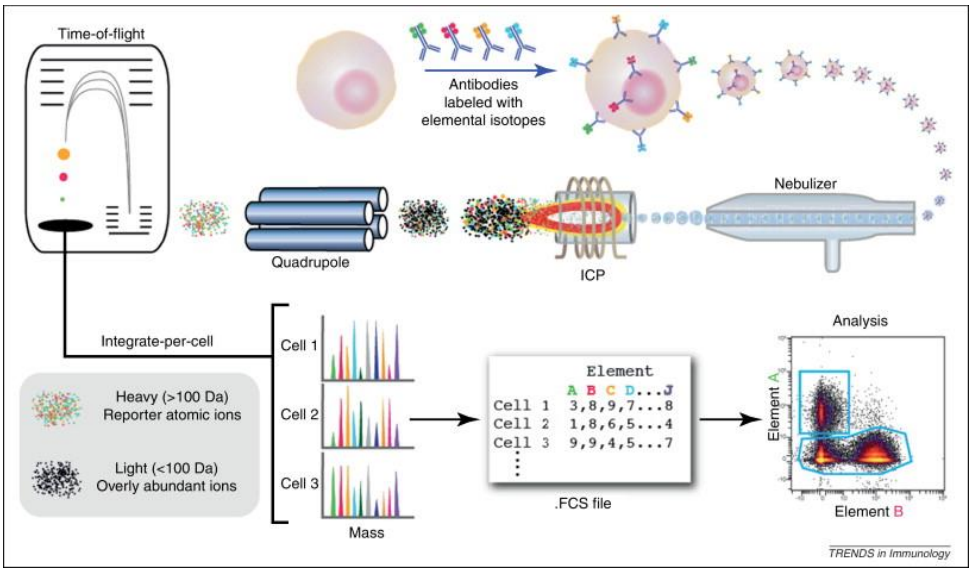

In flow cytometry, cells are detected by their light scatter. There is no mass cytometry analog to light scatter; only ion clouds containing metal isotopes (i.e. not the cells themselves) are detected by the mass cytometer and registered as "events". To be defined as an event and included in the FCS file, an ion cloud has to meet two criteria (which can be adjusted by the user): it must have an appropriate *event length*, reflecting its size, and the signal intensity in at least one mass channel must exceed the *lower convolution threshold*.[130] This implies that only ion clouds creating uninterrupted signals exceeding the lower convolution threshold for an appropriate duration of time are defined as events and recorded.

As cells themselves do not contain any metals in the detection range of the mass cytometer, they can be incubated with DNA-binding reagents containing iridium to allow identification of ion clouds originating from separate cells.

6.3.2 High dimensional data analysis

The high dimensionality of mass cytometry has introduced new challenges for data processing and analysis.[131] Cells are commonly classified into distinct subtypes based on expression of characteristic cluster of differentiation (CD) markers on their surface. Conventionally, the analysis of flow cytometry data has been performed by manually drawn gates in bivariate plots of CD markers. Such manual gating in bivariate plots becomes exponentially more complex with increasing numbers of markers, making this approach impractical for high-dimensional mass cytometry data.[132] The demand for new approaches to gain insight into the structure of complex mass cytometry data has driven the development of automated data analysis tools to classify cells into groups or clusters (optimally representing distinguished cell subtypes) based on their expression patterns of CD markers. Numerous unsupervised and semi-supervised algorithm-based analysis tools for clustering and dimensionality reduction have been developed over the past decade,[131, 133] two of which were employed in this study:

ViSNE[134] (Cytobank Inc., Beckman Coulter) is a widely used tool for dimensionality-reduction of high-dimensional data. Using the t-distributed stochastic neighbor embedding (t-SNE) algorithm, viSNE allows projection of the high-dimensional relationship between cells in a two-dimensional plot by constructing two new dimensions (t-SNE1 and t-SNE2). Cell populations in the two-dimensional plot can then be defined by either manual gating or automated clustering algorithms.

Citrus (cluster identification, characterization, and regression)[135] (Cytobank) is an algorithm that identifies cell types by hierarchical clustering and subsequently identifies statistically significant differences between pre-defined patient groups in these clusters.

6.3.3 Factors influencing mass cytometry data

The identification of meaningful variations in biological samples requires precise, standardized, and reproducible assays to distinguish true biological changes from technical artefacts.[136] Mass cytometry data can be influenced by factors contributing to specific and nonspecific signal and by experimental variation.

Specific and nonspecific signal

The specific signal in mass cytometry originates from metal conjugated antibodies bound to cellular epitopes of interest, while other sources can contribute to nonspecific signal.[137] In addition to nonspecific binding of antibodies to other than the epitopes of interest, there are three major contributors to nonspecific signal in mass cytometry: signal "spillover" of metal isotopes into neighboring ± 1 mass channels, isotope oxidation in the ICP causing signal in the + 16 mass channel, and incomplete isotope purification introducing signal from one or more other isotopes of the same metal element. The intensity of the nonspecific signal is dependent on the intensity of the signal in the primary channel, and careful panel design and titration of the antibody panel can minimize the effects on the data.[138] Metals in the detection range of the mass cytometer are not found in a typical biological sample, but contamination from either *in vivo* origins (for example gadolinium from intravenous MRI contrast or cisplatin used in chemotherapy) or environmental components such as soap (barium), reagent containers (lead), or water (iodine) are other potential sources of nonspecific signal.

The specific signal mainly depends on the cellular content of the epitope measured, but is also influenced by the metal content of the antibody, and the mass cytometers' detection sensitivity for each metal isotope.[130, 139] The antibody metal content, determined by the number of metal isotopes conjugated to an antibody, may differ between batches due to varying labeling efficacy in the process of antibody metal conjugation. The detection sensitivity for metal isotopes varies over the detection range of the mass cytometer, causing equal amounts of different metal isotopes to produce signals of differing intensity (figure 4).[137, 140] The most sensitive range is for

isotopes with atomic mass between 155 and 165 Dalton, and each mass cytometer has its own sensitivity pattern.

Figure 4: *Detection sensitivity varies due to different isotope transmission efficiency over the channels of the mass cytometer. Sensitivity is expressed as the ratio between observed and expected signal intensity of equal amounts of metal isotopes. The difference between the highest and lowest sensitivity is up to fivefold in CyTOF 1 and 2 mass cytometers, and lower in Helios mass cytometers. Reprinted by permission from Wiley: Cytometry A,*[140] *© 2015.*

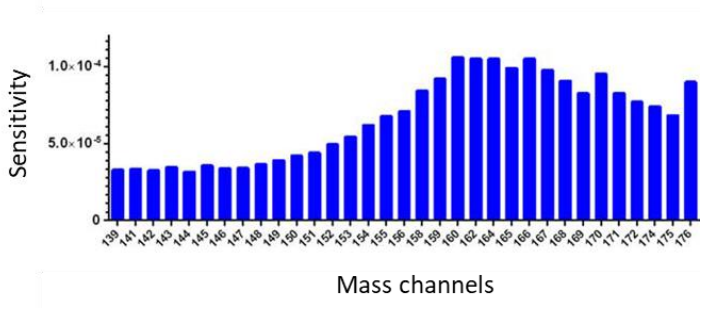

Variation and standardization

To accurately measure biological variations with cytometry, the experimental variation must be kept at an absolute minimum.[141] This is particularly important in mass cytometry, as the increased number of antibodies compared to flow cytometry magnifies potential variation.[136] General recommendations are common for mass and flow cytometry, such as standardized sample collection and antibody staining procedures. In addition, several procedures to specifically address variation in mass cytometry have been established. Barcoding samples with unique combinations of metal isotopes and pooling them prior to antibody staining simplifies sample handling, reduces antibody consumption and limits batch effects in staining.[142] During daily setup of the mass cytometer, instrument performance can be controlled with a standardized tuning solution containing five different elements (cesium, iridium, lanthanum, terbium and thulium), and with cell-sized EQ Four Element Beads containing one of four elements (cerium, europium, holmium, and lutetium) in the detection range of the mass cytometer. The mass cytometer is sensitive to temperature changes and buildup of cellular material during sample acquisition,

which requires several hours for a typical experiment. EQ Four Element Beads are therefore routinely spiked into the samples prior to acquisition to allow for normalization of signal variations over the acquisition time.[143] Methods for standardization across machines and over time, which are necessary in multicenter and longitudinal studies, are routinely used in flow cytometry, but not yet established in mass cytometry.[141, 144] Most mass cytometry studies have been performed in a single lab at a single site, and established normalization methods do not fully correct for variations across mass cytometers.[140, 145]

6.3.4 Receptor occupancy measurement with mass cytometry

Although RO assays are widely used in flow cytometry,[113, 120] no RO assay for mass cytometry has previously been published. High-parameter mass cytometry can enable the measurement of RO in more cell subtypes congruently with more cellular features of interest than what is currently achievable by flow cytometry. A mass cytometry RO assay shares many general methodological considerations with a flow cytometry assay, like the fundamental need for accurate quantitation of drug and receptor and the requirement for strict standardization and adequate controls.[120] Other challenges, such as the influence of factors contributing to specific and unspecific signal, are mass cytometry-specific (page 25). Varying detection sensitivity between different mass channels[140] (figure 4) could affect an RO an assay where bound drug and total receptor levels are measured by different antibodies. Measuring drug and receptor levels using antibodies conjugated to metal isotopes with different detection sensitivities can lead to either over- or underestimation of the RO, depending on which is detected in the most sensitive channel. Varying detection sensitivity patterns between mass cytometers[140] would make the degree of this effect unpredictable.

7. Aims of the study

The main aim of this thesis was to perform a mass cytometry study of natalizumab treated RRMS patients to investigate the relationship between natalizumab receptor occupancy (RO), the wearing-off phenomenon, and disease activity.

Objectives:

1. Develop a method for reliable and reproducible RO measurement with mass cytometry (paper I)

2. Investigate whether wearing-off symptoms at the end of the dosing interval are associated with natalizumab RO or clinical and demographic patient characteristics (paper II)

3. Evaluate whether wearing-off is associated with clinical or radiological outcomes (paper III)

8. Methods

8.1 Patients and outcomes

8.1.1 The cohort

We invited all patients with RRMS receiving natalizumab at the Department of Neurology, Haukeland University Hospital in October 2018 (n=45) to participate in the main project. All patients had been diagnosed with MS according to the 2010 McDonald diagnostic criteria[146] or earlier (prior to the latest revision in 2017). None had anti-natalizumab antibodies. Blood samples used for the method development were collected from a subgroup of 8 treated patients during 2016. Healthy controls were volunteering employees at the Department without any known neurological condition. The study was approved by the Regional Committee for Medical Research Ethics, Western Norway (REK 2016/579).

8.1.2 Patient outcome measures

Patients were evaluated for evidence of disease activity by assessing clinical relapses and disability progression as measured by EDSS[33], and by annual routine MRI scans without intravenous gadolinium contrast. We evaluated neurocognitive status using the Symbol Digit Modalities Test (SDMT),[147] a 90-second test where the patient links geometric figures to specific numbers and a higher score indicates better neurocognitive function. We evaluated fatigue using the Fatigue Severity Scale (FSS),[148] a survey where patients score their level of agreement (scores 1-7) on 9 statements regarding fatigue and a higher score indicates more severe fatigue. At inclusion, patients filled in forms regarding working status, smoking, weight and height, and whether they experienced wearing-off symptoms at the end of the 4-week interval between natalizumab infusions (Appendix 1). We had observed patients reporting various wearing-off symptoms and that not all patients had such symptoms regularly, therefore we categorized wearing-off symptoms based on their frequency – never, sometimes (at the end of some infusion intervals), and regularly (at the end of every infusion interval) – and patients could also record type of symptoms.

8.2 Neurofilament analysis

We measured the concentration of NF-L in serum samples with a single-molecule array (Simoa) assay (Quanterix, Billerica, MA). All serum samples were stored at -80°C and thawed on the day of analysis. In paper II we used only samples collected at inclusion. In paper III we compared samples collected at inclusion with samples collected at the 1-year follow-up. To avoid technical variations, the baseline samples were re-analyzed together with the 1-year samples, keeping sample pairs from each patient in the same analysis batch. NF-L levels are not affected by repeated thaw-freeze cycles of serum samples.[149]

8.3 Mass cytometry analysis

8.3.1 Samples

In the initial method development, we evaluated two sample types: peripheral blood leukocytes (PBLs) and peripheral blood mononuclear cells (PBMCs). PBLs were obtained from whole blood and fixed with Proteomic stabilizer (SmartTube, Inc.) shortly after collection and stored at -80°C, whereas PMBCs were isolated from whole blood by a 2-hour protocol and stored alive at -200°C. We observed lower RO in PBMCs compared to PBLs from the same patients and noted a downregulation of α4 integrin if we incubated live PBMCs with natalizumab which was not observed in fixed PBLs. Fixation of cells with proteomic stabilizer shortly after collection apparently prevented effects of *in vitro* processing of samples and we therefore conducted all further experiments with PBLs only.

We collected samples immediately before and 30 minutes after the 60-minute natalizumab infusions, at the expected time points for minimum and maximum natalizumab binding. Previous studies report that natalizumab RO is stable over time in patients receiving infusions with regular intervals.[96] We also observed this when comparing RO over 2 infusion cycles in a subgroup of 10 patients, and we therefore performed the main experiment on samples from one infusion day only.

8.3.2 Antibody panel and staining

Antibody panel design

We developed an antibody panel for the study of innate and adaptive peripheral blood immune cells with potential roles in disease activity and response to natalizumab therapy (table 1).[72, 150-152] CD34+ hematopoietic stem cells are the common precursors of these leukocytes and usually reside in the bone marrow, and natalizumab therapy increases levels of circulating CD34+ cells in peripheral blood.[81]

Table 1: Overview of peripheral blood leukocyte subtypes evaluated in the study and their associated cluster of differentiation (CD) markers.

	Leukocyte subtype	CD marker
	Hematopoietic stem cells	$CD45^{low}$ $CD34^{+}$
Innate immunity	**Granulocytes**	$CD45^{low}$ $CD66b^{+}$
Innate immunity	**Natural killer (NK) cells**	$CD56^{+}$
Innate immunity	**Monocytes**	$CD33^{+}$ $CD14^{+}$
Innate immunity	**Conventional dendritic cells (cDC)**	$CD33^{+}$ $CD11c^{+}$
Adaptive immunity	**Memory B lymphocytes**	$CD20^{+}$ $CD19^{+}$ $CD27^{+}/CD38^{-}$
Adaptive immunity	**CD8+ T lymphocytes**	
Adaptive immunity	Naive	$CD3^{+}$ $CD8^{+}$ $CD27^{+}/CD45RA^{+}$
Adaptive immunity	Central memory (T_{CM})	$CD3^{+}$ $CD8^{+}$ $CD27^{+}/CD45RA^{-}$
Adaptive immunity	Effector memory (T_{EM})	$CD3^{+}$ $CD8^{+}$ $CD27^{-}/CD45RA^{-}$
Adaptive immunity	Effector memory RA (T_{EMRA})	$CD3^{+}$ $CD8^{+}$ $CD27^{-}/CD45RA^{+}$
Adaptive immunity	**CD4+ T lymphocytes**	
Adaptive immunity	Naive	$CD3^{+}$ $CD4^{+}$ $CD27^{+}/CD45RA^{+}$
Adaptive immunity	Central memory (T_{CM})	$CD3^{+}$ $CD4^{+}$ $CD27^{+}/CD45RA^{-}$
Adaptive immunity	Effector memory (T_{EM})	$CD3^{+}$ $CD4^{+}$ $CD27^{-}/CD45RA^{-}$
Adaptive immunity	Effector memory RA (T_{EMRA})	$CD3^{+}$ $CD4^{+}$ $CD27^{-}/CD45RA^{+}$

We designed the antibody panel based on prior knowledge[137, 140] and the Maxpar antibody panel designer (Fluidigm). In the RO assay, we measured cell-bound natalizumab and total α4 integrin directly with two different antibodies. Bound natalizumab was detected with an anti-IgG4 antibody (conjugated to 169Tm) specific

to the Fc portion of human IgG4. Total α4 integrin was detected with an anti-CD49d antibody (conjugated to 141Pr) specific for a different epitope than natalizumab so that the antibody could bind to α4 integrin independently of bound natalizumab (figure 2).

We titrated antibody concentrations on samples using the same conditions as the samples for the main experiment. Anti-IgG4 and anti-CD49d were titrated to saturating concentrations (Figure 5). The remaining antibodies in the panel were titrated to the lowest separating concentrations that allowed discrimination of the populations of interest, while minimizing nonspecific signal in the ± 1 and + 16 mass channels.

Figure 5: Titration to saturating concentration. *Exemplified by titration of anti-IgG4 for detection of natalizumab in a treated patient (blue) and in a healthy donor (HD) as negative control (red). Vertical line representing the chosen dilution for saturating titration without increase in signal intensity in the negative control.*

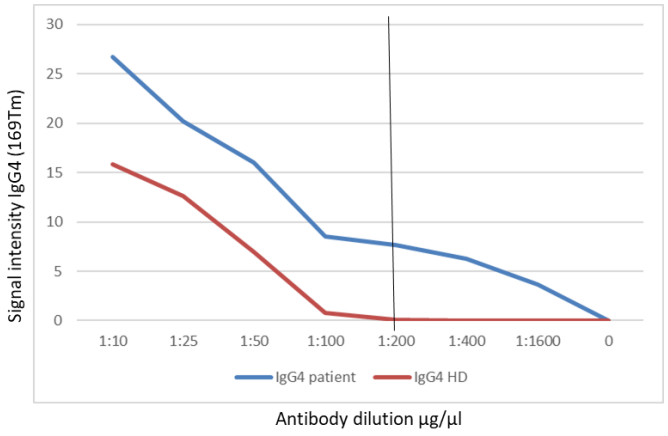

Standardization and quality control

Staining conditions such as temperature, incubation times, and cell numbers were standardized. PBLs were barcoded and pooled in batches of 20 samples before staining with aliquots of the same antibody cocktail to reduce variability in the staining procedure. Stained cells were fixed again with paraformaldehyde and

incubated with iridium-intercalator over night before acquisition. We adapted a method for controlling for experimental variation between samples with a common reference sample[153] by reserving one spot in each barcode batch for a standard healthy donor sample so that we could control for batch-to-batch variability. Pooling with patient samples did not lead to binding of natalizumab to the healthy donor cells.

Despite careful antibody panel design, we needed to ensure that we only measured specific signal in the two channels critical for the RO assay. We performed "mass minus one" (MMO) controls to check for spillover into the two channels by staining samples with the whole antibody cocktail minus anti-IgG4 (169Tm) or anti-CD49d (141Pr), respectively. To control for metal contamination, an aliquot of all samples was analyzed unstained. We controlled for competition between binding of anti-CD49d and natalizumab by comparing the anti-CD49d signal in a healthy donor sample with and without prior incubation with natalizumab. Negative controls for anti-IgG4 were untreated healthy donor cells and positive controls were sample aliquots that had been saturated *in vitro* with natalizumab.

8.3.3 Receptor occupancy measurement and standardization with beads

Based on prior knowledge, bound natalizumab was measured in a more sensitive channel (169) than α4 integrin (141) in our mass cytometry RO assay, which would lead to an overestimation of the natalizumab/α4 integrin ratio (figure 6). We therefore needed to standardize the signal between the two channels to obtain a correct RO.

In flow cytometry, a similar problem occurs when antibodies are conjugated to fluorophores with different brightness. This can be solved by employing antibody-binding polystyrene beads, such as Quantum Simply Cellular (QSC) beads, as a reference for standardization of signal from different fluorophore-labeled antibodies.[154] QSC beads are cell-sized polystyrene microspheres available in sets of four bead populations with known, gradually increasing antibody binding capacity (ABC).[155] In flow cytometry, these beads are used to convert signal intensity to numbers of cellular epitopes.

Figure 6: Differing mass cytometer detection sensitivity can affect RO results. *In our RO assay, bound natalizumab was detected with anti-IgG4 (169Tm), and total α4 integrin was detected with anti-CD49d (141Pr). Anti-IgG4 was measured in a more sensitive channel than anti-CD49d. Reprinted by permission from Wiley: Cytometry A,*[156] *© 2015*

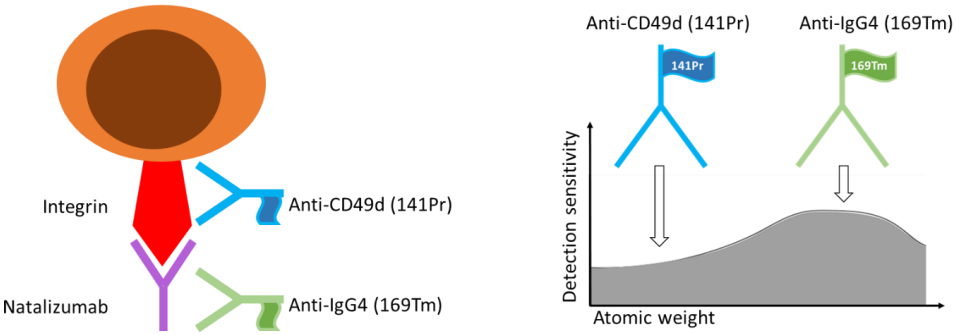

We aimed to employ QSC beads to standardize the signal from anti-IgG4 and anti-CD49d in our RO assay. In flow cytometry, beads can be detected by their light scatter, but as mass cytometry has no analog to light scatter and QSC beads do not contain any metal, they are not detectable by mass cytometry. When we saturated QSC beads with metal-conjugated antibodies, beads with the lowest ABC were incompletely detected by the mass cytometer, indicating that these beads did not contain enough metal ions to exceed the event length required to be detected as an event (figure 7A). Numerous unsuccessful attempts to overcome this problem included adjusting the mass cytometer settings for minimum event length and convolution threshold, titrating up the antibody concentration, and incubating the beads with various metals in the detection range of the mass cytometer, like cisplatin, iridium, and barcoding agents. However, at a cytometry conference (2018) a group from Berlin presented an unpublished method for adaption of QSC beads for mass cytometry by labeling them with Osmium Tetroxide (OsO_4), a highly reactive compound that binds to polystyrene.[157] When we labeled QSC beads with OsO_4 prior to antibody staining, we could identify the beads in the osmium channels of the mass cytometer independent of the signal from the antibody (figure 7B).

Figure 7: Adaption of QSC beads for mass cytometry. (A) *Five populations of QSC beads with increasing antibody binding capacity (ABC) stained with a metal-conjugated antibody. The beads per se are not detectable by the mass cytometer. Thus, beads with low ABC (low numbers of bound metal-conjugated antibodies) had insufficient event length for detection.* ***(B)*** *Mass cytometry rain plot during acquisition of QSC beads stained with anti-IgG4 (169Tm) without (top) and with (bottom) OsO_4 labeling. OsO_4 labeling allows detection of QSC beads in the osmium channels.*[157]

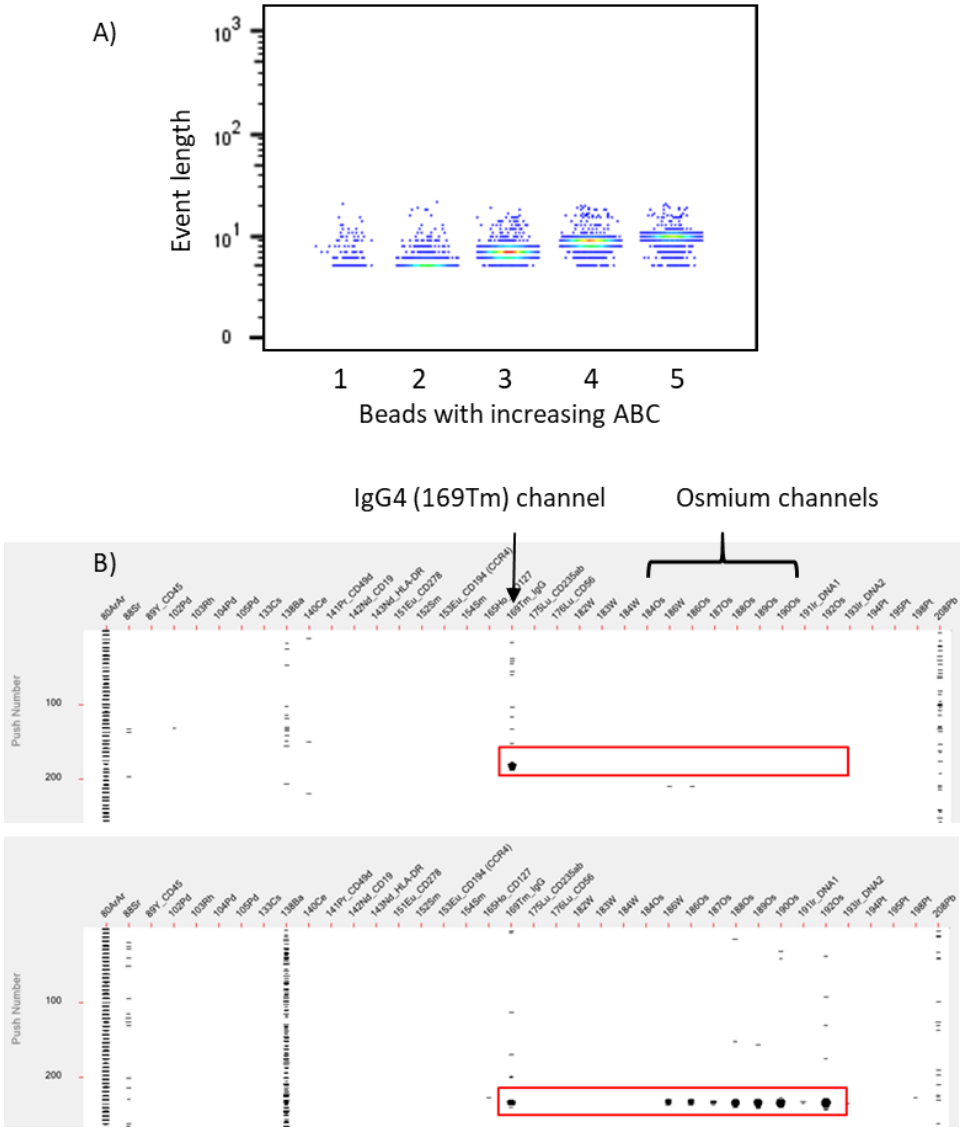

To cover the whole detection range of our samples, we purchased a custom-made bead population with extra low ABC, so that our set consisted of five bead populations. We analyzed the beads on the mass cytometer directly prior to acquisition of PBL samples and used the signal intensities of known amounts of anti-IgG and anti-CD49d on the beads as a reference for standardization of signal intensity of unknown amounts of anti-IgG and anti-CD49d in the samples.

8.3.4 Data analysis

FCS files from PBL samples in our main patient cohort were analyzed in parallel both by a manual and an automated approach as outlined in figure 8. Briefly, we separated PBLs into subtypes, estimated RO in these PBL subtypes, and compared RO between patient groups. FSC files were de-identified with a random number and data analysis was blinded. Low expression of target receptor may cause inaccurate RO estimation,[113] and cells with low α4 integrin levels (like naïve CD8+ and CD4+ T cells and granulocytes) were therefore excluded from the RO analyses.

Figure 8: Data analysis workflow for PBL samples acquired by mass cytometry

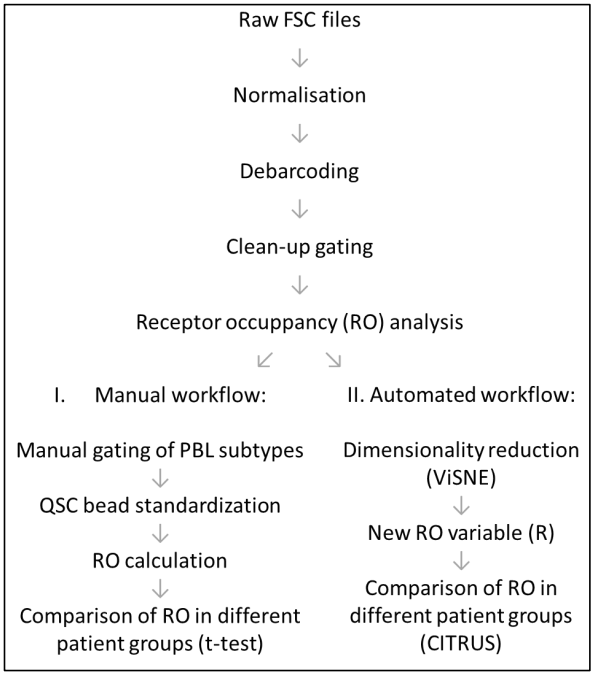

9. Results

Paper I: Optimization of Receptor Occupancy Assays in Mass Cytometry: Standardization Across Channels with QSC Beads

In paper I, we developed a receptor occupancy (RO) assay for mass cytometry which allowed simultaneous RO measurement and high-parameter immune phenotyping of peripheral blood leukocytes (PBLs). The method was evaluated in a natalizumab RO assay where anti-IgG4 and anti-CD49d were used to measure natalizumab and α4 integrin on eight PBL subtypes. Natalizumab was detected in a more sensitive mass channel than α4 integrin, leading to overestimation of the RO. We demonstrated how this could be solved by using antibody-binding quantum simply cellular (QSC) beads with known antibody binding capacity (ABC) for standardization across mass channels with different sensitivities before calculating RO (figure 9). In an *in vitro* drug saturated sample with expected RO of 100% (figure 10, dotted line), we found that the raw RO was significantly overestimated (left) and that QSC bead standardization generated reliable and reproducible RO results (right).

Figure 9. *Adapted and reprinted by permission from Wiley: Cytometry A,*[156] *© 2015*

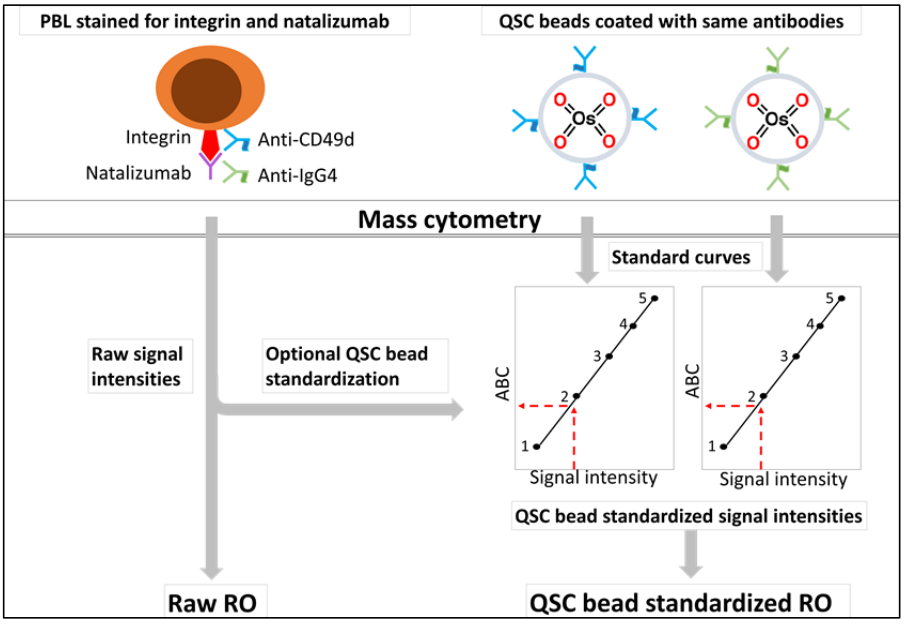

Figure 10. *Reprinted by permission from Wiley: Cytometry A,*[156] *© 2015*

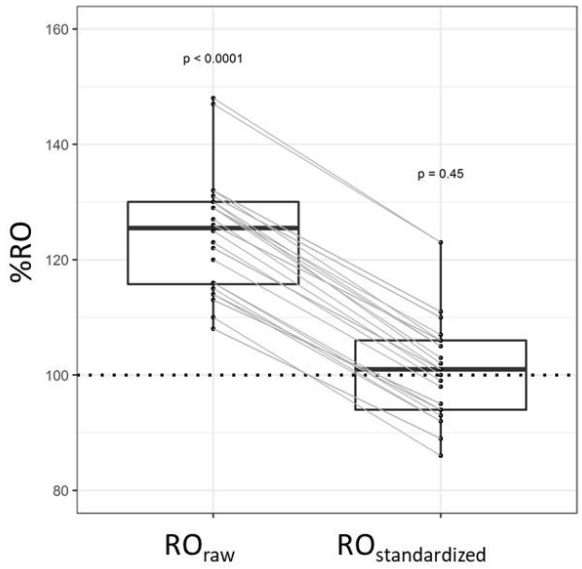

Paper II: Wearing-off at the end of natalizumab dosing intervals is associated with low receptor occupancy

In paper II, we investigated whether wearing-off symptoms at the end of the natalizumab dosing interval were associated with clinical and demographic patient characteristics or natalizumab RO on leukocytes.

In this cross-sectional study of 40 patients with relapsing-remitting MS (RRMS) receiving natalizumab at the Department of Neurology, Haukeland University Hospital, we recorded clinical and demographic data including age, body mass index (BMI), working status, smoking habits, disease characteristics, treatment duration, vitamin D levels, and wearing-off symptoms. We quantified neurofilament light chain in serum and measured natalizumab RO in 11 PBL subtypes by high-parameter mass cytometry. Associations with wearing-off symptoms were analyzed.

We found that eight (20.0%) patients reported regular occurrence of wearing-off symptoms, 9 (22.5%) sometimes had wearing-off symptoms, and 23 (57.5%) did not have wearing-off symptoms. Median RO values (figure 11) were lower in patients

who regularly had wearing-off symptoms (blue line) than in patients who reported having such symptoms sometimes (green line) or never (red line).

Figure 11. *Reprinted by permission from Wolters Kluwer Health, Inc.,*[158] *© 2020*

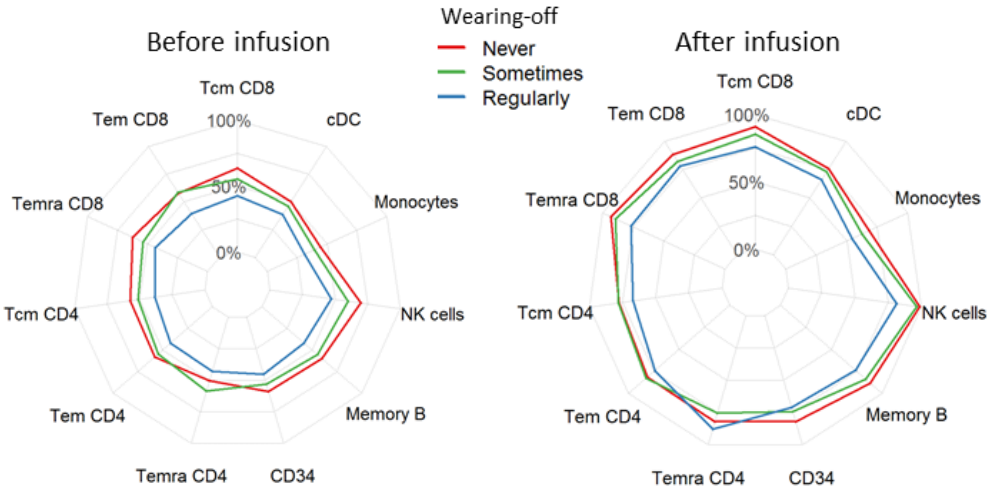

Patients who reported wearing-off symptoms regularly also had higher BMI and higher frequency of sick leave. High BMI was associated with low RO. No other demographic or disease characteristics were associated with the phenomenon. Thus, we concluded that low RO may explain the wearing-off phenomenon observed in some patients with RRMS treated with natalizumab, and that high BMI may contribute to this finding.

Paper III: Wearing-off at the end of natalizumab dosing interval and risk of MS disease activity: a prospective 1-year follow-up study.

In paper III, we evaluated the short-term risk of disease activity in a 1-year prospective follow-up of the same patient cohort (n=40). We found that all patients available for follow-up after one year (n=35) fulfilled the criteria for no evidence of disease activity (NEDA-3). Thus, wearing-off symptoms were not associated with short-term risk of disease activity. However, patients with wearing-off symptoms regularly had more severe fatigue and cognitive dysfunction.

10. Discussion

10.1 Receptor occupancy and QSC beads in mass cytometry

Measuring receptor occupancy (RO) of therapeutic antibodies with high-parameter mass cytometry could open new opportunities to explore therapeutic effects in complex biological systems.[123] However, variations in the mass cytometers detection sensitivity for different metal-conjugated antibodies can lead to misinterpretation of the results. We observed an overestimation of the RO in our assay where drug was detected in a more sensitive channel than receptor (paper I). In an effort to account different detection sensitivity, we adapted antibody-binding QSC beads from flow to mass cytometry to perform signal intensity standardization before RO calculation. Bead standardized results were consistent with the expected RO, demonstrating successful standardization of signal intensity from different metal-conjugated antibodies. This approach can easily be adapted to RO assays of therapeutic antibodies used in other diseases.

To be useful in clinical practice, RO results must be linked to robust clinical data, and standardization with QSC beads could be an important step in implementing mass cytometry RO assays in clinical trials. Standardization methods have been established in flow cytometry to allow comparison of experiments over time and between different instruments and laboratories which is necessary in multicenter and longitudinal trials.[159] Mass cytometry has just only started to address these topics, and much additional mass cytometry standardization remains on the scale needed for large multi-center studies.[139, 140, 145] Established normalization methods with tuning and EQ beads do not correct for sensitivity variations across the detection range which differs across mass cytometers, or for batch-to-batch differences in antibody metal content. It is plausible that QSC beads would correct for such machine- and reagent-based variability in mass like in flow cytometry,[120, 157] but that was not tested in this study. Importantly, QSC beads only offer standardization of the specific signal from metal conjugated antibodies and do not correct for unspecific signal caused by

poor panel design or sample contamination, or for pre-analytical variations in sample handling or antibody staining procedures.

In flow cytometry QSC beads are used for absolute quantitation of epitopes. It is unknown if this is possible in mass cytometry, as it is uncertain whether ion transmission efficiency is completely equal in QSC beads and cells when they pass through the mass cytometer. An RO assay only requires *standardization* of signal intensities and not quantitation of *absolute numbers* of epitopes. However, our collaborators in the adaption of QSC beads for mass cytometry report to obtain values in the range of expected absolute epitope numbers when using QSC beads.[157]

Several different RO assay formats are used in flow cytometry (figure 2).[113, 120] In our RO assay, variations in α4 integrin level required simultaneous measurement of bound drug and total receptor levels. We chose to directly measure bound drug (figure 2B), and total receptor levels (figure 2C) with two different metal-conjugated antibodies, necessitating standardization with QSC beads. This could have been avoided if we had instead chosen an assay where total receptor levels were measured indirectly with the same anti-drug antibody in an *in vitro* drug-saturated sample aliquot. However, staining and acquiring only two sets of QSC beads for the entire experiment instead of an *in vitro* drug-saturated aliquot of every sample cut the acquisition time and cost almost in two and reduced antibody and sample consumption. As QSC beads adapted for mass cytometry are not yet commercially available, antibody labeling needed to be preceded by OsO_4 labeling with multiple time-consuming washing steps with strict safety precautions due to the toxicity of OsO_4. Commercially available metal labeled QSC beads would ease the application.

Although mass cytometry currently outperforms flow cytometry in terms of multiplexing capacity with very little overlap between channels, the technology has some disadvantages.[130] The preferred speed of acquisition in mass cytometry is lower than in flow cytometry (<400 versus several thousand events per second) because the ion clouds are relatively large compared to the original cell and need to be analyzed one at a time to obtain correct analysis of single cell features. Sample transmission

efficiency is lower than in flow cytometry (approximately 50% in the Helios mass cytometer used in this study), which is problematic if sample amount is limited. Also, instrument handling is more technically demanding in mass than in flow cytometry and acquisition costs are considerably higher. These limitations should be considered in light of the study aim. While mass cytometry is superior in explorative studies of unknown terrain and in-depth characterization of complex biological systems, flow cytometry may be a more appropriate tool for measurement of predefined features in one or few cell types in many patients.

In our study, mass cytometry allowed the analysis of multiple cell subtypes where only some showed statistically significant associations between natalizumab RO and wearing-off (paper II). These significant cell types could have been overlooked in a flow cytometry assay with fewer parameters, and we would not have come to the same conclusions.

10.2 Natalizumab receptor occupancy and dosing

Accumulating evidence suggests that therapeutic efficacy is maintained in many patients when natalizumab dosing intervals are extended from 4 to 5-8 weeks.[108-110] An important motivation for individualized natalizumab therapy is the observed reduction of PML risk in extended interval dosing (EID).[112] EID also has socioeconomic benefits by reducing drug and administration costs with up to 50% (if intervals are extended to 8 weeks), and less frequent hospital visits are convenient for both patients and health care providers. Natalizumab is usually discontinued during pregnancy, but using the lowest effective dose is preferable to minimize fetal risk in cases where therapy is continued throughout pregnancy to avoid rebound MS disease activity in the mother.[160, 161] The PML risk reduction in EID is attributed to reduced end-of-interval RO compared to SID, which is thought to allow some immune surveillance of the CNS. Consistent with previous studies,[116, 118] we observed a considerable variability in natalizumab RO although patients received the same standard dose with 4-week intervals. Adequate RO of natalizumab apparently persists well beyond the standard dosing interval of 4 weeks in many patients.[96, 114, 118] Importantly, patients with lower than average natalizumab RO have increased risk of

disease breakthrough already 6-8 weeks after the last dose,[95, 96, 115] and could therefore be at risk of disease breakthrough when RO is reduced in EID schedules. Thus, natalizumab RO has been proposed as a biomarker to guide optimal dosing for individual patients to balance the risks and benefits of the therapy. However, there is no established cut-off-value for a minimal RO to maintain clinical efficacy. As the studies supporting maintained efficacy in EID[108-110] are observational and non-randomized, patients with less aggressive MS are more likely to be moved to EID schedule than patients with an active disease, and there is often even less disease activity in the EID than in SID group in these studies. Inversely, patients selected by clinicians for EID are likely to have more PML risk factors than patient who remain on SID regimens, and the risk reduction in EID may therefore be even more pronounced than observed in the studies.[116] These uncertainties will hopefully be dissolved in the ongoing randomized trial of EID versus SID (ClinicalTrials.gov identifier NCT03689972). It has been hypothesized that certain (unknown) leukocyte cell subsets play a more important role in JC virus surveillance while others contribute to MS disease activity,[116] and identifying the level of unbound integrin needed to allow the right subsets to access the CNS while constraining others would be a major advance for dose optimization. We consider high-parameter mass cytometry superior to flow cytometry as a tool to explore this in future studies of natalizumab RO and PML risk in different dosing schedules.

Natalizumab RO is a direct measure of the main biological effect of natalizumab, the blocking of interaction between α4β1 integrin and VCAM-1, but other biomarkers for therapeutic effect have been suggested. Measuring serum concentration of natalizumab may be easier, but the relationship between serum levels and RO is unpredictable due to influence of numerous known and unknown factors.[118] Return of disease activity is timely more linked to receptor desaturation than decrease of serum levels (which happens earlier), indicating that RO reflects therapeutic efficacy better than serum levels.[109] Natalizumab therapy leads to a rapid and sustained increase of circulating CD34+ hematopoietic stem cells possibly due to increased mobilization from the bone marrow, and the degree of natalizumab-induced mobilization of these cells has been suggested as a therapeutic biomarker because it correlates with

therapeutic efficacy.[81] Natalizumab also leads to increased levels of circulating lymphocytes, and lymphocyte count in peripheral blood has likewise been reported to correlate with therapeutic efficacy and suggested as a biomarker.[80] Natalizumab RO was not evaluated in these two studies.[80, 81] We found that both levels of CD34+ cells and lymphocytes in peripheral blood correlate with natalizumab RO (unpublished data). The degree of hematopoietic stem cell and lymphocyte mobilization may thus be associated with therapeutic efficacy through RO. Body weight has also been suggested as a parameter to navigate dosing.[162] The safety of weight-based dosing was evaluated in a phase II trial with only 6-month follow-up where effectiveness was not assessed,[84] and a fixed dose of 300 mg every 4 weeks is the only dose ever evaluated in phase III trials.[85, 163] Consistent with previous reports,[116, 118] we found that RO generally decreased with high BMI, but we could still observe low RO among patients with low BMI. The inter-individual variability in RO can thus only partly be explained by body weight and BMI, making these parameters imprecise for navigating dose adjustment. Overall, natalizumab RO stands out as the biomarker best suited to guide individualized therapy.

10.3 The wearing-off phenomenon

Subjective wearing-off symptoms at the end of the natalizumab dosing interval are frequently reported, but phenomenon is poorly understood and has been sparsely investigated. We found an association between low RO and regular wearing-off symptoms (paper II). Consistent with the literature, [118] we found that high BMI was associated with low natalizumab RO. As median BMI was higher in the patient group with wearing-off symptoms regularly, we suggested that high BMI, by reducing RO, was the underlying cause of wearing-off symptoms. In a 1-year follow-up of the patients, we found that all patients fulfilled the criteria for NEDA-3 (paper III), although patients with wearing-off symptoms regularly had significantly poorer scores on fatigue (higher FSS) and cognitive function (lower SDMT). Baseline and 1-year NF-L levels in serum were similar between groups, indicating no difference in axonal injury.

The possibility of a biological cause of the wearing-off phenomenon adds a new aspect to the debate on dosing intervals and may have several implications. Firstly, subjective wearing-off symptoms not associated with objective signs of disease activity may not be considered important by the physician or even be registered in the patient journal. Subjective complaints from patients are more likely to be emphasized by health care providers if they are supported by objective signs.[164] Secondly, if patients with wearing-off symptoms have lower than average natalizumab RO, they may have increased risk of therapeutic failure if dosing intervals are extended. Correspondingly, if high RO is a risk factor for PML,[116] patients with wearing-off symptoms could have lower than average PML risk so that EID is less beneficial. The effect of dosing intervals on the severity of wearing-off symptoms is uncertain and cannot be concluded from non-randomized observational studies of SID and EID because patients with such symptoms would be reluctant to extend dosing intervals and would thus be positively selected to the SID group.[101] In order to address these unanswered questions, wearing-off symptoms should be evaluated in prospective studies of randomized natalizumab dosing regimens. Acknowledgement of the phenomenon will hopefully promote the inclusion of wearing-off evaluation in such studies.

Fatigue and cognitive impairment are poorly captured in the NEDA-3 criteria, and poorer scores in patients with regular wearing-off symptoms could represent a suboptimal therapeutic effect. However, similar NF-L levels supports that there was no difference in disease activity between groups. Higher proportion of patients on permanent sick-leave in the group with wearing-off regularly could reflect cognitive impairment, which correlates with employment status.[90]

Pro-inflammatory cytokines are thought to contribute to MS-related fatigue,[165] and fluctuating cytokine levels have been suggested to induce the wearing-off symptoms in previous studies.[100, 101] A hypothetical mechanism is that low natalizumab RO towards the end of the dosing interval could increase the migratory capacity of some cytokine-producing lymphocytes into the CNS and cause wearing-off symptoms, but not enough to allow lesion formation. Not all patients with low RO have wearing-off

symptoms, indicating the involvement of other contributing factors. If the phenomenon reflects reappearance of previously experienced MS symptoms as the natalizumab effect wears off, patients with mild previous symptoms may not experience wearing-off symptoms although RO is low.

Only one previous study, published a few months before ours, has evaluated the relationship between the wearing-off phenomenon and natalizumab RO.[101] In contrast to our results, no association between wearing-off symptoms and natalizumab RO or patient characteristics was found. However, they found non-significant trends similar to our significant results, and differences between their study and ours may have contributed to different results. In their flow cytometry assay, RO was only measured in two cell types, and significant cell types may theoretically have been overlooked. Body weight, which is negatively associated with RO, was higher in our cohort than theirs and the difference was even more pronounced in the group with wearing-off symptoms regularly. Differences in categorization may also have contributed. In their study[101] patients were categorized based on whether they had symptoms currently (32%) or had ever had symptoms (54%), whereas we used the categories sometimes (22.5%) or regularly (20.0%), whereof only the latter was significantly associated with lower RO and high BMI. The study included a larger cohort than ours, but it contained both patients on SID (n=62) and EID (n=31) schedules and the number of patients on SID was only moderately higher than in our study (n=40).

We suggest that high BMI reduces RO and contributes to the wearing-off phenomenon, but we have no proof of causality. Wearing-off symptoms may simply be a psychological effect and other mechanisms could explain the correlations found. High BMI could be a confounding factor independently causing both wearing-off symptoms and low RO. High BMI is not only a risk factor for developing MS, but may also influence the disease severity negatively through various suggested mechanisms such as vascular comorbidity, insulin resistance, and epigenetic modulation of immune cells.[166-169] Such mechanisms could contribute to wearing-off symptoms independently of RO. However, symptom occurrence towards the end of the dosing interval follows the same temporal pattern as RO decline, unlike BMI,

which is relatively constant. Increased fatigue toward the end of the dosing interval may reflect less natalizumab-induced suppression of fatigue[91] when RO declines. Alternatively, fatigue could be a common underlying factor, causing inactivity, high BMI (leading to the observed lower RO[118]), and lower participation in work-life. However, the temporal relationship between RO and the wearing-off symptoms supports our conclusion. We also observed a dose-response tendency with significantly lower median RO in patients with wearing-off symptoms regularly and similar non-significant trends in patients with symptoms sometimes, compared to patients who never had such symptoms (figure 11). Varying classification of wearing-off symptoms across studies may lead to varying results when comparing natalizumab RO between groups.

The small patient cohort limits the interpretation of our results. However, we expect that the limited statistical power only allowed us to detect large effects and that there may be associations of smaller effect size that went unnoticed. We observed no disease activity in our patients, and short prospective follow-up time and a possible selection bias of patients with good therapeutic effect in our patient cohort (as elaborated in the next chapter) may contribute. Further follow-up of our patient cohort may reveal differences in patient outcome.

The main rationale for EID is reduced risk of PML in JC virus-positive patients. But should patients at high risk of PML receive natalizumab therapy? Better knowledge of the established PML risk factors – JCV index, natalizumab therapy duration, and prior use of immunosuppressants – has not lead to a decline in overall incidence of PML, and more caution in giving natalizumab to high-risk patients has been advised.[170] Observational studies show promising PML risk reduction in EID compared to SID. Although the initiative to try off-label dosing schedules to decrease PML risk has partly come from treating neurologists, several of the large studies that encourage continuation of natalizumab therapy in JC virus-positive patients have either been sponsored[109, 116] or funded[112] by Biogen, the manufacturer of natalizumab. The first ongoing randomized prospective trial of SID versus EID (ClinicalTrials.gov identifier NCT03689972) will hopefully improve our understanding of the

effectiveness and safety of EID. Further research is required to confirm whether wearing-off symptoms deteriorate with EID, or if the low RO in this group increases risk of disease breakthrough if intervals are extended. As long as this remains unknown, we recommend maintaining the current practice of switching to other highly effective DMT instead of continuing natalizumab in EID in JC virus positive patients with wearing-off symptoms. EID leads to a more pronounced decrease of RO in high weight patients than in normal weight patients,[116] motivating particular cautiousness with EID in patients with wearing-off symptoms and high BMI.

10.4 Methodological considerations

10.4.1 Patient cohort and study design

The main limitation of our study is the small patient cohort, but all natalizumab treated patients in our department were invited and the inclusion rate was high, reducing the risk of inclusion bias. Some routines at our neurological department may have contributed to differences in our cohort compared to other studies of natalizumab therapy. Firstly, natalizumab treated patients in our department are usually promptly switched to other DMTs if they develop antibodies against JC-virus. Thus, none were JC virus positive at inclusion, while other studies of natalizumab RO often include JC virus positive patients. However, this does not affect any of the outcome measures evaluated in our study. Secondly, less expensive DMTs with comparable efficacy and lower PML risk than natalizumab (primarily rituximab) are increasingly used in our department, and few new patients have started therapy with natalizumab at our department the last years. Thus, patients with side effects or poor therapeutic response to natalizumab may have been negatively selected over time so that the remaining pool of treated patients at the time of inclusion may have had less side effects and better therapeutic response. The same mechanisms could potentially contribute to a slightly lower prevalence of wearing-off symptoms than in other cohorts, although we did not observe that wearing-off symptoms were associated with cessation of therapy. Finally, our early use of highly effective DMTs like natalizumab

could contribute to a patient cohort with less severe disease than cohorts where natalizumab is preserved strictly for second line therapy.

The study design has some limitations. The predictive abilities of a biomarker are best studied prospectively,[23] and the cross sectional design in paper II thus limits the interpretation of the results. The prospective follow-up of 1 year in paper III may be too short to reveal subtle differences in therapeutic efficacy, especially considering that natalizumab is a highly effective DMT with low expected annual relapse rate. We did not collect demographic or clinical data before initiation of natalizumab therapy and can therefore not rule out any pre-treatment differences between patient groups.

10.4.2 Outcome measures

Clinically relevant and well-defined outcomes are necessary to identify biomarkers that reliably reflect these meaningful outcomes.[23] A strength of this study is that we evaluated established outcomes included in NEDA-3 as well as NF-L levels, patient reported outcomes, and neuropsychological measures that are poorly captured in NEDA-3, but are likely to be included in future NEDA definitions.[47]

Clinical and MRI disease activity

Clinical relapses correlate with accumulated disability and disease progression, but more so in the first two years of the diagnosis,[37] and may therefore be less relevant in our population with median disease duration of 13 years. MRI lesion activity is more sensitive and specific to disease activity than clinical relapses and reveals both asymptomatic and symptomatic lesions.[32] At our department, RRMS patients who are stable on DMT without clinical signs of disease activity are annually examined with MRI without gadolinium contrast. Accordingly, the patients in the cohort were only evaluated for new or enlarged T2 lesions and not for contrast-enhancement of lesions. We did not evaluate any other MRI metrics, like brain atrophy, which correlates better with cognitive impairment than lesion burden.[46]

EDSS emphasizes motor impairment and does not capture all aspects of disease progression, and the scale is not sensitive enough to reveal low levels of progression particularly in its lower ranges.[37] EDSS is more robust for measurements over long time periods, and despite high inter-rater variability, EDSS is so commonly used that it allows comparison of results across studies.[171, 172] A change in EDSS score of 1.0 to 1.5 points has been suggested as clinically meaningful.[171] In the context of this study, we consider EDSS suitable to control for confounding group-level differences in disability between the wearing-off groups (paper II), but a poor measure for disability progression over only a year in a cohort with a low median EDSS score of 2 (paper III).

Cognition

SDMT is considered the best psychometric measure available for cognitive status and processing speed in MS due to high reliability, predictive validity, sensitivity, and specificity. The test is not affected by mathematical ability or emotional burden, but some incidental learning of symbol–digit associations may occur.[42, 173] A deterioration of four or more points is considered clinically meaningful.[90]

Fatigue

FSS is widely used to assess fatigue in both clinical practice and research, allowing comparisons across studies, and the test has acceptable reliability, internal consistency, and sensitivity.[174] We did not evaluate depression and anxiety, which can negatively affect the severity of fatigue.

Wearing-off symptoms

Patient reported wearing-off symptoms is a central outcome measure in this study. We divided patients into categories based on symptom frequency, in addition to letting patients write freely which symptoms they had, but we did not assess severity of symptoms. Patient reported outcomes are being increasingly used to help detection and management of hidden RRMS symptoms and to bridge the gap between what matters most to patients and the focus of the physicians and regulatory authorities.[175]

To allow for comparison across studies, patient reported outcomes must be measured in a standardized and validated way. The few published studies of wearing-off symptoms[100, 101] have categorized the symptoms in various ways, which will weaken the comparability of results.

10.4.3 Molecular biomarkers used in the study

Several important challenges complicate the path from bench to bedside for molecular biomarkers in MS.[23] For implementation in clinical practice, MS biomarkers should be process-specific, preferably measurable in blood and clinically useful, and the test should have high analytic validity and be simple. Natalizumab RO is highly process-specific, directly measuring the most central biological effect: blocking of α4 integrin. However, RO analysis is technically demanding, time-consuming and expensive, and the clinical usefulness is not fully determined. We have addressed some of the technical challenges in this work, aiming to improve the analytic validity of the test. NF-L, a neuron-specific biomarker, is elevated in CSF and blood in many other neurological diseases than MS and is not natalizumab-specific. However, the analysis is less technically demanding and quicker than an RO assay. The clinical usefulness of NF-L in detecting disease activity and monitoring therapeutic response in MS has been increasingly documented.[52]

These use of two biomarkers that complement each other is a strength of this study. A drawback of both biomarkers is that there is no established clinically relevant cut-off value and uncertain reproducibility across machines.

10.4.4 Technical considerations

Sample types and receptor occupancy assays

Collection of blood is minimally invasive, and blood is convenient for the study of circulating immune cells and especially suited for the study of natalizumab RO because the therapeutic target is located on circulating cells. We collected samples immediately before and 30 minutes after natalizumab infusion, which allowed for the measurement of minimum and maximum RO levels, based on prior knowledge.[118]

Because RO is known to be stable over time within treated patients,[96] we only measured RO in samples collected at inclusion.

We used PBL fixed in proteomic stabilizer shortly after collection because we observed that early fixation apparently preserved the *in vivo* cell status better than processing of live PBMCs. Firstly, we observed that RO levels were lower in PBMCs that were processed and stored alive than in PBL fixed shortly after collection, and we suspected that processing unfixed cells led to natalizumab detachment. In line with this, van Kempen and colleagues used a correcting factor of 1.4 to obtain more correct RO values on PBMCs because they observed that natalizumab slowly dissociated from the cells during isolation and storage.[101] Secondly, we observed that *in vitro* incubation with natalizumab induced downregulation of α4 integrin in live PBMCs and not in fixed cells. Downregulation of target receptor after incubating live cells with drug is commonly seen in RO assays (less pronounced when incubating on ice than at room temperature),[120] and downregulation of α4 integrin is a well-known effect of natalizumab in treated patients.[122] Nonetheless, this effect is not always accounted for, like in two recently published studies of natalizumab RO.[101, 116] Both studies used live PBMCs in an RO assay format where α4 integrin levels were measured indirectly by anti-IgG4 in sample aliquots that had been incubated with natalizumab at room temperature. If incubation led to receptor downregulation in the sample aliquot used to measure receptor levels, the drug/receptor ratio would seem higher than it was *in vivo*, thus leading to an overestimation of the RO. The reported RO values in these two studies were higher than in our data, and in one of the studies[116] several patients had RO still exceeding 100% at the end of the 4-week dosing interval. We suspect the use of live PBMCs contributed to this.

Using flow versus mass cytometry techniques to measure RO could possibly also affect the results. Flow cytometry-based studies report various mean natalizumab RO values, often more than 75% at the end of 4-week dosing intervals,[96, 101] which is higher than in our study. Notably, the "background" RO in untreated patients is reported to be 10-15% in flow cytometry assays.[96] We have no other mass cytometry RO studies to compare to yet, but we saw very low "background" anti-IgG levels in

untreated healthy donors (supplementary figure 4D, paper I), consistent with considerably lower background signal in mass than in flow cytometry.[126]

Sample collection was performed in a standardized manner because inconsistent duration and temperature of incubation with Proteomic stabilizer across samples in a study may affect the results.[176] PBL samples collected and stored at -80°C at different time points were thawed on the same day so that antibody staining and mass cytometry analysis of PBL was performed on all samples simultaneously.

We titrated the quantitative antibodies to saturating concentrations in the same sample type and with the same cell concentration as used in the main experiment, as recommended.[120] Despite these efforts, patient-to-patient variations in receptor levels may impact the individual optimal saturating antibody concentration and result in some variability in RO.

Data analysis

Data analysis was performed blinded in both the manual and unsupervised analysis approach. Manual analysis is time consuming but allows supervision of the process. Unsupervised analysis is less time consuming but the precision, accuracy, and variability of unsupervised methods varies and none of the algorithms are perfect.[131] We consider the combination of the two approaches a good quality control to confirm the results in our main experiment (paper II).

10.5 Concluding remarks and future perspectives

High-dimensional mass cytometry provides an unprecedented opportunity to capture and understand the complexity and heterogeneity of human disease, and to identify individual molecular signatures that underlie clinical outcomes and therapeutic responses.[177] We developed a novel method for integrating an RO assay in high-dimensional mass cytometry and present the first study employing QSC beads in mass cytometry. The method is easily adaptable to other therapeutic antibodies that are increasingly applied in the treatment of cancer and a broad range of

immunological diseases. Considering the widespread use of QSC beads and RO assays in flow cytometry together with the exponentially increasing number of mass cytometry studies (740 peer-reviewed publications over the last 10 years; Source: Fluidigm), we believe our method to be a highly relevant scientific contribution.[123] Moreover, QSC beads may allow for the standardization across mass cytometers and over time that is already well established in flow cytometry. This is a critical step on the path of implementing mass cytometry in multi-center longitudinal clinical trials that is necessary to link high-dimensional data to relevant clinical outcomes and provide advances in the field of precision medicine.[177]

The utility of natalizumab RO as a biomarker to guide individualized dosing is hampered by the lack of a validated cut-off value for therapeutic efficacy. To establish such a cut-off, natalizumab RO measurement should be standardized and included in clinical trials of different dosing intervals. Such studies must be randomized to avoid selection bias of patients with non-active disease in EID groups. Using mass cytometry to measure RO in such trials would allow measurement of RO in a broad range of cell subtypes simultaneous with other potentially important therapeutic biomarkers.

We observed an association between low natalizumab RO and wearing-off symptoms at the end of the 4-week dosing interval, which is the first indication of a biological cause of the phenomenon. There have been remarkably few studies of this frequent phenomenon, which may be due to a tendency for neurologists to under-recognize subjective symptoms although they may be important to treated patients. We found that all patients, including those with wearing-off symptoms regularly, fulfilled the criteria for NEDA-3. However, cognitive impairment and fatigue were more pronounced in patients with wearing-off symptoms regularly. We hope that the characteristics and clinical significance of the wearing-off phenomenon will be evaluated future randomized studies of natalizumab in different dosing intervals to avoid positive selection of patients with wearing-off in the SID group. In light of our results, we would be cautious with extending the dosing intervals in patients reporting wearing-off symptoms regularly, especially in the overweight and obese.

11. Appendix: Patient form at inclusion

Forskningsprosjekt: Immun-karakterisering av pasienter som mottar sykdomsmodulerende behandling

I forbindelse med prosjektet du deltar i ønsker vi å registrere oppdaterte opplysninger om deg. Disse vil bli lagret anonymisert i forskningsdatabasen og dette skjema vil bli makulert av prosjektansvarlig (Gerd Haga Bringeland). Utfylt skjema leveres i luken på dagposten.

Navn: Dato:

1) Arbeidssituasjon:

□ Fast arbeid, stillingsprosent …….. % yrke ……..

□ korttidssykemeldt, sykemeldingsgrad ……..% yrke ……..

□ langtidssykemeldt/uføretrygdet

□ annet: ……

2) Røykevaner:

□ Aldri-røyker

□ tidligere røyker

□ nåværende av og til

□ nåværende fast

3) Vekt (kg) …… Høyde (cm) ……

4) Noen pasienter opplever økte symptomer på slutten av 4-ukersintervallet mellom Tysabridoser. Gjelder dette deg?

□ Nei

□ Ja, av og til Symptom(er):……

□ Ja, hver gang Symptom(er):……

12. References

1. Reich DS, Lucchinetti CF, Calabresi PA. Multiple Sclerosis. N Engl J Med 2018;378:169-180.
2. Koch-Henriksen N, Sorensen PS. The changing demographic pattern of multiple sclerosis epidemiology. Lancet Neurol 2010;9:520-532.
3. Collaborators GBDMS. Global, regional, and national burden of multiple sclerosis 1990-2016: a systematic analysis for the Global Burden of Disease Study 2016. Lancet Neurol 2019;18:269-285.
4. Browne P, Chandraratna D, Angood C, et al. Atlas of Multiple Sclerosis 2013: A growing global problem with widespread inequity. Neurology 2014;83:1022-1024.
5. Grytten N, Torkildsen O, Myhr KM. Time trends in the incidence and prevalence of multiple sclerosis in Norway during eight decades. Acta Neurol Scand 2015;132:29-36.
6. Charcot J-M. Histologie de la sclerose en plaques. Gaz Hop, Paris1868: 41: 554–555, 557–558, 566.
7. Oksenberg JR, Baranzini SE. Multiple sclerosis genetics--is the glass half full, or half empty? Nat Rev Neurol 2010;6:429-437.
8. Dendrou CA, Fugger L, Friese MA. Immunopathology of multiple sclerosis. Nat Rev Immunol 2015;15:545-558.
9. Ascherio A, Munger KL. Epidemiology of Multiple Sclerosis: From Risk Factors to Prevention-An Update. Semin Neurol 2016;36:103-114.
10. Olsson T, Barcellos LF, Alfredsson L. Interactions between genetic, lifestyle and environmental risk factors for multiple sclerosis. Nat Rev Neurol 2017;13:25-36.
11. International Multiple Sclerosis Genetics C, Wellcome Trust Case Control C, Sawcer S, et al. Genetic risk and a primary role for cell-mediated immune mechanisms in multiple sclerosis. Nature 2011;476:214-219.
12. Belbasis L, Bellou V, Evangelou E, Ioannidis JP, Tzoulaki I. Environmental risk factors and multiple sclerosis: an umbrella review of systematic reviews and meta-analyses. Lancet Neurol 2015;14:263-273.
13. Ffrench-Constant C. Pathogenesis of multiple sclerosis. Lancet 1994;343:271-275.
14. Trapp BD, Nave KA. Multiple sclerosis: an immune or neurodegenerative disorder? Annu Rev Neurosci 2008;31:247-269.
15. Stys PK, Zamponi GW, van Minnen J, Geurts JJ. Will the real multiple sclerosis please stand up? Nat Rev Neurosci 2012;13:507-514.
16. Grigoriadis N, van Pesch V, Paradig MSG. A basic overview of multiple sclerosis immunopathology. Eur J Neurol 2015;22 Suppl 2:3-13.
17. Abbas AKL, A. H.; Pillai S. Cellular and Molecular Immunology, 7th ed: Elsevier Inc., 2012.
18. Sallusto F, Geginat J, Lanzavecchia A. Central memory and effector memory T cell subsets: function, generation, and maintenance. Annu Rev Immunol 2004;22:745-763.
19. Mahnke YD, Brodie TM, Sallusto F, Roederer M, Lugli E. The who's who of T-cell differentiation: human memory T-cell subsets. Eur J Immunol 2013;43:2797-2809.

20. Bar-Or A, Fawaz L, Fan B, et al. Abnormal B-cell cytokine responses a trigger of T-cell-mediated disease in MS? Ann Neurol 2010;67:452-461.
21. Thompson AJ, Banwell BL, Barkhof F, et al. Diagnosis of multiple sclerosis: 2017 revisions of the McDonald criteria. Lancet Neurol 2018;17:162-173.
22. Brownlee WJ, Hardy TA, Fazekas F, Miller DH. Diagnosis of multiple sclerosis: progress and challenges. Lancet 2017;389:1336-1346.
23. Comabella M, Montalban X. Body fluid biomarkers in multiple sclerosis. Lancet Neurol 2014;13:113-126.
24. De Angelis F, John NA, Brownlee WJ. Disease-modifying therapies for multiple sclerosis. BMJ 2018;363:k4674.
25. Klotz L, Havla J, Schwab N, et al. Risks and risk management in modern multiple sclerosis immunotherapeutic treatment. Ther Adv Neurol Disord 2019;12:1756286419836571.
26. Rae-Grant A, Day GS, Marrie RA, et al. Practice guideline recommendations summary: Disease-modifying therapies for adults with multiple sclerosis: Report of the Guideline Development, Dissemination, and Implementation Subcommittee of the American Academy of Neurology. Neurology 2018;90:777-788.
27. Ontaneda D, Tallantyre E, Kalincik T, Planchon SM, Evangelou N. Early highly effective versus escalation treatment approaches in relapsing multiple sclerosis. Lancet Neurol 2019;18:973-980.
28. Montalban X, Hauser SL, Kappos L, et al. Ocrelizumab versus Placebo in Primary Progressive Multiple Sclerosis. N Engl J Med 2017;376:209-220.
29. Muraro PA, Martin R, Mancardi GL, Nicholas R, Sormani MP, Saccardi R. Autologous haematopoietic stem cell transplantation for treatment of multiple sclerosis. Nat Rev Neurol 2017;13:391-405.
30. Burt RK, Balabanov R, Burman J, et al. Effect of Nonmyeloablative Hematopoietic Stem Cell Transplantation vs Continued Disease-Modifying Therapy on Disease Progression in Patients With Relapsing-Remitting Multiple Sclerosis: A Randomized Clinical Trial. JAMA 2019;321:165-174.
31. Milligan NM, Newcombe R, Compston DA. A double-blind controlled trial of high dose methylprednisolone in patients with multiple sclerosis: 1. Clinical effects. J Neurol Neurosurg Psychiatry 1987;50:511-516.
32. Barkhof F, Scheltens P, Frequin ST, et al. Relapsing-remitting multiple sclerosis: sequential enhanced MR imaging vs clinical findings in determining disease activity. AJR Am J Roentgenol 1992;159:1041-1047.
33. Kurtzke JF. Rating neurologic impairment in multiple sclerosis: an expanded disability status scale (EDSS). Neurology 1983;33:1444-1452.
34. Giovannoni G, Bermel R, Phillips T, Rudick R. A brief history of NEDA. Mult Scler Relat Disord 2018;20:228-230.
35. Lu G, Beadnall HN, Barton J, Hardy TA, Wang C, Barnett MH. The evolution of "No Evidence of Disease Activity" in multiple sclerosis. Mult Scler Relat Disord 2018;20:231-238.
36. Kappos L, De Stefano N, Freedman MS, et al. Inclusion of brain volume loss in a revised measure of 'no evidence of disease activity' (NEDA-4) in relapsing-remitting multiple sclerosis. Mult Scler 2016;22:1297-1305.

37. Stangel M, Penner IK, Kallmann BA, Lukas C, Kieseier BC. Towards the implementation of 'no evidence of disease activity' in multiple sclerosis treatment: the multiple sclerosis decision model. Ther Adv Neurol Disord 2015;8:3-13.
38. Smith MM, Arnett PA. Factors related to employment status changes in individuals with multiple sclerosis. Mult Scler 2005;11:602-609.
39. Glanz BI, Degano IR, Rintell DJ, Chitnis T, Weiner HL, Healy BC. Work productivity in relapsing multiple sclerosis: associations with disability, depression, fatigue, anxiety, cognition, and health-related quality of life. Value Health 2012;15:1029-1035.
40. Flensner G, Landtblom AM, Soderhamn O, Ek AC. Work capacity and health-related quality of life among individuals with multiple sclerosis reduced by fatigue: a cross-sectional study. BMC Public Health 2013;13:224.
41. Janardhan V, Bakshi R. Quality of life in patients with multiple sclerosis: the impact of fatigue and depression. J Neurol Sci 2002;205:51-58.
42. Oreja-Guevara C, Ayuso Blanco T, Brieva Ruiz L, Hernandez Perez MA, Meca-Lallana V, Ramio-Torrenta L. Cognitive Dysfunctions and Assessments in Multiple Sclerosis. Front Neurol 2019;10:581.
43. Cortese M, Riise T, Bjornevik K, et al. Preclinical disease activity in multiple sclerosis: A prospective study of cognitive performance prior to first symptom. Ann Neurol 2016;80:616-624.
44. Skorve E, Lundervold AJ, Torkildsen O, Myhr KM. The Norwegian translation of the brief international cognitive assessment for multiple sclerosis (BICAMS). Mult Scler Relat Disord 2019;36:101408.
45. Damasceno A, Damasceno BP, Cendes F. No evidence of disease activity in multiple sclerosis: Implications on cognition and brain atrophy. Mult Scler 2016;22:64-72.
46. Benedict RH, Weinstock-Guttman B, Fishman I, Sharma J, Tjoa CW, Bakshi R. Prediction of neuropsychological impairment in multiple sclerosis: comparison of conventional magnetic resonance imaging measures of atrophy and lesion burden. Arch Neurol 2004;61:226-230.
47. Giovannoni G, Turner B, Gnanapavan S, Offiah C, Schmierer K, Marta M. Is it time to target no evident disease activity (NEDA) in multiple sclerosis? Mult Scler Relat Disord 2015;4:329-333.
48. Giovannoni G, Tomic D, Bright JR, Havrdova E. "No evident disease activity": The use of combined assessments in the management of patients with multiple sclerosis. Mult Scler 2017;23:1179-1187.
49. Comabella M, Sastre-Garriga J, Montalban X. Precision medicine in multiple sclerosis: biomarkers for diagnosis, prognosis, and treatment response. Curr Opin Neurol 2016;29:254-262.
50. Biomarkers Definitions Working G. Biomarkers and surrogate endpoints: preferred definitions and conceptual framework. Clin Pharmacol Ther 2001;69:89-95.
51. Sormani MP, Bruzzi P. MRI lesions as a surrogate for relapses in multiple sclerosis: a meta-analysis of randomised trials. Lancet Neurol 2013;12:669-676.
52. Varhaug KN, Torkildsen O, Myhr KM, Vedeler CA. Neurofilament Light Chain as a Biomarker in Multiple Sclerosis. Front Neurol 2019;10.

53. Lycke JN, Karlsson JE, Andersen O, Rosengren LE. Neurofilament protein in cerebrospinal fluid: a potential marker of activity in multiple sclerosis. J Neurol Neurosurg Psychiatry 1998;64:402-404.
54. Kuhle J, Plattner K, Bestwick JP, et al. A comparative study of CSF neurofilament light and heavy chain protein in MS. Mult Scler 2013;19:1597-1603.
55. Piehl F, Kockum I, Khademi M, et al. Plasma neurofilament light chain levels in patients with MS switching from injectable therapies to fingolimod. Mult Scler 2018;24:1046-1054.
56. Novakova L, Zetterberg H, Sundstrom P, et al. Monitoring disease activity in multiple sclerosis using serum neurofilament light protein. Neurology 2017;89:2230-2237.
57. Rissin DM, Kan CW, Campbell TG, et al. Single-molecule enzyme-linked immunosorbent assay detects serum proteins at subfemtomolar concentrations. Nat Biotechnol 2010;28:595-599.
58. Cai L, Huang J. Neurofilament light chain as a biological marker for multiple sclerosis: a meta-analysis study. Neuropsychiatr Dis Treat 2018;14:2241-2254.
59. Disanto G, Barro C, Benkert P, et al. Serum Neurofilament light: A biomarker of neuronal damage in multiple sclerosis. Ann Neurol 2017;81:857-870.
60. Varhaug KN, Barro C, Bjornevik K, et al. Neurofilament light chain predicts disease activity in relapsing-remitting MS. Neurol Neuroimmunol Neuroinflamm 2018;5:e422.
61. de Flon P, Gunnarsson M, Laurell K, et al. Reduced inflammation in relapsing-remitting multiple sclerosis after therapy switch to rituximab. Neurology 2016;87:141-147.
62. Gunnarsson M, Malmestrom C, Axelsson M, et al. Axonal damage in relapsing multiple sclerosis is markedly reduced by natalizumab. Ann Neurol 2011;69:83-89.
63. Meeter LH, Dopper EG, Jiskoot LC, et al. Neurofilament light chain: a biomarker for genetic frontotemporal dementia. Ann Clin Transl Neurol 2016;3:623-636.
64. Rosengren LE, Karlsson JE, Karlsson JO, Persson LI, Wikkelso C. Patients with amyotrophic lateral sclerosis and other neurodegenerative diseases have increased levels of neurofilament protein in CSF. J Neurochem 1996;67:2013-2018.
65. Thompson AGB, Luk C, Heslegrave AJ, et al. Neurofilament light chain and tau concentrations are markedly increased in the serum of patients with sporadic Creutzfeldt-Jakob disease, and tau correlates with rate of disease progression. J Neurol Neurosurg Psychiatry 2018;89:955-961.
66. Tiedt S, Duering M, Barro C, et al. Serum neurofilament light: A biomarker of neuroaxonal injury after ischemic stroke. Neurology 2018;91:e1338-e1347.
67. Fog M, de Fine Olivarius B. Lærebog i medicinsk neurologi: Gyldendal, 1974.
68. University of California SFMSET, Cree BA, Gourraud PA, et al. Long-term evolution of multiple sclerosis disability in the treatment era. Ann Neurol 2016;80:499-510.
69. Koch-Henriksen N, Laursen B, Stenager E, Magyari M. Excess mortality among patients with multiple sclerosis in Denmark has dropped significantly over the

past six decades: a population based study. J Neurol Neurosurg Psychiatry 2017;88:626-631.
70. Lunde HMB, Assmus J, Myhr KM, Bo L, Grytten N. Survival and cause of death in multiple sclerosis: a 60-year longitudinal population study. J Neurol Neurosurg Psychiatry 2017;88:621-625.
71. Biogen. Tysabri® (Natalizumab) Prescribing Information [online]. Available at: https://medinfo.biogen.com/secure.
72. Rudick RA, Sandrock A. Natalizumab: alpha 4-integrin antagonist selective adhesion molecule inhibitors for MS. Expert Rev Neurother 2004;4:571-580.
73. Elices MJ, Osborn L, Takada Y, et al. VCAM-1 on activated endothelium interacts with the leukocyte integrin VLA-4 at a site distinct from the VLA-4/fibronectin binding site. Cell 1990;60:577-584.
74. Yednock TA, Cannon C, Fritz LC, Sanchez-Madrid F, Steinman L, Karin N. Prevention of experimental autoimmune encephalomyelitis by antibodies against alpha 4 beta 1 integrin. Nature 1992;356:63-66.
75. Steinman L. The discovery of natalizumab, a potent therapeutic for multiple sclerosis. J Cell Biol 2012;199:413-416.
76. Krumbholz M, Meinl I, Kumpfel T, Hohlfeld R, Meinl E. Natalizumab disproportionately increases circulating pre-B and B cells in multiple sclerosis. Neurology 2008;71:1350-1354.
77. Traub JW, Pellkofer HL, Grondey K, et al. Natalizumab promotes activation and pro-inflammatory differentiation of peripheral B cells in multiple sclerosis patients. J Neuroinflammation 2019;16:228.
78. Alter A, Duddy M, Hebert S, et al. Determinants of human B cell migration across brain endothelial cells. J Immunol 2003;170:4497-4505.
79. Lehmann-Horn K, Sagan SA, Bernard CC, Sobel RA, Zamvil SS. B-cell very late antigen-4 deficiency reduces leukocyte recruitment and susceptibility to central nervous system autoimmunity. Ann Neurol 2015;77:902-908.
80. Signoriello E, Lanzillo R, Brescia Morra V, et al. Lymphocytosis as a response biomarker of natalizumab therapeutic efficacy in multiple sclerosis. Mult Scler 2016;22:921-925.
81. Mattoscio M, Nicholas R, Sormani MP, et al. Hematopoietic mobilization: Potential biomarker of response to natalizumab in multiple sclerosis. Neurology 2015;84:1473-1482.
82. Niino M, Bodner C, Simard ML, et al. Natalizumab effects on immune cell responses in multiple sclerosis. Ann Neurol 2006;59:748-754.
83. Stuve O, Marra CM, Jerome KR, et al. Immune surveillance in multiple sclerosis patients treated with natalizumab. Ann Neurol 2006;59:743-747.
84. Miller DH, Khan OA, Sheremata WA, et al. A controlled trial of natalizumab for relapsing multiple sclerosis. N Engl J Med 2003;348:15-23.
85. Polman CH, O'Connor PW, Havrdova E, et al. A randomized, placebo-controlled trial of natalizumab for relapsing multiple sclerosis. N Engl J Med 2006;354:899-910.
86. Butzkueven H, Kappos L, Pellegrini F, et al. Efficacy and safety of natalizumab in multiple sclerosis: interim observational programme results. J Neurol Neurosurg Psychiatry 2014;85:1190-1197.

87. Prosperini L, Sacca F, Cordioli C, et al. Real-world effectiveness of natalizumab and fingolimod compared with self-injectable drugs in non-responders and in treatment-naive patients with multiple sclerosis. J Neurol 2017;264:284-294.
88. Tramacere I, Del Giovane C, Salanti G, D'Amico R, Filippini G. Immunomodulators and immunosuppressants for relapsing-remitting multiple sclerosis: a network meta-analysis. Cochrane Database Syst Rev 2015:CD011381.
89. Review IIfCaE. Disease-Modifying Therapies for Relapsing-Remitting and Primary-Progressive Multiple Sclerosis: Effectiveness and Value. Final evidence report. [online]. Available at: https://icer-review.org/wp-content/uploads/2016/08/CTAF_MS_Final_Report_030617.pdf.
90. Morrow SA, O'Connor PW, Polman CH, et al. Evaluation of the symbol digit modalities test (SDMT) and MS neuropsychological screening questionnaire (MSNQ) in natalizumab-treated MS patients over 48 weeks. Mult Scler 2010;16:1385-1392.
91. Iaffaldano P, Viterbo RG, Paolicelli D, et al. Impact of natalizumab on cognitive performances and fatigue in relapsing multiple sclerosis: a prospective, open-label, two years observational study. PLoS One 2012;7:e35843.
92. Kunkel A, Fischer M, Faiss J, Dahne D, Kohler W, Faiss JH. Impact of natalizumab treatment on fatigue, mood, and aspects of cognition in relapsing-remitting multiple sclerosis. Front Neurol 2015;6:97.
93. Svenningsson A, Falk E, Celius EG, et al. Natalizumab treatment reduces fatigue in multiple sclerosis. Results from the TYNERGY trial; a study in the real life setting. PLoS One 2013;8:e58643.
94. Foley JF, Nair KV, Vollmer T, et al. Long-term natalizumab treatment is associated with sustained improvements in quality of life in patients with multiple sclerosis. Patient Prefer Adherence 2017;11:1035-1048.
95. Derfuss T, Kovarik JM, Kappos L, et al. alpha4-integrin receptor desaturation and disease activity return after natalizumab cessation. Neurol Neuroimmunol Neuroinflamm 2017;4:e388.
96. Plavina T, Muralidharan KK, Kuesters G, et al. Reversibility of the effects of natalizumab on peripheral immune cell dynamics in MS patients. Neurology 2017;89:1584-1593.
97. Calabresi PA, Giovannoni G, Confavreux C, et al. The incidence and significance of anti-natalizumab antibodies: results from AFFIRM and SENTINEL. Neurology 2007;69:1391-1403.
98. Gudesblatt M, Zarif M, Bumstead B, et al. Multiple sclerosis and natalizumab: "between the dose symptoms" [abstract 982]. Mult Scler 2012:18(suppl 14):P982.
99. Katz J, Lathi E, Heyda L. Characterizing the Natalizumab "Wearing Off" Effect [abstract]. ACTRIMS meeting; Poster DX36 2014.
100. Ratchford JN, Brock-Simmons R, Augsburger A, et al. Multiple sclerosis symptom recrudescence at the end of the natalizumab dosing cycle. Int J MS Care 2014;16:92-98.
101. van Kempen ZLE, Doesburg D, Dekker I, et al. The natalizumab wearing-off effect: End of natalizumab cycle; recurrence of MS symptoms. Neurology 2019.

102. Clerico M, Artusi CA, Di Liberto A, et al. Long-term safety evaluation of natalizumab for the treatment of multiple sclerosis. Expert Opin Drug Saf 2017;16:963-972.
103. Hirsch HH, Kardas P, Kranz D, Leboeuf C. The human JC polyomavirus (JCPyV): virological background and clinical implications. APMIS 2013;121:685-727.
104. Alstadhaug KB, Myhr KM, Rinaldo CH. Progressive multifocal leukoencephalopathy. Tidsskr Nor Laegeforen 2017;137.
105. Bloomgren G, Richman S, Hotermans C, et al. Risk of natalizumab-associated progressive multifocal leukoencephalopathy. N Engl J Med 2012;366:1870-1880.
106. Ho PR, Koendgen H, Campbell N, Haddock B, Richman S, Chang I. Risk of natalizumab-associated progressive multifocal leukoencephalopathy in patients with multiple sclerosis: a retrospective analysis of data from four clinical studies. Lancet Neurol 2017;16:925-933.
107. Major EO, Yousry TA, Clifford DB. Pathogenesis of progressive multifocal leukoencephalopathy and risks associated with treatments for multiple sclerosis: a decade of lessons learned. Lancet Neurol 2018;17:467-480.
108. Bomprezzi R, Pawate S. Extended interval dosing of natalizumab: a two-center, 7-year experience. Ther Adv Neurol Disord 2014;7:227-231.
109. Zhovtis Ryerson L, Frohman TC, Foley J, et al. Extended interval dosing of natalizumab in multiple sclerosis. J Neurol Neurosurg Psychiatry 2016;87:885-889.
110. Yamout BI, Sahraian MA, Ayoubi NE, et al. Efficacy and safety of natalizumab extended interval dosing. Mult Scler Relat Disord 2018;24:113-116.
111. Clerico M, De Mercanti SF, Signori A, et al. Extending the Interval of Natalizumab Dosing: Is Efficacy Preserved? Neurotherapeutics 2020;17:200-207.
112. Ryerson LZ, Foley J, Chang I, et al. Risk of natalizumab-associated PML in patients with MS is reduced with extended interval dosing. Neurology 2019;93:e1452-e1462.
113. Liang M, Schwickart M, Schneider AK, et al. Receptor occupancy assessment by flow cytometry as a pharmacodynamic biomarker in biopharmaceutical development. Cytometry B Clin Cytom 2016;90:117-127.
114. Fox RJ, Cree BA, De Seze J, et al. MS disease activity in RESTORE: a randomized 24-week natalizumab treatment interruption study. Neurology 2014;82:1491-1498.
115. Wipfler P, Harrer A, Pilz G, et al. Natalizumab saturation: biomarker for individual treatment holiday after natalizumab withdrawal? Acta Neurol Scand 2014;129:e12-15.
116. Foley JF, Goelz S, Hoyt T, Christensen A, Metzger RR. Evaluation of natalizumab pharmacokinetics and pharmacodynamics with standard and extended interval dosing. Mult Scler Relat Disord 2019;31:65-71.
117. Punet-Ortiz J, Hervas-Garcia JV, Teniente-Serra A, et al. Monitoring CD49d receptor occupancy: A method to optimize and personalize natalizumab therapy in multiple sclerosis patients. Cytometry B Clin Cytom 2017.
118. Muralidharan KK, Kuesters G, Plavina T, et al. Population Pharmacokinetics and Target Engagement of Natalizumab in Patients With Multiple Sclerosis. J Clin Pharmacol 2017;57:1017-1030.

119. Sheremata WA, Vollmer TL, Stone LA, Willmer-Hulme AJ, Koller M. A safety and pharmacokinetic study of intravenous natalizumab in patients with MS. Neurology 1999;52:1072-1074.
120. Green CL, Stewart JJ, Hogerkorp CM, et al. Recommendations for the development and validation of flow cytometry-based receptor occupancy assays. Cytometry B Clin Cytom 2016;90:141-149.
121. Suntharalingam G, Perry MR, Ward S, et al. Cytokine storm in a phase 1 trial of the anti-CD28 monoclonal antibody TGN1412. N Engl J Med 2006;355:1018-1028.
122. Defer G, Mariotte D, Derache N, et al. CD49d expression as a promising biomarker to monitor natalizumab efficacy. J Neurol Sci 2012;314:138-142.
123. Huse K. Expanding the Clinical Cytometry Toolbox-Receptor Occupancy by Mass Cytometry. Cytometry A 2019;95:1046-1048.
124. Perfetto SP, Chattopadhyay PK, Roederer M. Seventeen-colour flow cytometry: unravelling the immune system. Nat Rev Immunol 2004;4:648-655.
125. Bandura DR, Baranov VI, Ornatsky OI, et al. Mass cytometry: technique for real time single cell multitarget immunoassay based on inductively coupled plasma time-of-flight mass spectrometry. Anal Chem 2009;81:6813-6822.
126. Ornatsky O, Bandura D, Baranov V, Nitz M, Winnik MA, Tanner S. Highly multiparametric analysis by mass cytometry. Journal of immunological methods 2010;361:1-20.
127. Bendall SC, Nolan GP, Roederer M, Chattopadhyay PK. A deep profiler's guide to cytometry. Trends Immunol 2012;33:323-332.
128. Lou X, Zhang G, Herrera I, et al. Polymer-based elemental tags for sensitive bioassays. Angew Chem Int Ed Engl 2007;46:6111-6114.
129. Spidlen J, Moore W, Parks D, et al. Data File Standard for Flow Cytometry, version FCS 3.1. Cytometry A 2010;77:97-100.
130. Brodie TM, Tosevski V. High-Dimensional Single-Cell Analysis with Mass Cytometry. Current protocols in immunology 2017;118:5 11 11-15 11 25.
131. Liu X, Song W, Wong BY, et al. A comparison framework and guideline of clustering methods for mass cytometry data. Genome Biol 2019;20:297.
132. Newell EW, Cheng Y. Mass cytometry: blessed with the curse of dimensionality. Nat Immunol 2016;17:890-895.
133. Kimball AK, Oko LM, Bullock BL, Nemenoff RA, van Dyk LF, Clambey ET. A Beginner's Guide to Analyzing and Visualizing Mass Cytometry Data. J Immunol 2018;200:3-22.
134. Amir el AD, Davis KL, Tadmor MD, et al. viSNE enables visualization of high dimensional single-cell data and reveals phenotypic heterogeneity of leukemia. Nat Biotechnol 2013;31:545-552.
135. Bruggner RV, Bodenmiller B, Dill DL, Tibshirani RJ, Nolan GP. Automated identification of stratifying signatures in cellular subpopulations. Proc Natl Acad Sci U S A 2014;111:E2770-2777.
136. Montgomery RR. High standards for high dimensional investigations. Cytometry A 2016;89:886-888.
137. Takahashi C, Au-Yeung A, Fuh F, et al. Mass cytometry panel optimization through the designed distribution of signal interference. Cytometry A 2017;91:39-47.

138. Gullaksen SE, Bader L, Hellesoy M, et al. Titrating Complex Mass Cytometry Panels. Cytometry A 2019;95:792-796.
139. Leipold MD. Another step on the path to mass cytometry standardization. Cytometry A 2015;87:380-382.
140. Tricot S, Meyrand M, Sammicheli C, et al. Evaluating the efficiency of isotope transmission for improved panel design and a comparison of the detection sensitivities of mass cytometer instruments. Cytometry A 2015;87:357-368.
141. Mizrahi O, Ish Shalom E, Baniyash M, Klieger Y. Quantitative flow cytometry: Concerns and recommendations in clinic and research. Cytometry B Clin Cytom 2017.
142. Zunder ER, Finck R, Behbehani GK, et al. Palladium-based mass tag cell barcoding with a doublet-filtering scheme and single-cell deconvolution algorithm. Nat Protoc 2015;10:316-333.
143. Finck R, Simonds EF, Jager A, et al. Normalization of mass cytometry data with bead standards. Cytometry A 2013;83:483-494.
144. Finak G, Langweiler M, Jaimes M, et al. Standardizing Flow Cytometry Immunophenotyping Analysis from the Human ImmunoPhenotyping Consortium. Sci Rep 2016;6:20686.
145. Leipold MD, Obermoser G, Fenwick C, et al. Comparison of CyTOF assays across sites: Results of a six-center pilot study. Journal of immunological methods 2018;453:37-43.
146. Polman CH, Reingold SC, Banwell B, et al. Diagnostic criteria for multiple sclerosis: 2010 revisions to the McDonald criteria. Ann Neurol 2011;69:292-302.
147. Smith A. The Symbol Digit Modalities Test (SDMT) Symbol Digit Modalities Test: Manual. Western Psychological Services 1982.
148. Krupp LB, LaRocca NG, Muir-Nash J, Steinberg AD. The fatigue severity scale. Application to patients with multiple sclerosis and systemic lupus erythematosus. Arch Neurol 1989;46:1121-1123.
149. Keshavan A, Heslegrave A, Zetterberg H, Schott JM. Stability of blood-based biomarkers of Alzheimer's disease over multiple freeze-thaw cycles. Alzheimers Dement (Amst) 2018;10:448-451.
150. Chanvillard C, Jacolik RF, Infante-Duarte C, Nayak RC. The role of natural killer cells in multiple sclerosis and their therapeutic implications. Front Immunol 2013;4:63.
151. Mishra MK, Yong VW. Myeloid cells - targets of medication in multiple sclerosis. Nat Rev Neurol 2016;12:539-551.
152. Rumble JM, Huber AK, Krishnamoorthy G, et al. Neutrophil-related factors as biomarkers in EAE and MS. J Exp Med 2015;212:23-35.
153. Kleinsteuber K, Corleis B, Rashidi N, et al. Standardization and quality control for high-dimensional mass cytometry studies of human samples. Cytometry A 2016;89:903-913.
154. Zenger VE, Vogt R, Mandy F, Schwartz A, Marti GE. Quantitative flow cytometry: inter-laboratory variation. Cytometry 1998;33:138-145.
155. Bangs Laboratories I. Quantum™ Simply Cellular®, Product data sheet [online]. Available at: https://www.bangslabs.com/sites/default/files/imce/docs/PDS%20814%20Web.pdf.

156. Bringeland GH, Bader L, Blaser N, et al. Optimization of Receptor Occupancy Assays in Mass Cytometry: Standardization Across Channels with QSC Beads. Cytometry A 2019;95:314-322.
157. Budzinski L, Schulz AR, Baumgart S, et al. Osmium-Labeled Microspheres for Bead-Based Assays in Mass Cytometry. J Immunol 2019;202:3103-3112.
158. Bringeland GH, Blaser N, Myhr KM, Vedeler CA, Gavasso S. Wearing-off at the end of natalizumab dosing intervals is associated with low receptor occupancy. Neurol Neuroimmunol Neuroinflamm 2020;7.
159. Mittag A, Tarnok A. Basics of standardization and calibration in cytometry--a review. J Biophotonics 2009;2:470-481.
160. Portaccio E, Annovazzi P, Ghezzi A, et al. Pregnancy decision-making in women with multiple sclerosis treated with natalizumab: I: Fetal risks. Neurology 2018;90:e823-e831.
161. Portaccio E, Moiola L, Martinelli V, et al. Pregnancy decision-making in women with multiple sclerosis treated with natalizumab: II: Maternal risks. Neurology 2018;90:e832-e839.
162. Tanaka M, Kinoshita M, Foley JF, Tanaka K, Kira J, Carroll WM. Body weight-based natalizumab treatment in adult patients with multiple sclerosis. J Neurol 2015;262:781-782.
163. Rudick RA, Stuart WH, Calabresi PA, et al. Natalizumab plus interferon beta-1a for relapsing multiple sclerosis. N Engl J Med 2006;354:911-923.
164. Tintore M, Alexander M, Costello K, et al. The state of multiple sclerosis: current insight into the patient/health care provider relationship, treatment challenges, and satisfaction. Patient Prefer Adherence 2017;11:33-45.
165. Heesen C, Nawrath L, Reich C, Bauer N, Schulz KH, Gold SM. Fatigue in multiple sclerosis: an example of cytokine mediated sickness behaviour? J Neurol Neurosurg Psychiatry 2006;77:34-39.
166. Castro K, Ntranos A, Amatruda M, et al. Body Mass Index in Multiple Sclerosis modulates ceramide-induced DNA methylation and disease course. EBioMedicine 2019;43:392-410.
167. Mowry EM, Azevedo CJ, McCulloch CE, et al. Body mass index, but not vitamin D status, is associated with brain volume change in MS. Neurology 2018;91:e2256-e2264.
168. Oliveira SR, Simao AN, Kallaur AP, et al. Disability in patients with multiple sclerosis: influence of insulin resistance, adiposity, and oxidative stress. Nutrition 2014;30:268-273.
169. Tettey P, Simpson S, Jr., Taylor BV, van der Mei IA. Vascular comorbidities in the onset and progression of multiple sclerosis. J Neurol Sci 2014;347:23-33.
170. Derfuss T, Kappos L. PML risk and natalizumab: the elephant in the room. Lancet Neurol 2017;16:864-865.
171. Meyer-Moock S, Feng YS, Maeurer M, Dippel FW, Kohlmann T. Systematic literature review and validity evaluation of the Expanded Disability Status Scale (EDSS) and the Multiple Sclerosis Functional Composite (MSFC) in patients with multiple sclerosis. BMC Neurol 2014;14:58.

172. Amato MP, Fratiglioni L, Groppi C, Siracusa G, Amaducci L. Interrater reliability in assessing functional systems and disability on the Kurtzke scale in multiple sclerosis. Arch Neurol 1988;45:746-748.
173. Benedict RH, DeLuca J, Phillips G, et al. Validity of the Symbol Digit Modalities Test as a cognition performance outcome measure for multiple sclerosis. Mult Scler 2017;23:721-733.
174. Flachenecker P, Kumpfel T, Kallmann B, et al. Fatigue in multiple sclerosis: a comparison of different rating scales and correlation to clinical parameters. Mult Scler 2002;8:523-526.
175. Medina LD, Torres S, Alvarez E, Valdez B, Nair KV. Patient-reported outcomes in multiple sclerosis: Validation of the Quality of Life in Neurological Disorders (Neuro-QoL) short forms. Mult Scler J Exp Transl Clin 2019;5:2055217319885986.
176. Inc. ST. Protocol for using Smart Tube Proteomic Stabilizer to Bank Whole Blood Samples [online]. Available at: https://www.smarttubeinc.com/protocols/prot1/ST_BANK_STP1TF-120101B.pdf.
177. Baca Q, Cosma A, Nolan G, Gaudilliere B. The road ahead: Implementing mass cytometry in clinical studies, one cell at a time. Cytometry B Clin Cytom 2017;92:10-11.

I

Cytometry PART A
ISAC
Journal of Quantitative Cell Science

Optimization of Receptor Occupancy Assays in Mass Cytometry: Standardization Across Channels with QSC Beads

Gerd Haga Bringeland,[1,2*] Lucius Bader,[3,4] Nello Blaser,[5] Lisa Budzinski,[6] Axel R. Schulz,[6] Henrik E. Mei,[6] Kjell-Morten Myhr,[1,2] Christian A. Vedeler,[1,2] Sonia Gavasso[1,2*]

[1]Department of Neurology, Haukeland University Hospital, Bergen, Norway

[2]Department of Clinical Medicine, University of Bergen, Bergen, Norway

[3]Bergen group of Epidemiology and Biomarkers in Rheumatic Disease, Department of Rheumatology, Haukeland University Hospital, Bergen, Norway

[4]Department of Clinical Science, University of Bergen, Bergen, Norway

[5]Department of Mathematics, University of Bergen, Bergen, Norway

[6]German Rheumatism Research Centre Berlin (DRFZ), Berlin, Germany

Received 27 November 2018; Revised 3 January 2019; Accepted 8 January 2019

Grant sponsor: Novartis, Grant numberNorwegian Novartis' research grant for MS 2017

Additional Supporting Information may be found in the online version of this article.

*Correspondence to: Gerd Haga Bringeland or Sonia Gavasso, Department of Neurology, Haukeland University Hospital, Jonas Lies Vei 65, 5021 Bergen, Norway. Emails: gerd.haga.bringeland@helse-bergen.no; sonia.gavasso@helse-bergen.no

Published online 27 January 2019 in Wiley Online Library (wileyonlinelibrary.com)

DOI: 10.1002/cyto.a.23723

Abstract

Receptor occupancy, the ratio between amount of drug bound and amount of total receptor on single cells, is a biomarker for treatment response to therapeutic monoclonal antibodies. Receptor occupancy is traditionally measured by flow cytometry. However, spectral overlap in flow cytometry limits the number of markers that can be measured simultaneously. This restricts receptor occupancy assays to the analysis of major cell types, although rare cell populations are of potential therapeutic relevance. We therefore developed a receptor occupancy assay suitable for mass cytometry. Measuring more markers than currently available in flow cytometry allows simultaneous receptor occupancy assessment and high-parameter immune phenotyping in whole blood, which should yield new insights into disease activity and therapeutic effects. However, varying sensitivity across the mass cytometer detection range may lead to misinterpretation of the receptor occupancy when drug and receptor are detected in different channels. In this report, we describe a method for optimization of mass cytometry receptor occupancy measurements by using antibody-binding quantum simply cellular (QSC) beads for standardization across channels with different sensitivities. We evaluated the method in a mass cytometry-based receptor occupancy assay for natalizumab, a therapeutic antibody used in multiple sclerosis treatment that binds to α4-integrin, which is expressed on leukocyte cell surfaces. Peripheral blood leukocytes from a treated patient were stained with a panel containing metal-conjugated antibodies for detection of natalizumab and α4-integrin. QSC beads with known antibody binding capacity were stained with the same metal-conjugated antibodies and were used to standardize the signal intensity in the leukocyte sample before calculating receptor occupancy. We found that QSC bead standardization across channels corrected for sensitivity differences for detection of drug and receptor and generated more accurate results than observed without standardization. © 2019 The Authors. *Cytometry Part A* published by Wiley Periodicals, Inc. on behalf of International Society for Advancement of Cytometry.

Key terms

receptor occupancy; biomarkers; QSC beads; CyTOF; standardization; optimization; multiple sclerosis; natalizumab; quantitative analysis; mass cytometry

RECEPTOR occupancy (RO) by therapeutic monoclonal antibodies is a potential biomarker for therapeutic response and may support dose optimization in precision medicine (1,2). RO assays generally involve measuring bound drug relative to total target receptor on single cells by flow cytometry. *Mass* cytometry has rapidly evolved to become a relevant tool in several fields of translational clinical research (3–6). In mass cytometry, antibodies are conjugated to purified metal isotopes instead of fluorophores, which dramatically reduces signal overlap and allows simultaneous detection of more than 40 parameters in individual cells by inductively-coupled plasma mass spectrometry (7). Mass cytometry permits measurement of RO in

ISAC
International Society for Advancement of Cytometry

conjunction with more markers, and in more cell types of interest, than is currently possible by flow cytometry. In order to be useful, estimation of RO using mass cytometry must be reliable and reproducible. Mass cytometers have varying sensitivity over the detection range of metal isotopes (up to five-fold difference in CyTOF 1 and 2, lower in Helios), and each mass cytometer has its own sensitivity pattern (8,9). In a RO assay, differences in detection sensitivity of anti-drug and anti-receptor antibodies will result in either over- or underestimation of the RO, depending on which antibody is detected in the most sensitive channel.

Quantum simply cellular (QSC) beads are cell-sized particles with known antibody binding capacity that were developed for flow cytometry to enable determination of absolute numbers of cellular epitopes (10). We aimed to obtain more accurate RO estimation in mass cytometry by employing QSC beads for standardization across channels with varying detection sensitivity. We evaluated the applicability of QSC bead standardization in a mass cytometry-based RO assay for natalizumab. Natalizumab is a humanized monoclonal IgG4 antibody that binds to the α4 subunit of surface integrins on leukocytes, thereby preventing leukocytes from entering the central nervous system over the blood-brain-barrier. Natalizumab is used in the treatment of multiple sclerosis (MS) (11), and the natalizumab RO has been suggested as a biomarker for monitoring response to therapy (12,13). The assay used here was adapted from a natalizumab RO assay previously published for flow cytometry (14) in which bound natalizumab was detected by an anti-IgG4 and total α4 integrin was detected by an anti-α4 integrin antibody that binds to a different epitope of the α4 integrin than natalizumab. We demonstrated how the different detection sensitivities for natalizumab and α4 integrin influenced the mass cytometry-based RO assay results and how accurate and reproducible RO determination was achieved by standardization with QSC beads.

Materials and Methods

Subjects and Samples

The study was approved by the Regional Ethics Committee (approval REK 2016/579), and samples were collected after written informed consent from one healthy donor and one MS patient receiving natalizumab therapy (4 weeks after the last infusion) at the Department of Neurology, Haukeland University Hospital. Whole blood was obtained in heparinized vacutainer tubes (Greiner Bio-One GmbH, Kremsmünster, Austria), incubated with Proteomic stabilizer (Smart Tube, Inc., San Carlos, CA) for 10 min according to the manufacturer's protocol, and stored at −80°C.

Mass Cytometry Antibody Panel and Titration

The 34 marker mass cytometry antibody panel (Supporting Information Table S1a) consisted of 25 metal-conjugated antibodies purchased pre-conjugated from Fluidigm (South San Francisco, CA) and nine antibodies purchased from Biolegend (San Diego, CA), R&D Systems, (Minneapolis, MN) and Abcam (Cambridge, Great Britain) that were conjugated to metal isotopes with the Maxpar Antibody Labeling Kit (Fluidigm) according to the manufacturer's protocol. In the RO assay, bound natalizumab was measured with an anti-IgG4 (conjugated to ^{169}Tm) specific for the Fc portion of human IgG4 and total α4 integrin was measured with anti-α4 integrin (conjugated to ^{141}Pr) specific for a different epitope than natalizumab (Fig. 1). Antibody titrations were performed on the patient's peripheral blood leukocytes (PBLs) under the same conditions as the experiment (barcoded samples, staining volume 100 µl, 1.5×10^6 cells), and anti-IgG4 (^{169}Tm) and anti-α4 integrin (^{141}Pr) were titrated to saturating concentrations. An antibody cocktail containing the complete panel except anti-IgG4 and anti-α4 integrin was pre-made and stored in Maxpar Cell Staining Buffer (CSB; Fluidigm) in aliquots at −80°C for up to 9 days during which time the three replicate experiments were performed. Anti-IgG4 and anti-α4 integrin were added to the antibody cocktail aliquot on the day of the experiments.

Quality Control Experiments

Quality control (QC) experiments were performed on the same patient PBL sample under the same conditions as the main experiments. The following were analyzed:

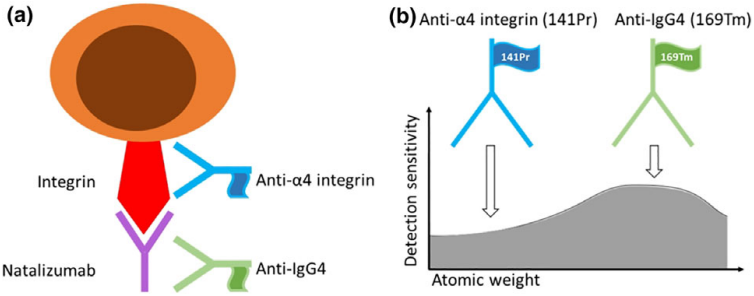

Figure 1. Natalizumab RO assay: (a) Natalizumab was detected with anti-IgG4 (^{169}Tm), and its receptor was detected with anti-α4 integrin (^{141}Pr). (b) Metal-conjugated antibodies are detected with different sensitivity depending on the atomic weight of the metal tag (graph adapted from Tricot et al.). [Color figure can be viewed at wileyonlinelibrary.com]

Unstained samples. To examine whether PBLs contained any metals in the detection range of the mass cytometer (in MS patients gadolinium can originate from intravenous contrast used in MRI scans), an unstained aliquot of the barcoded PBL sample, with only the DNA intercalation reagent used for cell detection, was acquired.

Mass-minus-one controls. Two mass-minus-one (MMO) controls were performed to test for spillover from other markers in the panel into the channels used for detection of anti-IgG4 and anti-α4 integrin. Barcoded PBLs were stained with the complete panel except for either anti-IgG4 or anti-α4 integrin.

Biological negative control. PBLs from an untreated healthy donor were barcoded and pooled with patient PBLs to serve as a negative control for binding of anti-IgG4 in the absence of natalizumab.

Positive control. Patient PBLs incubated with natalizumab, which were expected to have a RO of 100%, were used as a positive control. The same sample was also used as reference in some of the RO calculation methods.

Test of competitiveness between natalizumab and anti-α4 integrin. To examine whether natalizumab and anti-α4 integrin bound to different epitopes of α4 integrin without competition, detection of α4 integrin on PBLs from the healthy donor was compared with and without prior incubation with natalizumab.

Barcoding, Pooling, and Freezing of Aliquots

Whole blood samples stored in Proteomic stabilizer were thawed, and red blood cell lysis was performed with Thaw-Lyse buffer 1 (Smart Tube, Inc.) according to the manufacturer's manual. A total of 6×10^6 PBLs from each sample were permeabilized and barcoded using the Cell-ID 20-Plex Pd Barcoding kit (Fluidigm) according to the manufacturer's protocol. The two samples were washed in Maxpar PBS (Fluidigm), pooled, and stored in three aliquots each containing 3×10^6 cells in Maxpar PBS with 10% DMSO (Dimethyl sulfoxide, Sigma-Aldrich, Darmstadt, Germany) at −80°C for up to 9 days. All centrifugation steps were performed at room temperature at 800*g*.

In Vitro Incubation with Natalizumab and Antibody Staining

The in vitro incubation with natalizumab and antibody staining (Fig. 2a) was performed by the same operator in the same lab on three separate days. On each of the days, one aliquot of 3×10^6 barcoded and pooled PBLs was thawed and washed in Maxpar CSB. For optional incubation in vitro with natalizumab, the sample was split into two tubes, which were both incubated for 20 min at room temperature in Maxpar CSB with 100 U/ml heparin (LEO Pharma A/S, Ballerup, Denmark) to avoid nonspecific eosinophil antibody binding (15). To one of the tubes, natalizumab (Lot 28918, Biogen, Cambridge, Massachusetts) was added to a final concentration of 10 μg/ml. Both tubes were incubated for 30 min at room temperature with intermittent vortexing and washed thoroughly in Maxpar CSB. Prior to antibody staining, the number of cells in each tube was adjusted to 1×10^6, and cells were incubated again for 20 min at room temperature in Maxpar CSB with 100 U/ml heparin. Aliquots of the metal-conjugated antibody cocktail were thawed, anti-IgG4 and anti-α4 integrin were added, and antibody staining was performed in a total volume of 100 μl. After 30-min incubation at room temperature with intermittent vortexing, samples were washed with Maxpar CSB, and a 10-min post-staining fixation was performed in fresh 2% paraformaldehyde (Thermo Scientific, Waltham, MA) in Maxpar PBS at room temperature. Samples were washed with Maxpar PBS, resuspended in 1 ml of 125 nM Cell-ID™ Intercalator-Ir in Maxpar Fix and Perm Buffer (Fluidigm), and stored at 4°C for 3–4 h. Immediately prior to acquisition, PBL were washed in Maxpar PBS and Maxpar Water (Fluidigm), resuspended in 0.1× EQ Four Element Calibration Beads (Fluidigm) in Maxpar Water and filtered (Corning Falcon Test Tube with Cell Strainer Snap Cap, Fisher Scientific, Hampton, NN). All centrifugation steps were performed at room temperature at 800*g*.

Adaptation of QSC Bead Protocol for Mass Cytometry

QSC anti-mouse beads (Cat code 815A, Bangs Laboratories Inc., Fishers, IN) with increasing antibody binding capacity (ABC) for mouse-IgG were stained and acquired on the same days as PBL samples (Fig. 2b) and used to create standard curves of signal intensity (dual counts) from known numbers of anti-IgG4 (^{169}Tm) and anti-α4 integrin (^{141}Pr) (Fig. 2c). The QSC bead kit consisted of four bead populations with known ABC (12,319–814,348, lot 13,359). To cover the range of anti-IgG4 (^{169}Tm) and anti-α4 integrin (^{141}Pr) dual count values in our PBL samples, we purchased one additional QSC bead population with low ABC (2,685, lot 13,289), resulting in five QSC bead populations with ABC range of 2,685–814,548.

QSC beads are identified by forward and side scatter in flow cytometry, and they do not contain any metal in the detection range of the mass cytometer. To enable identification of QSC beads on the mass cytometer, the manufacturer's staining protocol was modified by addition of an osmium tetroxide (OsO_4) labeling step prior to antibody staining. Four drops of each of the QSC bead populations were incubated separately with 0.01–0.001% OsO_4 (CAS#20816-12-0, Electron Microscopy Sciences, Hatfield, PA) diluted in Maxpar PBS. After 30 min, beads were washed four times in Maxpar PBS, once in Maxpar CSB, and stained separately with 1 μg of either anti-IgG4 (^{169}Tm) or anti-α4 integrin (^{141}Pr) in a total volume of 100 μl Maxpar CSB for 30 min at room temperature. QSC beads were washed twice in Maxpar PBS and once in Maxpar Water, resuspended in 200 μl 0.1 × EQ Four Element Calibration Beads in Maxpar water, and filtered. The five QSC bead populations were kept separate through all staining and acquisition steps, and all centrifugation steps were performed at room temperature at 2500*g*.

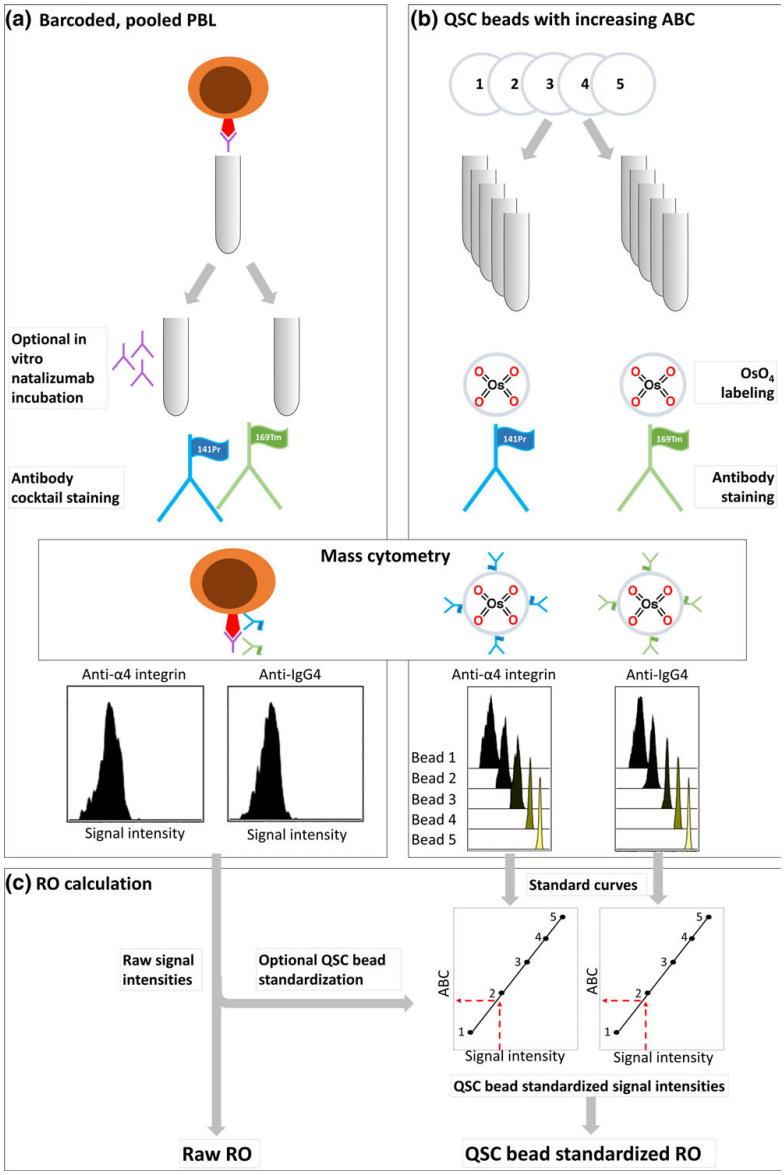

Figure 2. Experimental workflow: (a) peripheral blood leukocytes (PBLs) were split into two aliquots for optional in vitro incubation with natalizumab, stained with an antibody cocktail containing anti-IgG4 and anti-α4 integrin, and analyzed on a Helios mass cytometer. (b) Quantum simply cellular (QSC) beads with known antibody binding capacity (ABC) were labeled with OsO4, stained with anti-IgG4 or anti-α4 integrin, and acquired on the same mass cytometer on the same day. (c) Standard curves were created based on anti-IgG4 and anti-α4 integrin signal intensities from QSC beads with known ABC, and signal intensities of the same antibodies from the PBL samples were plotted into the standard curves for standardization before RO calculation. [Color figure can be viewed at wileyonlinelibrary.com]

A flow cytometry QC experiment was performed to examine whether OsO_4 labeling affected the ABC of QSC beads. QSC beads with and without OsO_4 labeling prior to antibody incubation with anti-IgG-PE (Abcam, Supporting Information Table S1b) were acquired on a flow cytometer (BD LSR Fortessa, BD Biosciences, Franklin Lakes, NJ). Apart

from staining QSC beads with a fluorochrome labeled anti-IgG4-PE antibody, instead of a metal-conjugated antibody, the QSC bead protocol described above was followed. To evaluate the correlation between QSC beads on mass and flow cytometry, QSC beads coated with anti-IgG4 (^{169}Tm) or anti-IgG4-PE were acquired by mass or flow cytometry, respectively, and signal intensities were compared.

Acquisition on the Helios® Instrument

In each of the three replicate experiments, freshly stained QSC beads and PBL samples were analyzed with the same standard settings on a Helios mass cytometer (Fluidigm). Before acquisition, tuning (CyTOF Tuning Solution, Fluidigm) and calibration (EQ Four Element Calibration Beads, Fluidigm) were performed according to the manufacture's guidelines. PBL sample acquisition was performed at a rate of 300–400 events per second.

Mass Cytometry Data Processing and Analysis

FCS files from analyses of QSC beads and PBL samples were normalized to the EQ beads using the Fluidigm normalizer (Fluidigm). Normalized QSC bead FCS files were exported to Cytobank software (Cytobank Inc., Santa Clara, CA) for gating and downstream analysis. Signal intensity (median dual counts) of QSC beads stained with anti-IgG4 and anti-α4 integrin, respectively, and the corresponding ABC values were plotted using QuickCal template (Bangs Laboratories) to create individual standard curves for the antibodies.

Normalized PBL sample FCS files were debarcoded (Fluidigm Debarcoder) and exported to Cytobank software for gating and downstream analysis. Cleanup gating was performed to obtain single PBL cells, and eight cell types of interest were identified by manual gating: memory B cells, monocytes, CD4 effector memory (T_{EM}), central memory (T_{CM}), effector memory RA (T_{EMRA}) T cells, and CD8 T_{EM}, T_{CM}, and T_{EMRA} cells.

In patient PBLs, 90th percentiles of anti-IgG4 (^{169}Tm) and anti-α4 integrin (^{141}Pr) dual counts in the eight cell types were exported for further calculations (Fig. 2c, left). Ninetieth percentiles were used instead of medians because of the bimodal distribution of α4 integrin and natalizumab in some cell types. For optional QSC bead standardization (Fig. 2c, right), these 90th percentiles were plotted against the respective standard curves in the QuickCal template and the corresponding ABC values, which will be referred to as QSC bead standardized signal intensities, were used in subsequent calculations. Untreated PBLs from the healthy donor were used as negative controls.

Calculation of Receptor Occupancy

In patient PBLs with and without in vitro natalizumab incubation, RO was calculated as a percent ratio between signal intensities of anti-IgG4 (^{169}Tm) and anti-α4 integrin (^{141}Pr) with and without QSC bead standardization (Fig. 2c):

i. Raw RO (RO_{raw}) based on raw 90th percentile dual counts:

$$\%RO_{raw} = 100 \times \frac{\text{Dual counts anti} - \text{IgG4 (169Tm)}}{\text{Dual counts anti} - \alpha4 \text{ integrin (141Pr)}}$$

ii. QSC bead standardized RO ($RO_{standardized}$) based on QSC bead standardized signal intensities:

$$\%RO_{standardized} = 100 \times \frac{\text{QSC bead standardized anti} - \text{IgG4 (169Tm)}}{\text{QSC bead standardized anti} - \alpha4 \text{ integrin (141 Pr)}}$$

In patient PBLs not incubated with natalizumab, we calculated RO by an additional approach by determining the ratio between RO (as calculated above) in the sample and RO in the in vitro natalizumab saturated aliquot of the same sample:

iii. RO_{raw} in the sample relative to RO_{raw} in the 100% saturated aliquot:

$$\%RO_{vs.100\%raw} = 100 \times \frac{\%\text{RO raw in sample}}{\%\text{RO raw in 100\%saturated sample}}$$

iv. $RO_{standardized}$ in the sample relative to $RO_{standardized}$ in the 100% saturated aliquot:

$$\%RO_{vs.\ 100\%standardized} = 100 \times \frac{\%\text{RO stand in sample}}{\%\text{RO stand in 100\%saturated sample}}$$

Statistics

In the sample incubated in vitro with natalizumab, RO results were compared to 100% using a one-sample *t* test. Otherwise, results from different RO calculation methods were compared using a paired *t* test. Statistical significance was defined as $P < 0.05$. We used R version 3.4.3 (16) for statistical analysis and Inkspace (Free Software Foundation, Inc., Boston, MA) for illustrations.

Results

Quantification of Natalizumab and α4 Integrin in PBL Cell Subtypes

Memory B cells, monocytes, CD4 T_{EM}, T_{CM}, and T_{EMRA} cells, and CD8 T_{EM}, T_{CM}, and T_{EMRA} cells were gated in PBL samples as illustrated in Supporting Information Figure S1a. The 90th percentile dual counts of anti-IgG4 (^{169}Tm) and anti-α4 integrin (^{141}Pr) of these cell types in the patient PBL samples with and without natalizumab incubation in vitro (Supporting Information Fig. S1b) were exported for RO calculations.

QSC Beads Were Used for Standardization of Signal Intensities

QSC beads were gated as illustrated in Supporting Information Figure S2a. Median dual counts of anti-IgG4 (^{169}Tm) and anti-α4 integrin (^{141}Pr) in the five QSC bead populations were determined (Fig. 3; Supporting Information Fig. S2b) and used to create standard curves for each of the antibodies in the QuickCal Template. QSC bead standardization of the PBL samples was performed by plotting raw signal intensities (90th percentile dual counts) of anti-IgG4 (^{169}Tm) and anti-α4 integrin (^{141}Pr) in the cell types against the respective standard curves, as shown in detail in Supporting Information Figure S2c. OsO_4 labeling of the QSC beads prior to antibody staining did not alter antibody binding capacity (Supporting Information Fig. S3a). Moreover, there was a linear correlation between ABC of the same QSC beads acquired by mass cytometry and by flow cytometry (Supporting Information Fig. S3b).

Bead Standardization Compensated for Overestimation of RO

Table 1 shows RO values from different calculation methods based on data collected on patient PBLs with and without in vitro incubation with natalizumab. Samples incubated with natalizumab were expected to have ROs of 100% in all cell subtypes. We compared two calculation methods (Fig. 4a): RO_{raw} and $RO_{standardized}$. We found that RO_{raw} was significantly different from the expected 100% in all eight cell subtypes identified ($p < 0.0001$, median 126%, IQR: 116–130%), whereas $RO_{standardized}$ was not significantly different from 100% ($p = 0.45$, median 101%, IQR: 94–106%).

In the samples not incubated with natalizumab, RO was unknown. Four different RO calculation methods were compared (Fig. 4b): In addition to RO_{raw} and $RO_{standardized}$, we calculated $RO_{vs100\%raw}$ and $RO_{vs100\%standardized}$ based on RO in the sample relative to RO in the corresponding 100% saturated sample. As for the in vitro saturated samples, we found that RO_{raw} was higher than $RO_{standardized}$ in each of the eight cell subtypes (p values, medians and ranges are shown in Fig. 4b). Neither $RO_{standardized}$ nor $RO_{vs100\%raw}$ were significantly different from $RO_{vs100\%standardized}$ in any of the subtypes (p values, medians and ranges are shown in Fig. 4b).

To determine whether the overestimation of RO could be caused by interfering factors, such as unwanted signal in the channels for detection of anti-IgG4 (^{169}Tm) and anti-α4 integrin (^{141}Pr), several control experiments were performed. First, unstained PBL samples did not contain any detectable metals (Supporting Information Fig. S4a). Second, MMO controls did not reveal spillover into either of the two channels (Supporting Information Fig. S4b). Third, there was minimal nonspecific binding of anti-IgG4 in the absence of natalizumab in untreated PBLs from the healthy donor (Supporting Information Fig. S4c). Finally, detection of α4 integrin by the anti-α4 integrin antibody was not reduced by bound natalizumab (Supporting Information Fig. S4d).

Discussion

Embedding RO assays into high-parameter mass cytometry may be a valuable addition to therapy monitoring. However, to be useful, mass cytometry-based RO assay results

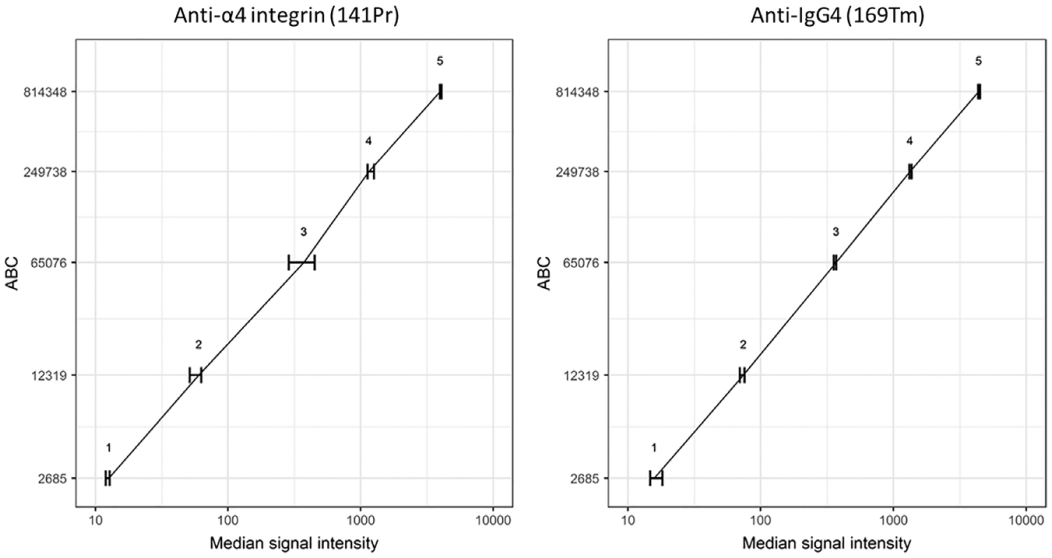

Figure 3. Median signal intensity of anti-α4 integrin (^{141}Pr) and anti-IgG4 (^{169}Tm) on QSC beads with known antibody binding capacity (ABC). Error bars show the range of measured signal intensities in three replicate experiments. The same data for each of the experiments are shown in Supporting Information Figure. S2b.

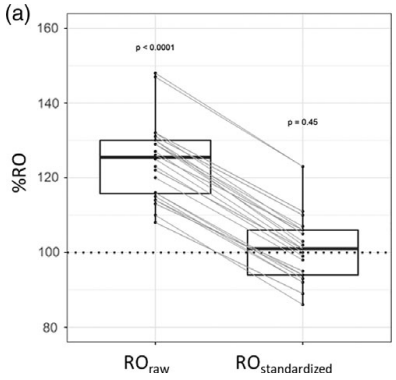

Figure 4a. Receptor occupancy (RO) in three replicate experiments with patient PBL aliquots. RO raw and RO stand in the PBLs incubated in vitro with natalizumab (all cell types combined) with expected RO 100% (marked by a horizontal line). Each dot represents RO in one cell type, and lines connect RO values determined in the same measurement using the two calculation methods. *P* values for comparison of mean RO to the expected (100%) in a one-sample *t* test.

must be reliable and reproducible. In this article, we showed how direct comparison of drug and receptor detected in mass cytometer channels with different sensitivities led to misinterpretation of RO. We demonstrated that reliable results can be obtained by standardization across channels using QSC beads with known ABC. A QSC bead protocol was adapted from flow to mass cytometry. In the mass cytometry assay, signal intensities from metal-conjugated antibodies in the sample were standardized with standard curves created from QSC beads coated with known numbers of the same metal-conjugated antibodies.

We performed our mass cytometry RO assay for the therapeutic antibody natalizumab on PBLs from one treated patient with one healthy donor as a negative control in three replicate experiments. An in vitro natalizumab-saturated aliquot with expected RO of 100% was used as a positive control. Natalizumab was detected with anti-IgG4 (^{169}Tm) and its target receptor was detected with anti-α4 integrin (^{141}Pr). Based on prior knowledge, 169 is a more sensitive channel of the mass cytometer than 141, and we therefore expected overestimation of the RO. Indeed, we observed a consistent overestimation of the RO_{raw} in all cell types (median 126%) of the sample saturated in vitro with natalizumab with *known* RO of 100%. After QSC bead standardization of anti-IgG4 (^{169}Tm) and anti-α4 integrin (^{141}Pr) signal intensities, the resulting $RO_{standardized}$ was no longer significantly different from the expected (median 101%). The same pattern was observed in

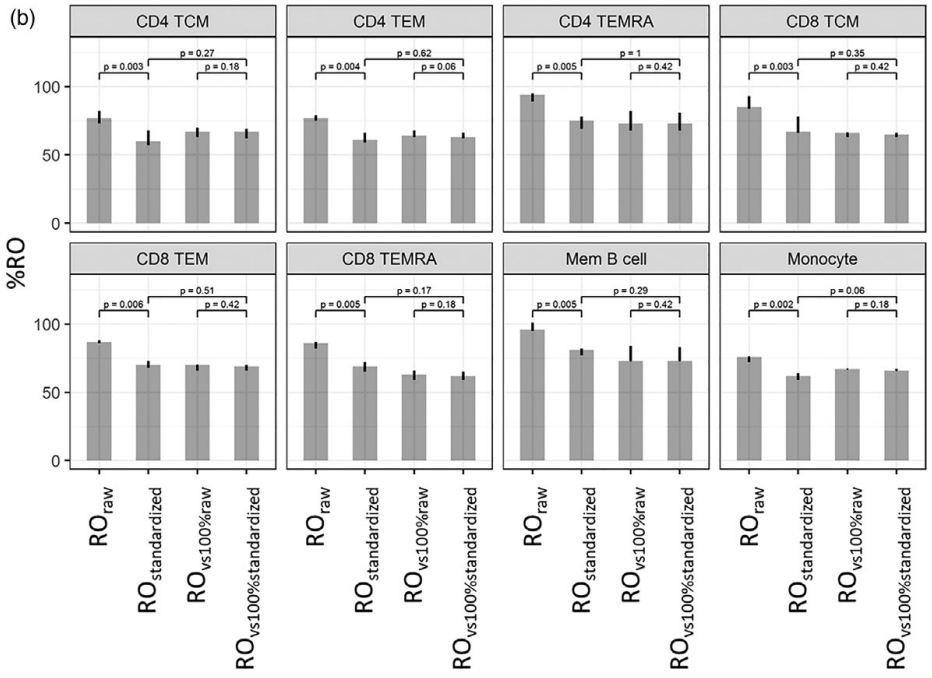

Figure 4b. Receptor occupancy (RO) in three replicate experiments with patient PBL aliquots. RO_{raw}, $RO_{standardized}$, $RO_{vs.\ 100\%\ raw}$, and $RO_{vs.\ 100\%\ standardized}$ in PBL aliquots with unknown RO. Heights of the bars are median values, and the error bars indicate the range of measured values in three replicate experiments. *P* values for comparison of mean RO using a paired *t* test.

Table 1. Receptor occupancy (RO) in eight cell types in three replicate experiments with the same patient PBL sample

(A) RO_{RAW} AND $RO_{STANDARDIZED}$ IN PATIENT PBLS SATURATED IN VITRO WITH NATALIZUMAB WITH EXPECTED RO OF 100%.

	RO RAW			*RO STANDARD ZED*		
	DAY 1	*DAY 2*	*DAY 3*	*DAY 1*	*DAY 2*	*DAY 3*
Mem B cell	*120%*	*129%*	*132%*	*98%*	*105%*	*111%*
Monocyte	*114%*	*108%*	*113%*	*94%*	*89%*	*95%*
CD4 T_{CM}	*115%*	*110%*	*122%*	*92%*	*86%*	*101%*
CD4 T_{EM}	*114%*	*116%*	*126%*	*92%*	*94%*	*106%*
CD4 T_{EMRA}	*116%*	*130%*	*129%*	*93%*	*102%*	*107%*
CD8 T_{CM}	*129%*	*127%*	*148%*	*103%*	*101%*	*123%*
CD8 T_{EM}	*123%*	*125%*	*131%*	*99%*	*100%*	*110%*
CD8 T_{EMRA}	*130%*	*132%*	*147%*	*105%*	*106%*	*123%*

(B) RO_{RAW}, $RO_{STANDARDIZED}$, $RO_{VS100\%RAW}$, AND $RO_{VS100\%STANDARDIZED}$ in patient PBL with unknown RO (i.e., not incubated with natalizumab in vitro).

	RO RAW			*RO STANDARDIZED*			*RO VS. 100% RAW*			*RO VS. 100% STANDARDIZED*		
	DAY 1	*DAY 2*	*DAY 3*	*DAY 1*	*DAY 2*	*DAY 3*	*DAY 1*	*DAY 2*	*DAY 3*	*DAY 1*	*DAY 2*	*DAY 3*
Mem B cell	*101%*	*95%*	*96%*	*82%*	*77%*	*81%*	*84%*	*73%*	*73%*	*83%*	*73%*	*73%*
Monocyte	*76%*	*72%*	*76%*	*62%*	*59%*	*64%*	*67%*	*67%*	*67%*	*66%*	*66%*	*67%*
CD4 T_{CM}	*73%*	*77%*	*82%*	*57%*	*60%*	*68%*	*63%*	*70%*	*67%*	*62%*	*69%*	*67%*
CD4 T_{EM}	*77%*	*75%*	*79%*	*61%*	*59%*	*66%*	*68%*	*64%*	*63%*	*66%*	*63%*	*62%*
CD4 T_{EMRA}	*95%*	*89%*	*94%*	*75%*	*69%*	*78%*	*82%*	*68%*	*73%*	*81%*	*68%*	*73%*
CD8 T_{CM}	*85%*	*84%*	*93%*	*67%*	*66%*	*78%*	*66%*	*66%*	*63%*	*65%*	*66%*	*63%*
CD8 T_{EM}	*86%*	*88%*	*87%*	*68%*	*70%*	*73%*	*70%*	*70%*	*66%*	*69%*	*70%*	*66%*
CD8 T_{EMRA}	*82%*	*87%*	*86%*	*65%*	*69%*	*72%*	*63%*	*66%*	*59%*	*62%*	*65%*	*59%*

the sample with unknown RO: RO_{raw} was higher in all cell types compared to $RO_{standardized}$.

QC experiments did not reveal other explanations for the overestimation of RO: We did not detect preexisting (in vivo) metal in the sample, spillover from other markers in the panel into channels of interest, or nonspecific binding of anti-IgG4, and bound natalizumab did not interfere with detection of integrin. Overall, our results indicate that deviance in channel sensitivity for anti-IgG4 (^{169}Tm) and anti-α4 integrin (^{141}Pr) was indeed the cause of the overestimation of RO and that this could be corrected by QSC bead standardization. In the sample with unknown RO, after correcting for RO in the corresponding 100% saturated sample, the effect of QSC bead standardization disappeared so that there was no significant difference between $RO_{vs100\%raw}$ and $RO_{vs100\%standardized}$ in any of the cell types. There was also no difference between $RO_{standardized}$ and $RO_{vs100\%standardized}$. This indicates that using RO in a 100% saturated sample as a reference mitigates overestimation of RO.

The general effect of the deviance in detection sensitivity on RO results can be predicted by the relative location of the antibody metal tags in the detection spectrum (8): If the drug is detected in a more sensitive channel than the receptor, the RO will be overestimated and vice versa. However, the detection sensitivity pattern varies between machines and cannot be exactly predicted by existing tools. EQ calibration beads and tuning solution only contain certain metals, whereas QSC beads are stained with the actual metal-conjugated antibodies used to stain the samples. The approach described here may also correct for differences in batch-to-batch variability in labeling efficiency (how many metal isotopes are conjugated to the antibody) of in-house conjugated antibodies but that was not tested in our study.

As no studies of RO in mass cytometry have yet been published, the problem with diverging detection sensitivity has not yet been addressed, but a similar problem arises in flow cytometry where antibodies are conjugated to fluorophores with different brightness. Some have addressed this by using various antibody-binding beads (1,10). Others have avoided measuring receptors in various ways: for example, comparing bound drug in the sample to an in vitro drug-saturated sample as an indirect measure of total receptor level (17) or comparing bound drug during treatment to a baseline before treatment (18). The latter method does not take into account changes in total receptor levels during treatment. Advantages of using QSC beads instead of staining several aliquots of the sample as a reference are that less sample is consumed and that acquisition time is decreased. Measuring drug and receptor on the same cells in the same run means that there is no batch-to-batch variability and takes into account varying receptor level during treatment. Labeling QSC beads with metal before antibody staining is time-consuming, and commercial antibody capture beads pre-labeled with metal in the detection range of mass cytometer would simplify the protocol.

Importantly, we here used QSC beads only for standardization and not for absolute quantitation of ABC. In mass

cytometry, signal intensity is proportional to the amount of metal-conjugated antibody bound per QSC bead or cell, but no actual counting of epitopes is performed by the instrument. Therefore, ABC values obtained by mass cytometry require careful interpretation, and we refer to the resulting semi-quantitative value as QSC bead standardized signal intensity.

Despite efforts to reduce experimental variability by using frozen aliquots of one barcoded sample and one antibody cocktail, we observed some day-to-day variability in the three replicate experiments performed over a period of 9 days. This could be due to variations in sample handling, staining, cell numbers, and pipetting in the many steps of the protocol. A superior approach for isolating the effect of QSC bead standardization and eliminating other experimental variation would be to run the same stained beads and PBL samples on different mass cytometers simultaneously.

Reproducibility over time and between instruments is crucial in longitudinal and multicenter studies. In flow cytometry, QSC beads allow comparison of experiments over time and between different instruments (19,20). In mass cytometers, individual detection sensitivity patterns for different machines and variations in machine performance over time may affect results in longitudinal and multicenter studies. Acquisition of data on samples and on QSC beads labeled with the same metal-conjugated antibodies as used to stain the samples on the same mass cytometer on same day may correct for such variations.

In conclusion, our findings suggest that QSC bead standardization offers an effective means to standardize signal intensities across channels of different sensitivity resulting in reliable and accurate RO results. We demonstrated this in a natalizumab RO assay, but the approach is applicable for RO assays of any drug-receptor pair or in other mass cytometry experiments involving comparison of abundance of two or more markers. QSC beads should cover the whole range of dual count values in the samples and may be labeled with any metal within the detection range of the mass cytometer, but alterations of bead ABC should be examined. There are certain factors that use of beads cannot correct. QC experiments should be performed to evaluate unspecific binding and spillover into the channels for detection of drug or receptor, and we suggest use of an in vitro drug-saturated sample with known RO as a reference to validate the results. Future studies should evaluate whether QSC beads can, as in flow cytometry, be used for standardization of experiments performed on different mass cytometers and over time, which would be an important step toward applicability of mass cytometry in multicenter and longitudinal clinical studies.

ACKNOWLEDGMENTS

The authors thank the Neurological Research Laboratory at Haukeland University Hospital for cooperation on sample collection, the Flow Cytometry Core at the University of Bergen for technical support and helpful discussions, and Novartis for financial research support.

Literature Cited

1. Moulard M, Ozoux ML. How validated receptor occupancy flow cytometry assays can impact decisions and support drug development. Cytometry B Clin Cytom 2016;90(2):150–158.
2. Stewart JJ, Green CL, Jones N, Liang M, Xu Y, Wilkins DEC, Moulard M, Czechowska K, Lanham D, McCloskey TW, et al. Role of receptor occupancy assays by flow cytometry in drug development. Cytometry B Clin Cytom 2016;90(2): 110–116.
3. Gaudillière B, Fragiadakis GK, Bruggner RV, Nicolau M, Finck R, Tingle M, Silva J, Ganio EA, Yeh CG, Maloney WJ, et al. Clinical recovery from surgery correlates with single-cell immune signatures. Sci Transl Med 2014;6(255): 255ra131.
4. Gaudillière B, Ganio EA, Tingle M, Lancero HL, Fragiadakis GK, Baca QJ, Aghaeepour N, Wong RJ, Quaintance C, El-Sayed YY, et al. Implementing mass Cytometry at the bedside to study the immunological basis of human diseases: Distinctive immune features in patients with a history of term or preterm birth. Cytometry A 2015;87(9):817–829.
5. Nair N, Mei HE, Chen SY, Hale M, Nolan GP, Maecker HT, Genovese M, Fathman CG, Whiting CC. Mass cytometry as a platform for the discovery of cellular biomarkers to guide effective rheumatic disease therapy. Arthritis Res Ther 2015; 17:127.
6. O'Gorman WE, Hsieh EWY, Savig ES, Gherardini PF, Hernandez JD, Hansmann L, Balboni IM, Utz PJ, Bendall SC, Fantl WJ, et al. Single-cell systems-level analysis of human toll-like receptor activation defines a chemokine signature in patients with systemic lupus erythematosus. J Allergy Clin Immunol 2015;136(5):1326–1336.
7. Bandura DR, Baranov VI, Ornatsky OI, Antonov A, Kinach R, Lou X, Pavlov S, Vorobiev S, Dick JE, Tanner SD. Mass cytometry: Technique for real time single cell multitarget immunoassay based on inductively coupled plasma time-of-flight mass spectrometry. Anal Chem 2009;81(16):6813–6822.
8. Tricot S, Meyrand M, Sammicheli C, Elhmouzi-Younes J, Corneau A, Bertholet S, Malissen M, le Grand R, Nuti S, Luche H, et al. Evaluating the efficiency of isotope transmission for improved panel design and a comparison of the detection sensitivities of mass cytometer instruments. Cytometry A 2015;87(4):357–368.
9. Takahashi C, Au-Yeung A, Fuh F, Ramirez-Montagut T, Bolen C, Mathews W, O'Gorman WE. Mass cytometry panel optimization through the designed distribution of signal interference. Cytometry A 2017;91(1):39–47.
10. Engelberts PJ, Badoil C, Beurskens FJ, Boulay-Moine D, Grivel K, Parren PWHI, Moulard M. A quantitative flow cytometric assay for determining binding characteristics of chimeric, humanized and human antibodies in whole blood: Proof of principle with rituximab and ofatumumab. J Immunol Methods 2013;388(1–2):8–17.
11. Hutchinson M. Natalizumab: A new treatment for relapsing remitting multiple sclerosis. Ther Clin Risk Manag 2007;3(2):259–268.
12. Wipfler P, Harrer A, Pilz G, Oppermann K, Afazel S, Haschke-Becher E, Sellner J, Trinka E, Kraus J. Natalizumab saturation: Biomarker for individual treatment holiday after natalizumab withdrawal? Acta Neurol Scand 2014;129(3):e12–e15.
13. Puñet-Ortiz J, Hervás-García JV, Teniente-Serra A, Cano-Orgaz A, Mansilla MJ, Quirant-Sánchez B, Navarro-Barriuso J, Fernández-Sanmartín MA, Presas-Rodríguez S, Ramo-Tello C, et al. Monitoring CD49d receptor occupancy: A method to optimize and personalize natalizumab therapy in multiple sclerosis patients. Cytometry B Clin Cytom. 2018;94(2):327–333.
14. Schneider-Hohendorf T, Rossaint J, Mohan H, Böning D, Breuer J, Kuhlmann T, Gross CC, Flanagan K, Sorokin L, Vestweber D, et al. VLA-4 blockade promotes differential routes into human CNS involving PSGL-1 rolling of T cells and MCAM-adhesion of TH17 cells. J Exp Med 2014;211(9):1833–1846.
15. Rahman AH, Tordesillas L, Berin MC. Heparin reduces nonspecific eosinophil staining artifacts in mass cytometry experiments. Cytometry A 2016;89(6):601–607.
16. R core team. R: A Language and Environment for Statistical Computing. Vienna, Austria: R Foundation for Statistical Computing, 2017.
17. Reilly M, Miller RM, Thomson MH, Patris V, Ryle P, McLoughlin L, Mutch P, Gilboy P, Miller C, Broekema M, et al. Randomized, double-blind, placebo-controlled, dose-escalating phase I, healthy subjects study of intravenous OPN-305, a humanized anti-TLR2 antibody. Clin Pharmacol Ther 2013;94(5):593–600.
18. Bensinger W, Maziarz RT, Jagannath S, Spencer A, Durrant S, Becker PS, Ewald B, Bilic S, Rediske J, Baeck J, et al. A phase 1 study of lucatumumab, a fully human anti-CD40 antagonist monoclonal antibody administered intravenously to patients with relapsed or refractory multiple myeloma. Br J Haematol 2012;159(1):58–66.
19. Perfetto SP, Ambrozak D, Nguyen R, Chattopadhyay PK, Roederer M. Quality assurance for polychromatic flow cytometry using a suite of calibration beads. Nat Protoc 2012;7(12):2067–2079.
20. Mizrahi O, Ish Shalom E, Baniyash M, Klieger Y. Quantitative flow cytometry: Concerns and recommendations in clinic and research. Cytometry B Clin Cytom 2018; 94(2):211–218.

Supplementary Table 1: Antibodies used in the experiments.

a) Mass cytometry antibody panel: 25 metal conjugated antibodies were purchased pre-conjugated from Fluidigm (South San Francisco, CA, USA). Nine antibodies purchased from Biolegend (San Diego, CA, USA), R&D Systems (Minneapolis, MN, USA) and Abcam (Cambridge, Great Britain) were conjugated to metals in-house using MaxPar X8 conjugation kits (Fluidigm).

Isotope tag	Target	clone	Company
141Pr	CD49d	9F10	Fluidigm
142Nd	CD19	HIB19	Fluidigm
143Nd	HLA-DR	L243	Fluidigm
144Nd	CD146	P1H12	Biolegend
145Nd	CD4	RPA-T4	Fluidigm
146Nd	CD8a	RPA-T8	Fluidigm
147Sm	CD20	2H7	Fluidigm
148Nd	CD34	581	Fluidigm
149Sm	CD25 (IL-2R)	2A3	Fluidigm
150Nd	CD61	VI-PL2	Fluidigm
151Eu	CD278/ICOS	C398.4A	Biolegend
152Sm	CD66b	80H3	Fluidigm
153Eu	CD194 (CCR4)	205410	Fluidigm
154Sm	CD3	UCHT1	Fluidigm
155Gd	CD161	HP-3G10	Biolegend
158Gd	CD27	L128	Fluidigm
159Tb	CD45RO	UCHL1	Biolegend
160Gd	CD14	M5E2	Fluidigm
161Dy	CD183 (CXCR3)	G025H7	Biolegend
162Dy	CD11c	Bu15	Fluidigm
163Dy	CD33	WM53	Fluidigm
165Ho	CD127 (IL7-Ra)	A019D5	Fluidigm
166Er	CD123 (IL-3R)	AO19D5	Biolegend
167Er	CD162	KPL-1	Fluidigm
168Er	CD185 (CXCR5)	51505	R&D Systems
169Tm	Human IgG4	HP6025	Abcam
170Er	CD45RA	HI100	Fluidigm
172Yb	CD38	HIT2	Fluidigm
173Yb	CD196/CCR6	G034E3	Biolegend
174Yb	CD279 (PD-1)	EH12.2H7	Fluidigm
175Lu	CD235ab (Glycophorin)	HIR2	Fluidigm
176Yb	CD56	NCAM16.2	Fluidigm
209Bi	CD16	3G8	Fluidigm
89Y	CD45	HI30	Fluidigm

b) Anti-human IgG4-PE was purchased pre-conjugated from Abcam and used for quality control experiments in flow cytometry.

Fluorochrome tag	Target	clone	Company
Phycoerythrin (PE)	Human IgG4	HP6025	Abcam

Supplementary Figure 1:

a) Gating strategy for PBL samples. Eight cell types of interest were identified: memory B cells, monocytes, CD4 effector memory (T_{EM}), central memory (T_{CM}), effector memory RA (T_{EMRA}) T cells, and CD8 T_{EM}, T_{CM}, and T_{EMRA} cells.

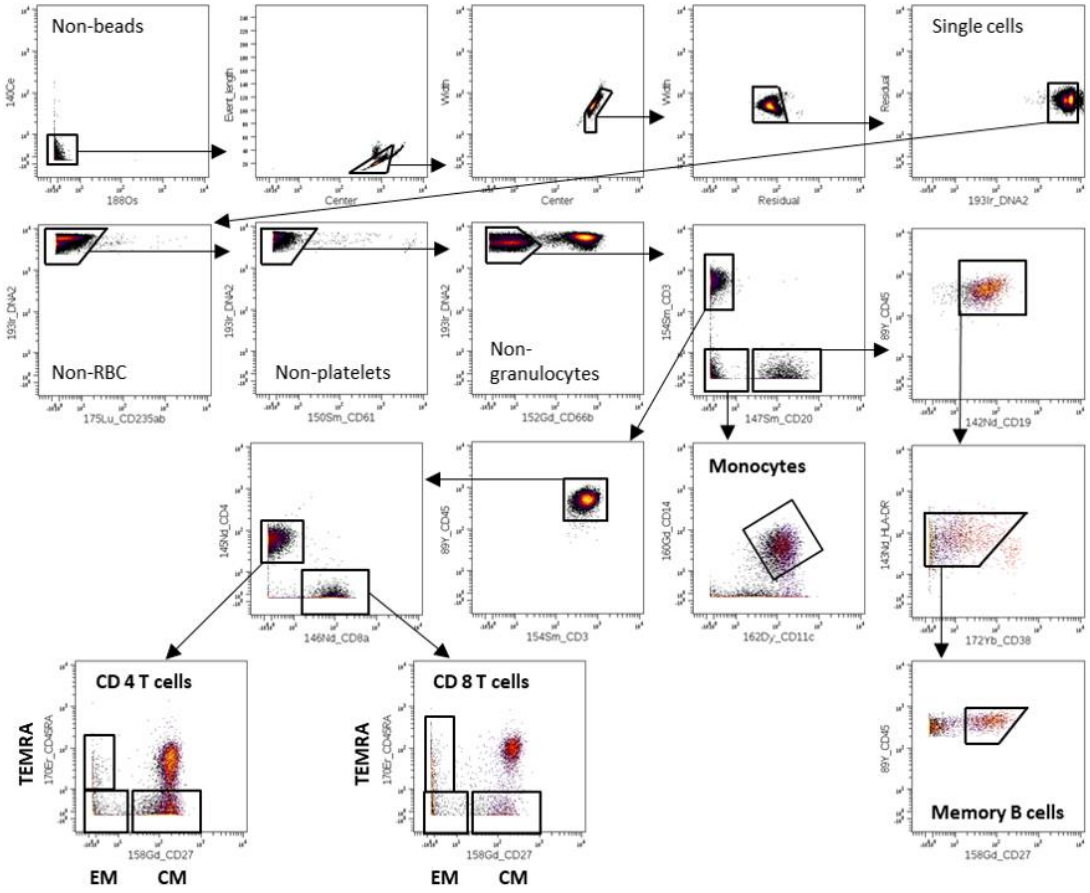

b) Eight cell types in patient PBL samples without (-nata) and with (+nata) *in vitro* natalizumab incubation. Shown are 90th percentile of anti-IgG4 and anti-α4 integrin dual counts in experiments conducted on three separate days.

Memory B cells

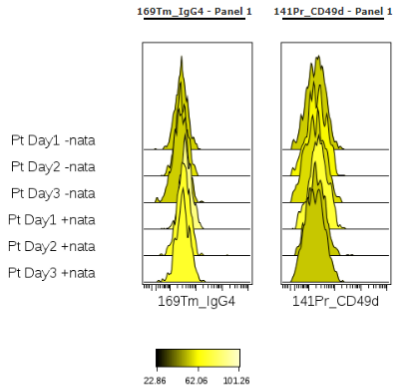

Calculated Raw values of Percentile using X-Axis channel(s): Panel/Channel Values

	169Tm_IgG4 - Panel 1	141Pr_CD49d - Panel 1
Pt Day1 -nata	55.01	54.36
Pt Day2 -nata	57.9	61.04
Pt Day3 -nata	54.64	56.83
Pt Day1 +nata	87.27	72.6
Pt Day2 +nata	69.79	53.9
Pt Day3 +nata	70.32	53.47

Monocytes

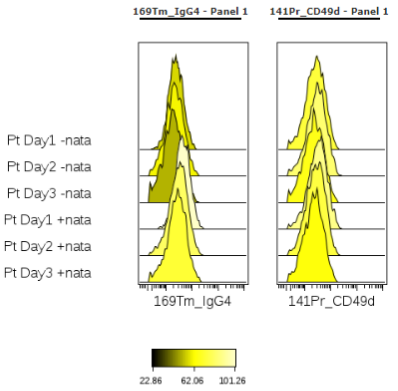

Calculated Raw values of Percentile using X-Axis channel(s): Panel/Channel Values

	169Tm_IgG4 - Panel 1	141Pr_CD49d - Panel 1
Pt Day1 -nata	56.07	73.63
Pt Day2 -nata	60.76	83.99
Pt Day3 -nata	50.45	66.76
Pt Day1 +nata	101.26	88.73
Pt Day2 +nata	81.18	74.89
Pt Day3 +nata	72.57	64.21

CD4 Tcm

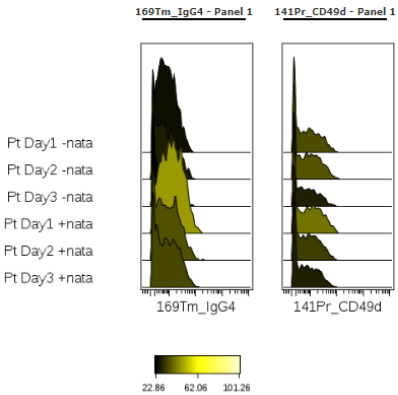

Calculated Raw values of Percentile using X-Axis channel(s): Panel/Channel Values

	169Tm_IgG4 - Panel 1	141Pr_CD49d - Panel 1
Pt Day1 -nata	25.28	34.83
Pt Day2 -nata	27.45	35.86
Pt Day3 -nata	22.86	27.83
Pt Day1 +nata	46.57	40.54
Pt Day2 +nata	35.46	32.35
Pt Day3 +nata	33.92	27.87

CD4 Tem

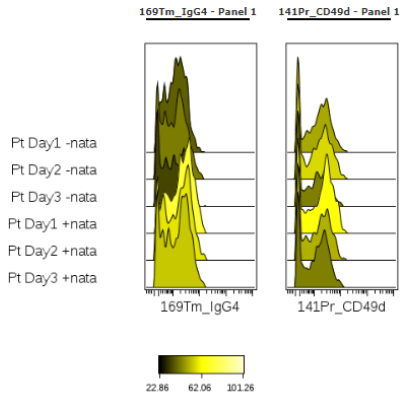

Calculated Raw values of Percentile using X-Axis channel(s): Panel/Channel Values

	169Tm_IgG4 - Panel 1	141Pr_CD49d - Panel 1
Pt Day1 -nata	37.49	48.73
Pt Day2 -nata	42.04	56.34
Pt Day3 -nata	33.57	42.44
Pt Day1 +nata	72.47	63.75
Pt Day2 +nata	58.16	49.94
Pt Day3 +nata	53.61	42.42

CD4 Temra

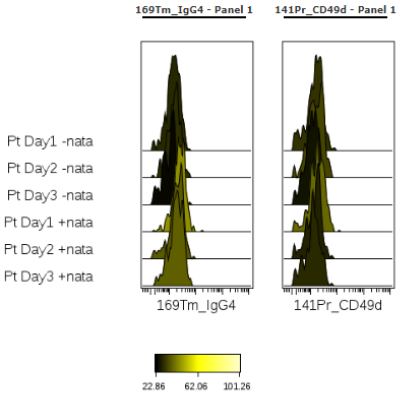

Calculated Raw values of Percentile using X-Axis channel(s): Panel/Channel Values

	169Tm_IgG4 - Panel 1	141Pr_CD49d - Panel 1
Pt Day1 -nata	29.05	30.6
Pt Day2 -nata	29.74	33.53
Pt Day3 -nata	24.1	25.73
Pt Day1 +nata	45.28	39.0
Pt Day2 +nata	36.79	28.23
Pt Day3 +nata	37.6	29.26

CD8 Tcm

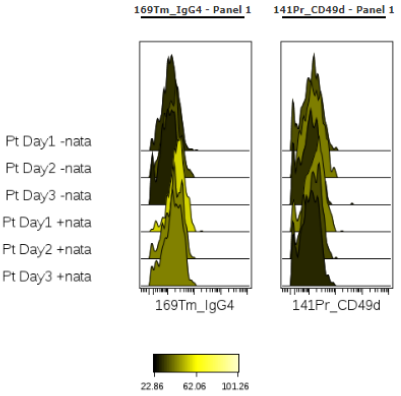

Calculated Raw values of Percentile using X-Axis channel(s): Panel/Channel Values

	169Tm_IgG4 - Panel 1	141Pr_CD49d - Panel 1
Pt Day1 -nata	30.15	35.27
Pt Day2 -nata	35.64	42.26
Pt Day3 -nata	28.14	30.18
Pt Day1 +nata	55.58	43.18
Pt Day2 +nata	43.13	33.92
Pt Day3 +nata	42.82	28.95

CD8 Tem

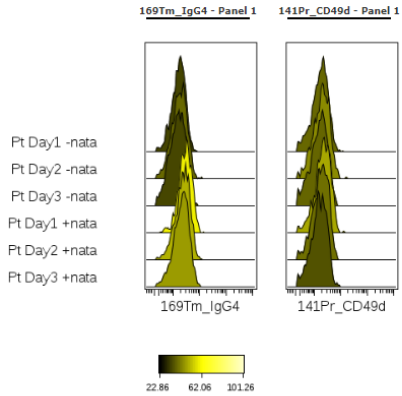

Calculated Raw values of Percentile using X-Axis channel(s): Panel/Channel Values

	169Tm_IgG4 - Panel 1	141Pr_CD49d - Panel 1
Pt Day1 -nata	33.39	38.84
Pt Day2 -nata	38.97	44.16
Pt Day3 -nata	33.63	38.53
Pt Day1 +nata	59.88	48.67
Pt Day2 +nata	50.1	40.0
Pt Day3 +nata	46.74	35.57

CD8 Temra

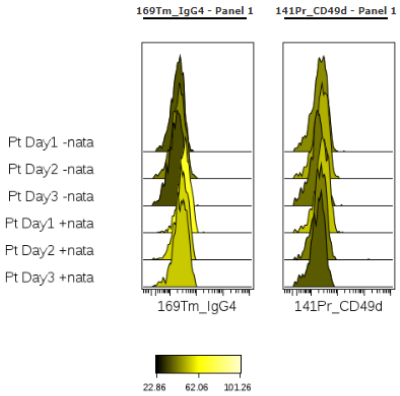

Calculated Raw values of Percentile using X-Axis channel(s): Panel/Channel Values

	169Tm_IgG4 - Panel 1	141Pr_CD49d - Panel 1
Pt Day1 -nata	36.1	44.24
Pt Day2 -nata	43.45	49.92
Pt Day3 -nata	34.68	40.38
Pt Day1 +nata	68.84	53.13
Pt Day2 +nata	55.62	42.08
Pt Day3 +nata	53.86	36.73

Supplementary Figure 2:

a) Gating strategy of QSC beads labeled with OsO_4 prior to metal conjugated antibody.

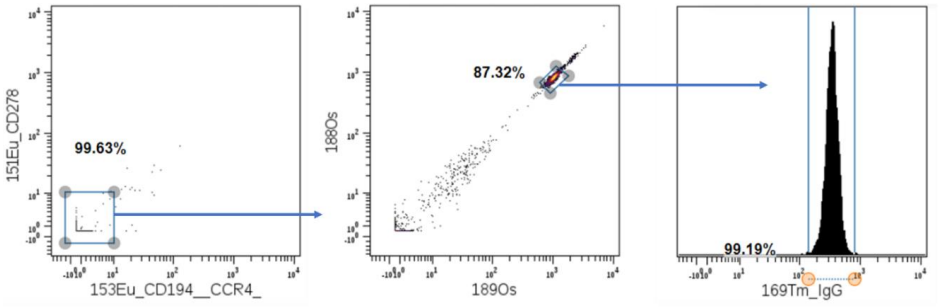

Gating out EQ beads | Bead singlets: Osmium double positive | Antibody positive QSC beads

b) Signal intensity (median dual counts) of the five QSC bead populations stained with anti-IgG4 (^{169}Tm) (top) and anti-α4 integrin (^{141}Pr) (bottom) in each of the three experiments.

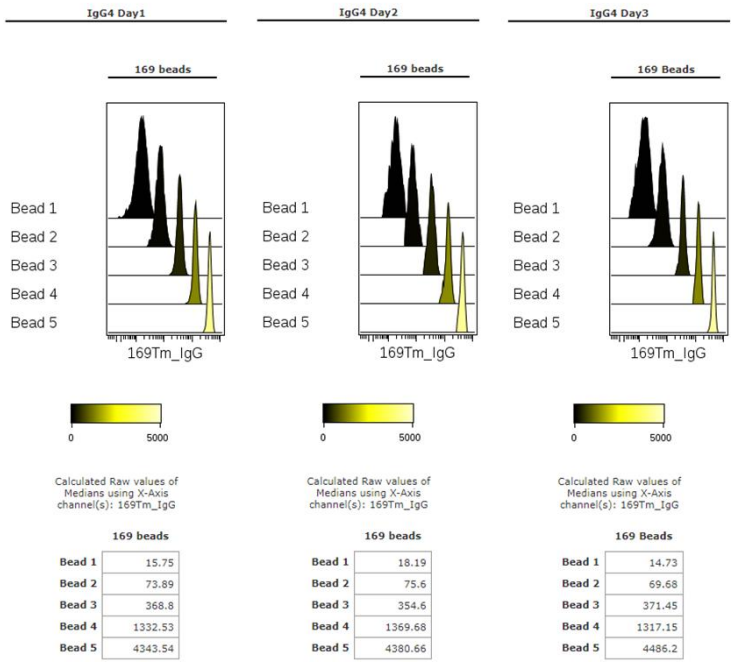

Calculated Raw values of Medians using X-Axis channel(s): 169Tm_IgG

169 beads	
Bead 1	15.75
Bead 2	73.89
Bead 3	368.8
Bead 4	1332.53
Bead 5	4343.54

Calculated Raw values of Medians using X-Axis channel(s): 169Tm_IgG

169 beads	
Bead 1	18.19
Bead 2	75.6
Bead 3	354.6
Bead 4	1369.68
Bead 5	4380.66

Calculated Raw values of Medians using X-Axis channel(s): 169Tm_IgG

169 Beads	
Bead 1	14.73
Bead 2	69.68
Bead 3	371.45
Bead 4	1317.15
Bead 5	4486.2

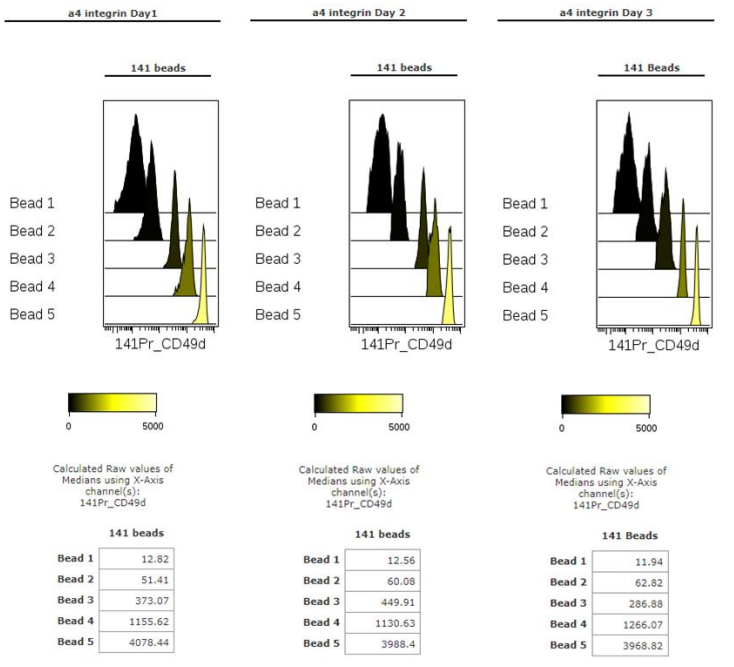

Calculated Raw values of Medians using X-Axis channel(s): 141Pr_CD49d

141 beads	
Bead 1	12.82
Bead 2	51.41
Bead 3	373.07
Bead 4	1155.62
Bead 5	4078.44

Calculated Raw values of Medians using X-Axis channel(s): 141Pr_CD49d

141 beads	
Bead 1	12.56
Bead 2	60.08
Bead 3	449.91
Bead 4	1130.63
Bead 5	3988.4

Calculated Raw values of Medians using X-Axis channel(s): 141Pr_CD49d

141 Beads	
Bead 1	11.94
Bead 2	62.82
Bead 3	286.88
Bead 4	1266.07
Bead 5	3968.82

c) QSC bead standardization of patient PBL samples: Standard curves were created in QuickCal (Bangs Laboratories) based on median dual counts of anti-IgG4 (^{169}Tm) and anti-α4 integrin (^{141}Pr) (previous panel) in five QSC bead populations with increasing ABC. For bead standardization of patient PBL samples, raw signal intensities (dual count 90th percentiles, shown in supplementary Figure 1b) of the same antibodies in eight cell types were plotted into the correlating standard curves and translated into ABC values. Standard curves in the three replicate experiments (days 1, 2, and 3) are shown.

Day 1, Anti-IgG4 (^{169}Tm)

Bangs Laboratories, Inc. — **QuickCal v 2.3**

QSC® anti-Mouse IgG Lot # 13359 + custom low peak

Acquisition Date	
Entry Date	

Bead	ABC	Dual counts
Blank		0
Bead #1	2685	15,75
Bead #2	12319	73,89
Bead #3	65076	368,8
Bead #4	249738	1332,53
Bead #5	814348	4343,54

Comments:	
	Day 1
Instrument	
Make/Model:	
PMT Setting:	
Antibody Used:	Anti-IgG4 (169Tm)
Regression Coefficient	0,9999
Detection Threshold:	#NUM!

#	Sample Name	Dual counts	ABC
1	Mem B cell	55,01	9 413
2	Monocyte	56,07	9 598
3	CD4 CM T	25,28	4 254
4	CD4 EM T	37,49	6 362
5	CD4 EMRA T	29,05	4 903
6	CD8 CM T	30,15	5 092
7	CD8 EF T	33,39	5 652
8	CD8 EMRA T	36,1	6 121
9	100% sat:		
10	Mem B cell	87,27	15 082
11	Monocyte	101,26	17 556
12	CD4 CM T	46,57	7 940
13	CD4 EM T	72,47	12 474
14	CD4 EMRA T	45,28	7 715
15	CD8 CM T	55,58	9 512
16	CD8 EF T	59,88	10 265
17	CD8 EMRA T	68,84	11 836
18			
19			
20			
21			

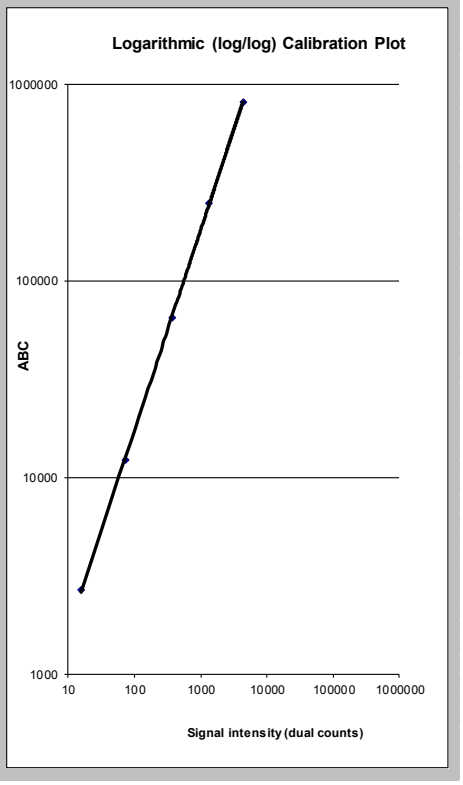

Day 1, Anti-α4 integrin (^{141}Pr)

Bangs Laboratories, Inc. — **QuickCal v 2.3**

QSC® anti-Mouse IgG Lot # 13359 + custom low peak

Acquisition Date	
Entry Date	

Bead	ABC	Dual counts
Blank		0
Bead #1	2685	12,82
Bead #2	12319	51,41
Bead #3	65076	373,07
Bead #4	249738	1155,62
Bead #5	814348	4078,44

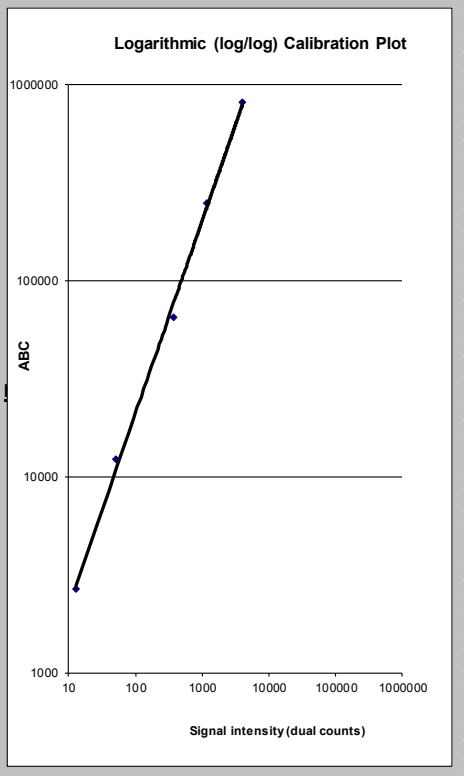

Comments:	
	Day 1
Instrument	
Make/Model:	
PMT Setting:	
Antibody Used:	Anti-α4 integrin (141Pr)
Regression Coefficient	0,9989
Detection Threshold:	#NUM!

#	Sample Name	Dual counts	ABC
1	Mem B cell	54,36	11 542
2	Monocyte	73,63	15 553
3	CD4 CM T	34,83	7 452
4	CD4 EM T	48,73	10 366
5	CD4 EMRA T	30,6	6 561
6	CD8 CM T	35,27	7 544
7	CD8 EF T	38,84	8 294
8	CD8 EMRA T	44,24	9 427
9	100% sat:		
10	Mem B cell	72,6	15 339
11	Monocyte	88,73	18 683
12	CD4 CM T	40,54	8 651
13	CD4 EM T	63,75	13 499
14	CD4 EMRA T	39	8 328
15	CD8 CM T	43,18	9 205
16	CD8 EF T	48,67	10 354
17	CD8 EMRA T	53,13	11 286
18			
19			
20			
21			

Day 2, Anti-IgG4 (^{169}Tm)

Bangs Laboratories, Inc. QuickCal v 2.3

QSC® anti-Mouse IgG Lot # 13359 + custom low peak

Acquisition Date	
Entry Date	

Bead	ABC	Dual counts
Blank		0
Bead #1	2685	18,19
Bead #2	12319	75,6
Bead #3	65076	354,6
Bead #4	249738	1369,68
Bead #5	814348	4380

Comments:	
	Day 2
Instrument	
Make/Model:	
PMT Setting:	
Antibody Used:	Anti-IgG4 (169Tm)
Regression Coefficient	0,9999
Detection Threshold:	#NUM!

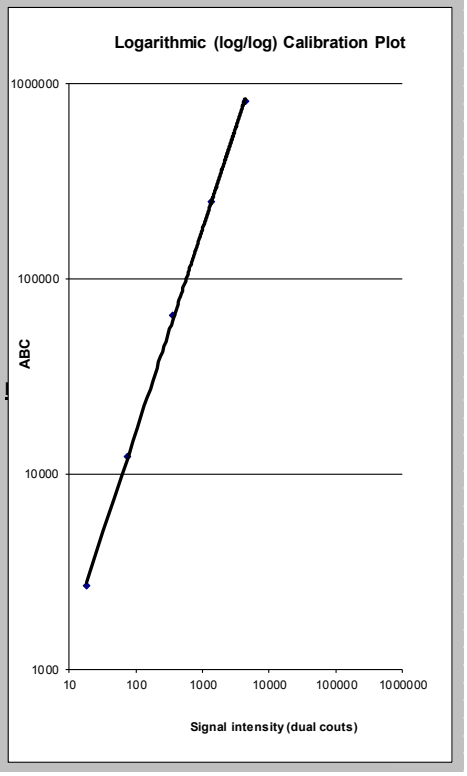

#	Sample Name	Dual counts	ABC
1	Mem B cell	57,9	9 267
2	Monocyte	60,76	9 744
3	CD4 CM T	27,45	4 257
4	CD4 EM T	42,04	6 638
5	CD4 EMRA T	29,74	4 628
6	CD8 CM T	35,64	5 589
7	CD8 EF T	38,97	6 134
8	CD8 EMRA T	43,45	6 870
9	100% sat:		
10	Mem B cell	69,79	11 258
11	Monocyte	81,18	13 179
12	CD4 CM T	35,46	5 559
13	CD4 EM T	58,16	9 310
14	CD4 EMRA T	36,79	5 777
15	CD8 CM T	43,13	6 818
16	CD8 EF T	50,1	7 970
17	CD8 EMRA T	55,62	8 887
18			
19			
20			
21			

Day 2, Anti-α4 integrin (^{141}Pr)

Bangs Laboratories, Inc. QuickCal v 2.3

QSC® anti-Mouse IgG Lot # 13359 + custom low peak

Acquisition Date	
Entry Date	

Bead	ABC	Dual counts
Blank		0
Bead #1	2685	12,56
Bead #2	12319	60,08
Bead #3	65076	449,91
Bead #4	249738	1130,63
Bead #5	814348	3988,4

Comments:	
	Day 2
Instrument	
Make/Model:	
PMT Setting:	
Antibody Used:	Anti- α4 integrin (141Pr)
Regression Coefficient	0,9972
Detection Threshold:	#NUM!

#	Sample Name	Dual counts	ABC
1	Mem B cell	61,04	12 113
2	Monocyte	83,99	16 615
3	CD4 CM T	35,86	7 153
4	CD4 EM T	56,34	11 189
5	CD4 EMRA T	33,53	6 693
6	CD8 CM T	42,26	8 416
7	CD8 EF T	44,16	8 791
8	CD8 EMRA T	49,92	9 926
9	100% sat:		
10	Mem B cell	53,9	10 709
11	Monocyte	74,89	14 831
12	CD4 CM T	32,35	6 460
13	CD4 EM T	49,94	9 930
14	CD4 EMRA T	28,23	5 644
15	CD8 CM T	33,92	6 770
16	CD8 EF T	40	7 971
17	CD8 EMRA T	42,08	8 381
18			
19			
20			
21			

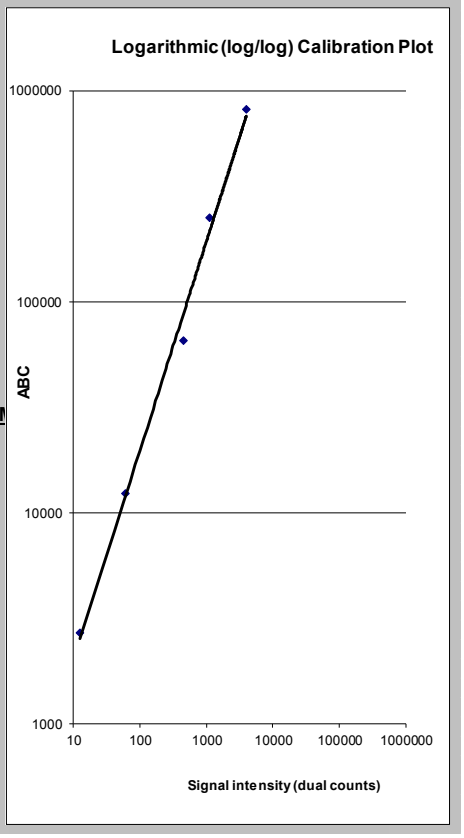

Day 3, Anti-IgG4 (^{169}Tm)

Bangs Laboratories, Inc. — **QuickCal v 2.3**

QSC® anti-Mouse IgG Lot # 13359 + custom low peak

Acquisition Date	
Entry Date	

Bead	ABC	Dual counts
Blank		0
Bead #1	2685	14,73
Bead #2	12319	69,68
Bead #3	65076	371,45
Bead #4	249738	1317,15
Bead #5	814348	4486,2

Comments:	
	Day 3
Instrument	
Make/Model:	
PMT Setting:	
Antibody Used:	Anti-IgG4 (169Tm)
Regression Coefficient	0,9999
Detection Threshold:	#NUM!

#	Sample Name	Dual counts	ABC
1	Mem B cell	54,64	9 824
2	Monocyte	50,45	9 068
3	CD4 CM T	22,86	4 096
4	CD4 EM T	33,57	6 024
5	CD4 EMRA T	24,1	4 319
6	CD8 CM T	28,14	5 046
7	CD8 EF T	33,63	6 035
8	CD8 EMRA T	34,68	6 224
9	100% sat:		
10	Mem B cell	70,32	12 656
11	Monocyte	72,57	13 063
12	CD4 CM T	33,92	6 087
13	CD4 EM T	53,61	9 638
14	CD4 EMRA T	37,6	6 750
15	CD8 CM T	42,82	7 691
16	CD8 EF T	46,74	8 399
17	CD8 EMRA T	53,86	9 683
18			
19			
20			
21			

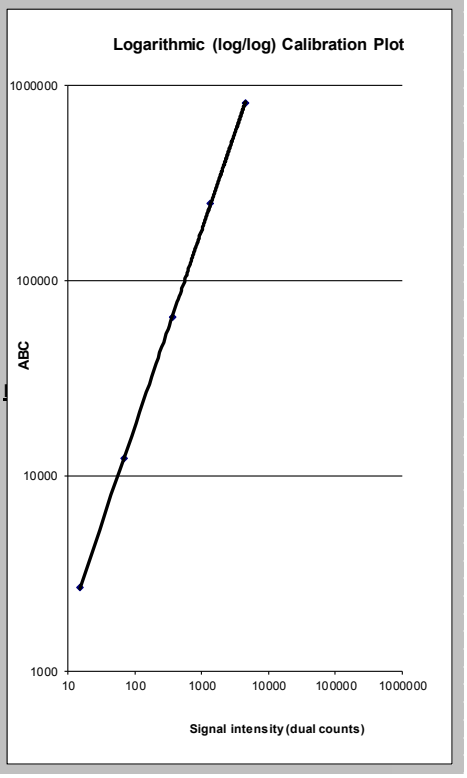

Day 3, Anti-α4 integrin (^{141}Pr)

Bangs Laboratories, Inc. QuickCal v 2.3

QSC® anti-Mouse IgG Lot # 13359 + custom low peak

Acquisition Date	
Entry Date	

Bead	ABC	Dual counts
Blank		0
Bead #1	2685	11,94
Bead #2	12319	62,82
Bead #3	65076	286,88
Bead #4	249738	1266,07
Bead #5	814348	3968,82

Comments:	
	Day 3
Instrument	
Make/Model:	
PMT Setting:	
Antibody Used:	Anti- α4 integrin (141Pr)
Regression Coefficient	0,9996
Detection Threshold:	#NUM!

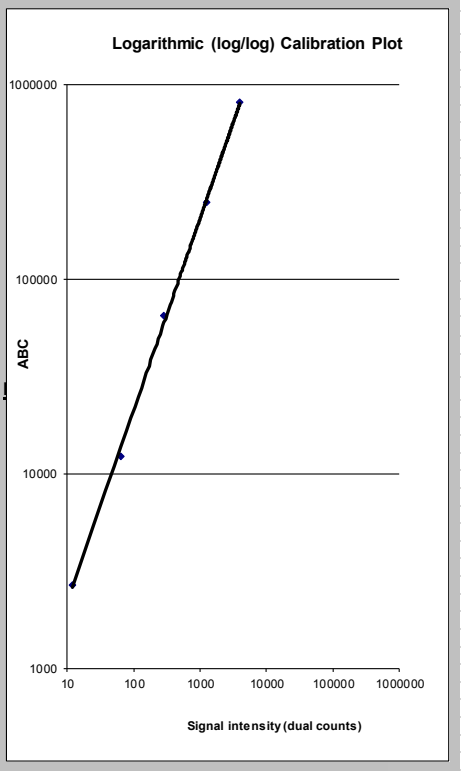

#	Sample Name	Dual counts	ABC
1	Mem B cell	56,83	12 140
2	Monocyte	66,76	14 232
3	CD4 CM T	27,83	5 998
4	CD4 EM T	42,44	9 099
5	CD4 EMRA T	25,73	5 551
6	CD8 CM T	30,18	6 498
7	CD8 EM T	38,53	8 271
8	CD8 EMRA T	40,38	8 663
9	100% sat:		
10	Mem B cell	53,47	11 431
11	Monocyte	64,21	13 695
12	CD4 CM T	27,87	6 007
13	CD4 EM T	42,42	9 095
14	CD4 EMRA T	29,26	6 302
15	CD8 CM T	28,95	6 236
16	CD8 EF T	35,57	7 643
17	CD8 EMRA T	36,73	7 889
18			
19			
20			
21			

Supplementary Figure 3:

a) QSC beads acquired on a Fortessa flow cytometer without (left) and with (right) OsO_4 labeling prior to antibody staining stained with anti-IgG4-PE. Median fluorescence intensity (MFI) in the four standard beads are shown.

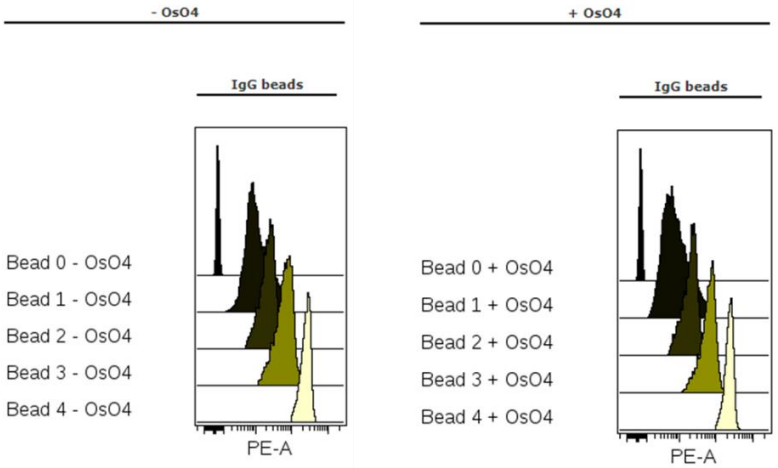

Calculated Raw values of Medians using X-Axis channel(s): PE-A

	IgG beads
Bead 0 - OsO4	29.89
Bead 1 - OsO4	999.18
Bead 2 - OsO4	2187.77
Bead 3 - OsO4	6324.48
Bead 4 - OsO4	23982.15

Calculated Raw values of Medians using X-Axis channel(s): PE-A

	IgG beads
Bead 0 + OsO4	28.67
Bead 1 + OsO4	711.87
Bead 2 + OsO4	2045.03
Bead 3 + OsO4	6292.76
Bead 4 + OsO4	22310.14

b) Correlation of signal intensity of the same five QSC bead populations stained with either anti-IgG4-PE or anti-IgG4 (^{169}Tm) and acquired with flow or mass cytometry, respectively.

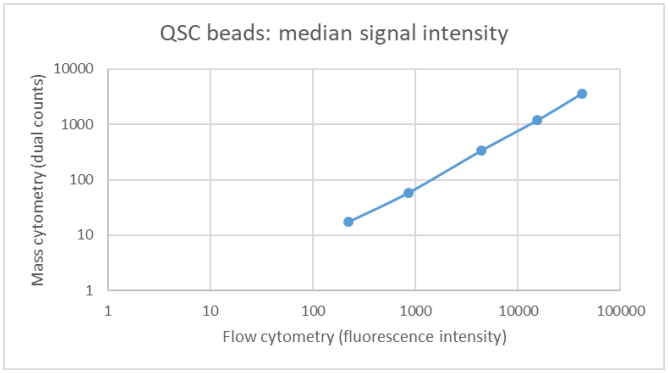

Supplementary Figure 4: Quality control experiments using PBL samples:

a) Preexisting metal in the detection channels for natalizumab (IgG4 ^{169}Tm, left) or α4 integrin (CD49d ^{141}Pr, right) in unstained PBL samples from the healthy donor (top) and the patient (bottom). Samples were barcoded and Ir-intercalated for event detection.

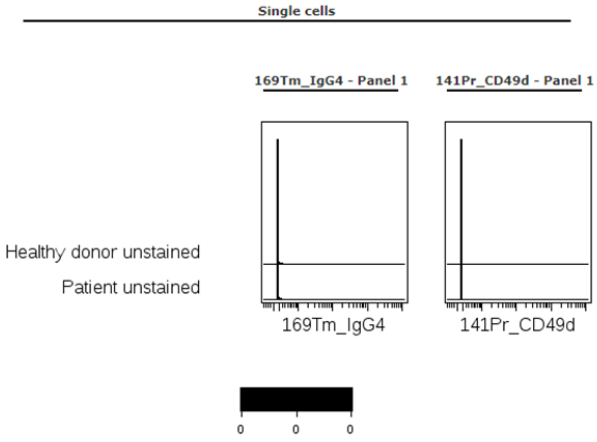

Calculated Raw values of Medians using X-Axis channel(s): Panel/Channel Values

	169Tm_IgG4 - Panel 1	141Pr_CD49d - Panel 1
Healthy donor unstained	0.0	0.0
Patient unstained	0.0	0.0

b) Mass-minus-one (MMO) controls in patient PBLs: 141 signal in sample stained with the panel minus anti-α4 integrin (left) and 169 signal in sample stained with the panel minus anti-IgG4 (right).

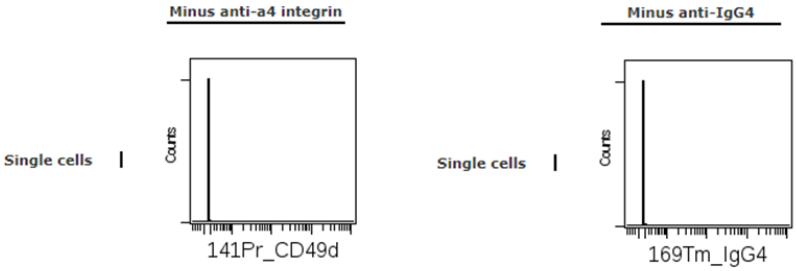

Calculated Raw values of Medians using X-Axis channel(s): 141Pr_CD49d

	Minus anti-a4 integrin
Single cells	0.0

Calculated Raw values of Medians using X-Axis channel(s): 169Tm_IgG4

	Minus anti-IgG4
Single cells	0.0

c) Healthy donor PBLs not treated with natalizumab. Median dual counts of anti-IgG4 in each of the eight cell types are shown.

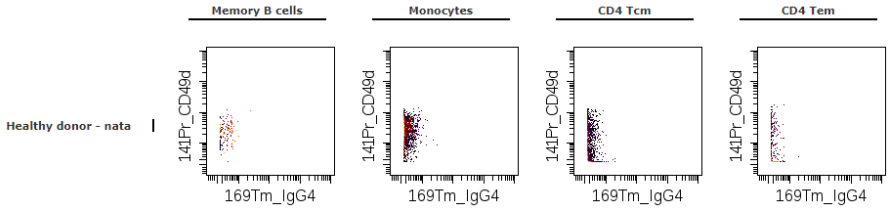

Calculated Raw values of Medians using X-Axis channel(s): 169Tm_IgG4

	Memory B cells	Monocytes	CD4 Tcm	CD4 Tem
Healthy donor - nata	1.77	0.57	0.0	0.35

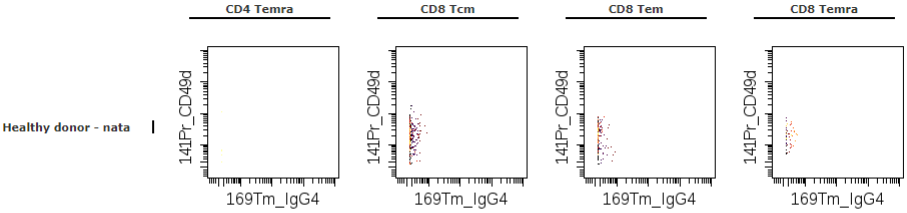

Calculated Raw values of Medians using X-Axis channel(s): 169Tm_IgG4

	CD4 Temra	CD8 Tcm	CD8 Tem	CD8 Temra
Healthy donor - nata	0.0	0.04	0.0	0.33

d) Healthy donor PBLs with (top) and without (bottom) *in vitro* incubation with natalizumab. The presence of drug (IgG4, left) did not affect detection of α4 integrin (CD49d, right), indicating non-competitive binding of anti-α4 integrin and natalizumab to different epitopes of α4 integrin. The 90th percentiles of anti-IgG4 and anti- α4 integrin in non-granulocytes are shown.

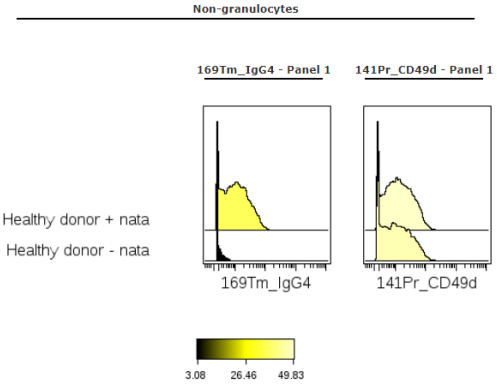

Calculated Raw values of Percentile using X-Axis channel(s): Panel/Channel Values

	169Tm_IgG4 - Panel 1	141Pr_CD49d - Panel 1
Healthy donor + nata	37.2	49.83
Healthy donor - nata	3.08	47.45

II

ARTICLE OPEN ACCESS

Wearing-off at the end of natalizumab dosing intervals is associated with low receptor occupancy

Gerd Haga Bringeland, MD, Nello Blaser, PhD, Kjell-Morten Myhr, MD, PhD, Christian Alexander Vedeler, MD, PhD, and Sonia Gavasso, PhD

Correspondence
Dr. Bringeland
gerd.haga.bringeland@helse-bergen.no

Neurol Neuroimmunol Neuroinflamm 2020;7:e678. doi:10.1212/NXI.0000000000000678

Abstract

Objective

We aimed to investigate whether wearing-off symptoms at the end of the natalizumab dosing interval were associated with clinical and demographic patient characteristics or natalizumab receptor occupancy (RO) on leukocytes.

Methods

In this cross-sectional study of 40 patients with relapsing-remitting MS (RRMS) receiving natalizumab at the Department of Neurology, Haukeland University Hospital, we recorded clinical and demographic data including age, body mass index (BMI), working status, smoking habits, disease characteristics, treatment duration, vitamin D levels, and wearing-off symptoms. We quantified neurofilament light chain in serum and measured natalizumab RO in leukocyte subtypes by high-parameter mass cytometry. Associations with wearing-off symptoms were analyzed.

Results

Eight (20.0%) patients who reported regular occurrence of wearing-off symptoms, 9 (22.5%) who sometimes had wearing-off symptoms, and 23 (57.5%) who did not have wearing-off symptoms were evaluated. Patients who regularly had wearing-off symptoms had lower natalizumab RO than patients who reported having such symptoms sometimes or never. The former group also had higher BMI and higher frequency of sick leave. High BMI was associated with low RO. No other demographic or disease characteristics were associated with the phenomenon.

Conclusions

Low RO may explain the wearing-off phenomenon observed in some patients with RRMS treated with natalizumab, and high BMI may be the underlying cause.

From the Neuro-SysMed (G.H.B., K.-M.M., C.A.V., S.G.), Department of Neurology, Haukeland University Hospital, Bergen, Norway; Department of Clinical Medicine (G.H.B., K.-M.M., C.A.V., S.G.), University of Bergen, Bergen, Norway; and Department of Informatics (N.B.), University of Bergen, Bergen, Norway.

Go to Neurology.org/NN for full disclosures. Funding information is provided at the end of the article.

The Article Processing Charge was funded by the authors.

Glossary

BMI = body mass index; **cDC** = conventional dendritic cell; **EID** = extended interval dosing; **PBL** = peripheral blood leukocyte; **PML** = progressive multifocal leukoencephalopathy; **RRMS** = relapsing-remitting MS; **RO** = receptor occupancy.

Natalizumab (Tysabri®, Biogen, Cambridge, MA) is a therapeutic monoclonal antibody used to treat patients with relapsing-remitting MS (RRMS). It prevents leukocyte migration across the blood-brain barrier into the CNS by binding to the α4 subunit of the α4β1 integrin (α4 integrin) on leukocyte surfaces.[1] Natalizumab is administered IV at a standard dose of 300 mg every 4 weeks.

Although highly efficacious in preventing disease activity, many patients report the so-called wearing-off symptoms at the end of the 4-week dosing interval. Although wearing-off symptoms are often reported, only a few previous studies have described the phenomenon, and little is known about the underlying causes of these symptoms.[2–5]

Natalizumab receptor occupancy (RO) is defined as the level of natalizumab bound to α4 integrin on leukocytes and is a potential biomarker to monitor and individualize natalizumab therapy.[6] RO has traditionally been measured with flow cytometry. Mass cytometry is a novel technology for high-parameter single-cell analysis. For mass cytometry, detection antibodies are conjugated to metals instead of fluorophores, allowing analysis of over 40 parameters simultaneously on single cells.[7] This permits measurement of RO in conjunction with more markers and in more cell types of interest than is currently possible by flow cytometry. We aimed to investigate whether clinical and demographic patient characteristics or natalizumab RO were associated with the wearing-off phenomenon by using high-parameter mass cytometry to measure natalizumab RO in patients with RRMS treated with natalizumab who do and do not report wearing-off symptoms at the end of dosing intervals.

Methods

Patients

We invited all patients older than 18 years with a diagnosis of RRMS who had received a minimum of 6 natalizumab infusions at the Department of Neurology, Haukeland University Hospital (n = 45) to participate in this cross-sectional study; 40 agreed to participate. At inclusion, we obtained baseline demographic and clinical patient characteristics from the patients' medical journal including age, sex, disease duration (years since first MS symptoms), natalizumab treatment duration (years since first natalizumab infusion), numbers of new MRI lesions and clinical relapses in the last year before inclusion, serum vitamin D level, Symbol Digit Modalities Test score,[8] and Expanded Disability Status Scale score.[9] Each patient filled in questionnaires on fatigue (Fatigue Severity Scale),[10] and on working status, smoking habits, weight, height, and whether they had wearing-off symptoms (never, sometimes, and regularly), and, if applicable, type of symptoms.

Standard protocol approvals, registrations, and patient consents

The study was approved by the Regional Committee for Medical Research Ethics, Western Norway (REK 2016/579), and written informed consent was obtained from all participating patients.

Blood samples

At inclusion, we collected blood before and after natalizumab infusion. For mass cytometry analysis, whole blood was collected in heparinized Vacutainer tubes (Greiner Bio-One GmbH, Kremsmünster, Austria), incubated with Proteomic Stabilizer (Smart Tube, Inc, San Carlos, CA) for 10 minutes, and stored at −80°C. Whole blood was then thawed, and red blood cell lysis was performed with Thaw-lyse buffer I (Smart Tube, Inc) to obtain peripheral blood leukocytes (PBLs). For neurofilament measurement, whole blood was collected in Vacutainer tubes with no additives (BD, Plymouth, United Kingdom), incubated at room temperature for 60 minutes, and centrifuged at room temperature at 3,200*g* for 13 minutes before the serum was retrieved and stored at −80°C.

Neurofilament measurement

Serum samples were thawed, and the concentration of neurofilament light chain (NF-L) was measured with a single-molecule array (Simoa) assay (Quanterix, Billerica, MA) according to the manufacturer's protocol.

Mass cytometry RO assay

PBLs were stained with a 36-parameter mass cytometry antibody panel (table e-1, links.lww.com/NXI/A190). Bound natalizumab was detected with an anti-IgG4 antibody (conjugated to ^{169}Tm). Total α4 integrin was detected with an anti-CD49d antibody (conjugated to ^{141}Pr) specific for a different epitope than natalizumab. The 36 metal-conjugated antibodies were purchased preconjugated (Fluidigm, South San Francisco, CA), or antibodies were purchased (BioLegend, San Diego, CA, R&D Systems, Minneapolis, MN, and Abcam, Cambridge, Great Britain) and conjugated in-house to metals with the Maxpar Antibody Labeling Kit (Fluidigm). Briefly, we thawed, barcoded (Cell-ID 20-Plex Pd Barcoding Kit, Fluidigm), and pooled PBL samples in batches of 20 randomly distributed samples, keeping paired samples from the same patients in the same batch. A control PBL sample from 1 healthy donor was included in each batch. Pooled PBLs were first incubated in Maxpar cell stain buffer with 100 U/mL heparin (LEO Pharma A/S) for 20 minutes at room temperature[11] and then incubated with the antibody cocktail

Table 1 Demographic and clinical characteristics of patients with RRMS and the frequency of wearing-off symptoms

		Wearing-off symptoms				
	Total	Never	Sometimes	Regularly	p Value[a]	*p* Value (age adjusted)[b]
Patients with RRMS, n (%)	40 (100)	23 (57.5)	9 (22.5)	8 (20.0)		
Age, y	43.0 (34.0–49.3)	45.0 (35.5–52.0)	34.0 (31.0–51.0)	43.0 (37.0–43.8)	0.382	—
Sex, female, n (%)	25 (62.5)	15 (65.2)	3 (33.3)	7 (87.5)	0.069	0.063
Height, cm	171 (166–179)	169 (165–173)	180 (177–182)	171 (167–173)	0.078	0.047
Weight, kg	75.0 (67.0–82.5)	75.0 (60.0–79.5)	73.0 (67.0–82.0)	81.5 (76.5–87.8)	0.107	0.022
BMI	25.3 (22.6–27.2)	25.1 (22.2–26.6)	23.9 (22.5–25.2)	27.8 (26.5–31.2)	0.023	0.006
Current smoker, n (%)	7 (17.5)	4 (17.4)	2 (22.2)	1 (12.5)	0.873	0.860
Sick leave, n (%)	9 (22.5)	2 (8.7)	3 (33.3)	4 (50.0)	0.04	0.013
Disease duration, y	13.0 (8.0–17.0)	13.0 (8.0–17.5)	13.0 (8.0–17.0)	12.5 (8.8–16.0)	0.949	0.798
Treatment duration, y	4.0 (3.0–7.3)	4.0 (3.0–8.5)	5.0 (3.0–6.0)	4.5 (2.0–8.0)	0.999	0.904
Dose number	56.5 (39.0–102.3)	49.0 (39.0–107.5)	69.0 (41.0–78.0)	63.5 (33.5–111.8)	0.974	0.816
Days since last dose	28.0 (28.0–28.0)	28.0 (28.0–28.5)	28.0 (28.0–28.0)	28.00 (27.0–28.0)	0.358	0.375
EDSS score	2.0 (1.0–3.5)	2.0 (1.0–3.5)	2.0 (1.5–2.5)	2.0 (1.5–3.1)	0.880	0.682
FSS score	4.8 (3.3–5.7)	4.6 (3.3–5.4)	4.3 (3.0–6.1)	5.3 (4.8–5.8)	0.223	0.186
SDMT	57.0 (50.0–67.3)	64.0 (52.5–68.5)	58.0 (54.0–64.0)	48.5 (45.5–56.0)	0.151	0.109
New lesions detected by MRI in last year	0.0 (0.0–0.0)	0.0 (0.0–0.0)	0.0 (0.0–0.0)	0.0 (0.0–0.0)	—	—
Relapse activity in last year	0.0 (0.0–0.0)	0.0 (0.0–0.0)	0.0 (0.0–0.0)	0.0 (0.0–0.0)	—	—
Serum vitamin D, nmol/L	74.50 (58.00–93.25)	76.0 (61.0–99.5)	74.0 (29.0–86.0)	73.0 (62.5–90.5)	0.796	0.773
Serum NF-L, pg/mL	6.1 (4.5–8.9)	8.0 (5.8–9.6)	5.1 (4.3–5.9)	4.6 (4.1–5.3)	0.011	0.390

Abbreviations: BMI = body mass index; EDSS = Expanded Disability Status Scale; FSS = Fatigue Severity Scale; SDMT = Symbol Digit Modalities Test; NF-L = neurofilament light chain. RRMS = relapsing-remitting MS.
Numbers are median (interquartile range) unless otherwise stated.
[a] Unadjusted *p* values are calculated using a Kruskal-Wallis test.
[b] Age-adjusted *p* values are calculated with a likelihood ratio test between a linear model with only age and a linear model with age and the relevant baseline variable as predictors.

for 30 minutes at room temperature. Stained PBLs were washed, fixed in fresh 2% paraformaldehyde (Thermo Scientific, Waltham, MA) in Maxpar PBS for 10 minutes at room temperature, and then incubated in 125 nM Cell-ID™ Intercalator-Ir in Maxpar Fix and Perm Buffer (Fluidigm) at 4°C overnight. We performed all centrifugation steps at room temperature at 800*g*.

Before mass cytometry analysis, PBLs were resuspended in 0.1× EQ Four Element Calibration Beads (Fluidigm) in Maxpar cell acquisition solution (Fluidigm) and filtered (Corning Falcon Test Tube with Cell Strainer Snap Cap, Fisher Scientific, Hampton, NN). We used antibody binding QSC beads (Bangs Laboratories, Inc., catalog number 815A, Fishers, IN) to standardize signal intensities from anti-IgG4 (conjugated to ^{169}Tm) and anti-CD49d (conjugated to ^{141}Pr) as previously described in detail.[12] We analyzed PBL and QSC beads with the same standard settings on a Helios® mass cytometer (Fluidigm) after tuning (CyTOF Tuning Solution, Fluidigm) and calibration (EQ Four Element Calibration Beads, Fluidigm) according to the manufacture's guidelines. Healthy control PBLs served as a negative control for anti-IgG4 in the absence of natalizumab, and patient PBLs incubated in vitro with natalizumab to an expected RO of 100%

Table 2 Frequency of reported wearing-off symptoms

	Wearing-off symptoms	
Symptom	**Sometimes**	**Regularly**
Fatigue	67%	63%
Psychological	33%	25%
Walking difficulty	11%	25%
Spasms	11%	13%
Pain	0%	13%

served as positive controls. Further quality control experiments were performed as previously described in detail.[12]

Data processing, analysis, and statistics

After acquisition of QSC beads, we normalized (Fluidigm normalizer) and exported FCS files to Cytobank software (Cytobank, Inc., Beckman Coulter, Brea, CA) and created QSC bead standard curves (QuickCal template, Bangs Laboratories). After acquisition of PBL samples, we normalized (Fluidigm normalizer), debarcoded (Fluidigm Debarcoder), and exported the FSC files to Cytobank software for gating and downstream analysis (figure e-1, links.lww.com/NXI/A190). We performed clean-up gating to obtain single PBLs, and the data were arcsinh transformed with a scale argument of 5.[13] We then performed 2 independent analyses for RO calculation in single PBLs: one was a manual analysis, and one used an unsupervised approach.

In the manual approach, we first identified the following 11 leukocyte subtypes of interest by manual gating: $CD8^+$ central memory (T_{CM}), effector memory (T_{EM}), effector memory RA (T_{EMRA}) T cells; $CD4^+$ T_{EM}, T_{CM}, and T_{EMRA} cells; $CD34^+$ cells; memory B cells; natural killer (NK) cells; monocytes; and conventional dendritic cells (cDCs). We then plotted the signal intensities (dual count 90th percentiles) of anti-IgG4 and anti-CD49d in each of these cell types with the QSC bead standard curves to obtain bead standardized values and calculated %RO by the following formula:

$$\%\mathrm{RO} = 100 \times \frac{\text{QSC bead standardized anti} - \text{IgG4 (169Tm)}}{\text{QSC bead standardized anti} - \text{CD49d (141Pr)}}$$

We compared ROs in the leukocyte subtypes in different patient groups using a Kruskal-Wallis test.

In the unsupervised approach, we used R (version 3.4.3) to add an extra variable into the FSC files: the ratio between signal intensities of anti-IgG4 and anti-CD49d in each cell. This resulted in an RO estimate for each cell. For visualization of high-dimensional single-cell data, we performed automated dimensionality reduction with stochastic neighborhood embedding (viSNE, Cytobank).[14] We analyzed the new RO variable with the cluster identification, characterization, and regression tool CITRUS (Cytobank), an algorithm that automatically identifies statistically significant differences between patient groups.[15] We applied the correlative model Significance Analysis of Microarrays with a false discovery rate (adjusted for multiple hypothesis testing) of 1%. CITRUS was run with 10 repetitions.

The relationship between baseline demographic variables and wearing-off was compared using a Kruskal-Wallis test. Statistical differences with $p < 0.05$ were considered significant using a 2-sided comparison. To test the age-corrected relationship between baseline variables and wearing-off, we used a likelihood ratio test between a linear model with only age and a linear model with age and the relevant baseline variable as predictors. We conducted a linear regression of the association between RO and body mass index (BMI) and used a t test to assess whether the slope was significantly different from zero. We used R version 3.4.3[16] for statistical analysis and correlation plots.

Data availability

FCS files from anonymized patient PBL samples can be accessed in the Flow Repository (ID: FR-FCM-Z2A9).

Results

Patient characteristics

Of the 45 patients who were eligible for inclusion, 40 (89%) consented to participate in the study. Of 5 (11%) nonconsenting patients, 1 refused participation, and 4 had infusion time points outside of the opening hours of the routine laboratory where blood samples were collected. Eight (20.0%) of the 40 participating patients reported having wearing-off symptoms regularly at the end of every dosing interval, 9 (22.5%) sometimes did, and 23 (57.5%) reported never having wearing-off symptoms (table 1). The most frequent wearing-off symptom was fatigue (table 2). Patients who regularly had wearing-off symptoms had significantly higher BMI and higher frequency of sick leave than patients who never or only sometimes experienced such symptoms (table 1). After age adjustment, weight was also significantly increased in patients with wearing-off symptoms regularly, whereas height was increased in patients with symptoms only sometimes. None of the other demographic or clinical patient characteristics were significantly different between the groups, and none of the included patients had clinical relapses or new lesions on MRI in the year before inclusion in the study. Age-adjusted median serum NF-L levels were similar between groups. There was no association between NF-L and BMI (data not shown).

Receptor occupancy

Manual gating of PBLs correlated well with the automated mapping with viSNE (figure 1A). We observed a broad range of natalizumab RO values. The median RO values in all leukocyte subtypes before infusion and in 10 of 11 leukocyte subtypes after infusion (figure 1B) were lower in patients who regularly experienced wearing-off symptoms than in patients who never or only sometimes experienced such symptoms. The differences were statistically significant in $CD8^+$ T_{EM}, $CD4^+$ T_{EM}, and

Figure 1 Natalizumab receptor occupancy (RO) in patients reporting wearing-off symptoms never, sometimes, or regularly

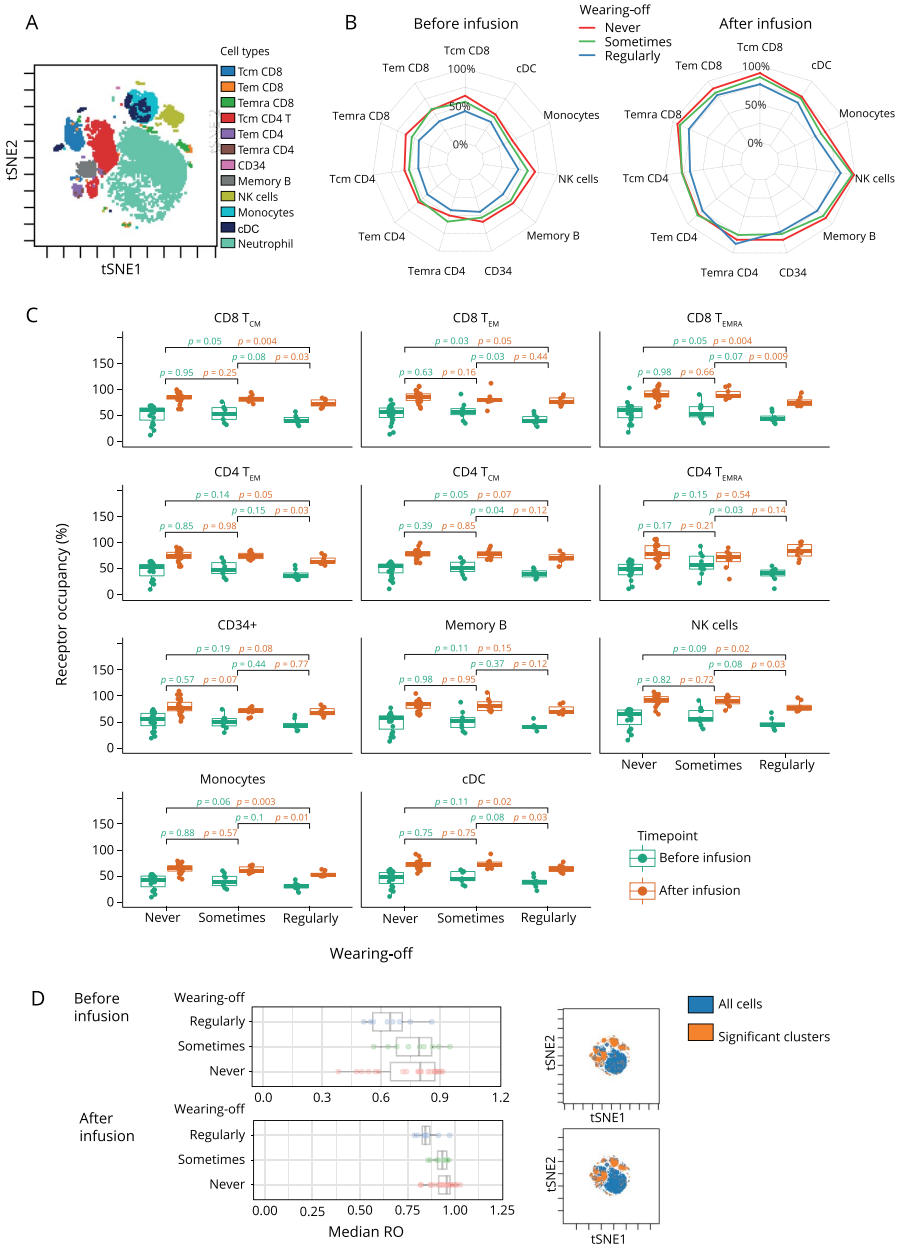

(A) Manually gated PBLs visualized on a viSNE map. RO was analyzed in 11 cell subtypes: $CD8^+$ central memory (T_{CM}), effector memory (T_{EM}), effector memory RA (T_{EMRA}) cells; $CD4^+$ T_{EM}, T_{CM}, and T_{EMRA} cells; $CD34^+$ cells; memory B cells; natural killer (NK) cells; monocytes; and conventional dendritic cells (cDCs). Neutrophils were not included in RO analysis. (B) Spider plot of median RO values in 11 cell subtypes in patients before and after natalizumab infusion. (C) RO values in 11 cell subtypes before and after natalizumab infusion. *p* values (Kruskal-Wallis test) comparing ROs in different wearing-off groups. (D) Left: median RO values in cell clusters significantly different between wearing-off groups (SAM analysis in CITRUS). Right: significant cell clusters are visualized on the viSNE map. PBL = peripheral blood leukocyte; SAM = Significance Analysis of Microarrays.

$CD4^+$ T_{EMRA} cells before infusion and in $CD8^+$ T_{CM}, $CD8^+$ T_{EMRA}, $CD4^+$ T_{CM} cells, NK cells, monocytes, and cDCs after infusion (figure 1C). Furthermore, in $CD8^+$ and $CD4^+$ T cells not stratified into subtypes, RO was significantly lower in both $CD8^+$ and $CD4^+$ T cells before infusion and in $CD8^+$ T cells after infusion in patients who regularly had wearing-off symptoms (figure e-2, links.lww.com/NXI/A190). Unsupervised analysis of median ROs with CITRUS also showed lower median natalizumab ROs in patients with regular wearing-off symptoms (figure 1D). Neither of the 2 analysis approaches showed significant differences between patients reporting wearing-off symptoms sometimes and never.

High BMI was associated with significantly lower RO in $CD8^+$ T_{EM} cells and cDCs before infusion and in $CD8^+$ T_{EMRA} cells, $CD34^+$ cells, and monocytes after infusion (figure 2).

Discussion

Natalizumab prevents disease activity in RRMS and has positive effects on subjective symptoms such as mood, fatigue, and cognitive function.[17,18] However, subjective wearing-off symptoms at the end of the 4-week interval are frequently reported by patients. In this study, wearing-off symptoms were reported by 42.5% of the patients (20.0% regularly and 22.5% only sometimes). We found lower natalizumab ROs in patients who regularly experienced wearing-off symptoms compared with patients who reported such symptoms never or only sometimes. The result was replicated in 2 separate data analysis pipelines. Furthermore, patients who reported regularly experiencing wearing-off symptoms had higher median body weight and BMI and higher sick leave frequency than those who rarely or never experienced such symptoms. Median height was increased in patients with symptoms only sometimes. Other clinical and demographic factors were similar between the patient groups. High BMI was associated with low RO in several leukocyte subtypes.

The main limitation of our study is the small patient cohort. As a consequence of this limited statistical power, we were only able to detect large effects and acknowledge that there may be associations of smaller effect size that went unnoticed. Wearing-off symptoms were less frequent in our study than the prevalence of 54%–63% reported in other studies, but as previously reported, the most frequent wearing-off symptom was fatigue.[2–5] In contrast to our results, a recent study found no association between the wearing-off effect and natalizumab RO or patient characteristics.[5] The previously reported study used flow cytometry to measure RO in $CD8^+$ T_{EM} cells and $CD8^+$ effector T cells. By using high-parameter mass cytometry, we were able to measure RO in 11 cell subtypes simultaneously. We found that patients who regularly experienced wearing-off symptoms had higher BMI than those who did not, and we also observed an association between high BMI and low RO. Body weight was higher in our cohort than in the previous study[5] (median 75.0 vs mean 72.9 kg) and was even more pronounced in the group with wearing-off symptoms regularly (median 81.5 vs mean 74.6 kg). van Kempen et al.[5] reported nonsignificant trends similar to our significant results. Our wearing-off population had higher body weight than theirs, which may explain why we observed statistically significant differences despite our small cohort size. The association between high BMI and low RO suggests that high BMI, by decreasing natalizumab RO, may be the underlying cause of the wearing-off phenomenon. Others have previously reported such an association between low natalizumab RO and high body weight or BMI, and some have suggested that the dose of natalizumab should be adjusted for body weight.[6,19,20] We found no associations between wearing-off symptoms and disease activity markers such as clinical relapses, new lesions detected by MRI in the past year, or serum NF-L levels.[21]

Figure 2 Linear regression analysis demonstrates an association between RO and BMI

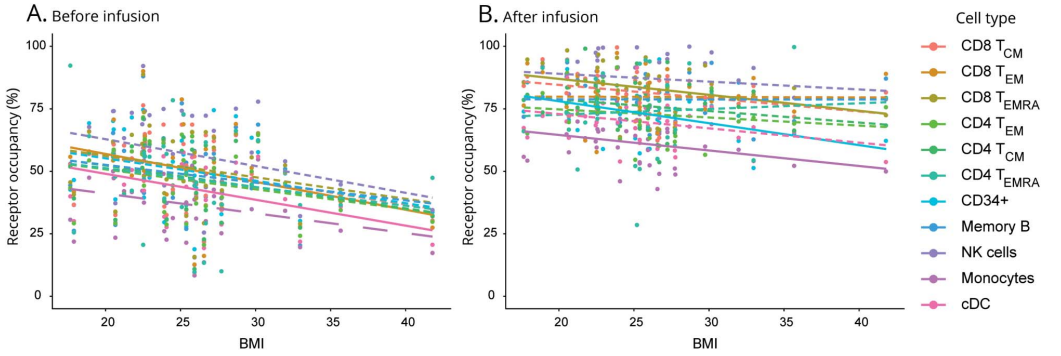

Plot of receptor occupancies (A) before and (B) after infusion for indicated cell types as a function of BMI. Solid lines have slopes that are significantly different from zero ($p < 0.05$), and dashed lines have slopes that are not significantly different from zero. BMI = body mass index; RO = receptor occupancy.

As also reported by others,[19] we observed large interindividual variations in natalizumab RO, and not all patients with low RO had high BMI. A previous study reported that body weight only partly predicts variability in natalizumab RO and suggested other factors such as density and turnover of α4β1 integrin that may drive the variability.[22]

It has been hypothesized that cytokines could induce the wearing-off symptoms.[4,5] We speculate that lower natalizumab RO at the end of the dosing interval could increase the migratory capacity of cytokine-producing leukocytes into the CNS resulting in the wearing-off symptoms. We found significantly lower RO in the T-cell subtypes $CD8^+$ T_{EM}, $CD4^+$ T_{EM}, and $CD4^+$ T_{EMRA} cells before infusion in patients who regularly had wearing-off symptoms. T_{EM} and T_{EMRA} cells home to the site of inflammation where they have effector functions such as secretion of proinflammatory cytokines and cytotoxicity; in contrast, T_{CM} cells and naive T cells home to secondary lymphoid organs.[23,24]

Our results suggest that low RO may be a contributing factor to the wearing-off phenomenon and that higher BMI may be an underlying cause. This supports the suggestion that natalizumab dosing should be personalized. Personalization has been mainly focused on extended interval dosing (EID).[19] This has particularly been driven by the risk of progressive multifocal leukoencephalopathy (PML), a serious complication of natalizumab therapy in patients previously exposed to JC virus.[25] Retrospective studies of off-label treatment with EID have shown maintained efficacy[26,27] and reduced PML risk[28] compared with standard interval dosing. However, these studies are limited by possible selection bias due to nonrandomized design, and the efficacy and safety of EID is not fully known. As patients who regularly experience wearing-off symptoms already have lower RO and report symptoms at the end of dosing intervals, extending dosing intervals could increase the risk of disease activity. We therefore do not recommend EID in patients reporting wearing-off symptoms regularly, as this could lead to an even lower RO at the end of the interval than observed with standard dosing.[6,19] Further studies should investigate whether wearing-off symptoms are associated with increased risk of RRMS disease activity and whether increasing RO by reduced dosing intervals or weight loss may mitigate the symptoms.

Acknowledgment

The authors thank Fritz og Ingrid Nilsens legat for financial research support and Hanne Linda Nakkestad at the Neurological Research Laboratory at Haukeland University Hospital for performing SiMOA analyses. The mass cytometry was performed at the Flow Cytometry Core Facility, Department of Clinical Science, University of Bergen. The Helios mass cytometer was funded by the Bergen Research Foundation. Neuro-SysMed is jointly hosted by Haukeland University Hospital and University of Bergen and supported as a Centre for Clinical Treatment Research (FKB) by grants from The Research Council of Norway, project number 288164.

Study funding

Supported by Fritz og Ingrid Nilsens legat for Forskning på Multippel sklerose.

Disclosure

G.H. Bringeland has received research support from Novartis and institutional support from the Regional Heath Authority of Western Norway. N. Blaser reports no disclosures. K.-M. Myhr has received grants and personal fees from Biogen and Novartis; personal fees from Genzyme, Roche, Almirall, and Merck; personal fees and nonfinancial support from Teva; and a research grant from the Norwegian Research Council (grant number 288164). C.A. Vedeler has received institutional support from the Regional Heath Authority of Western Norway and research grant support from the Norwegian Research Council (grant number 288164). Dr. Gavasso has received institutional support from the Regional Heath Authority of Western Norway. Go to Neurology.org/NN for full disclosures.

Publication history

Received by *Neurology: Neuroimmunology & Neuroinflammation* October 22, 2019. Accepted in final form December 20, 2019.

Appendix Authors

Name	Location	Role	Contribution
Gerd Haga Bringeland, MD	University of Bergen, and Haukeland University Hospital, Bergen, Norway	Author	Conception and design of the study; major role in the acquisition of data; interpretation of data; analysis of data; and revision of the manuscript for intellectual content
Nello Blaser, PhD	University of Bergen, Bergen, Norway	Author	Interpretation of data; analysis of data; and revision of the manuscript for intellectual content
Kjell-Morten Myhr, MD, PhD	University of Bergen, and Haukeland University Hospital, Bergen, Norway	Author	Conception and design of the study and revision of the manuscript for intellectual content
Christian Alexander Vedeler, MD, PhD	University of Bergen, and Haukeland University Hospital, Bergen, Norway	Author	Conception and design of the study and revision of the manuscript for intellectual content
Sonia Gavasso, PhD	University of Bergen, and Haukeland University Hospital, Bergen, Norway	Author	Conception and design of the study; interpretation of data; and revision of the manuscript for intellectual content

References

1. Polman CH, O'Connor PW, Havrdova E, et al. A randomized, placebo-controlled trial of natalizumab for relapsing multiple sclerosis. N Engl J Med 2006;354:899–910.
2. Katz J, Lathi E, Heyda L. Characterizing the Natalizumab "Wearing off" Effect [abstract]. ACTRIMS meeting; Poster DX36; 2014.
3. Gudesblatt M, Zarif M, Bumstead B, et al. Multiple sclerosis and natalizumab: "between the dose symptoms" [abstract 982]. Mult Scler 2012;18(suppl 14):P982.
4. Ratchford JN, Brock-Simmons R, Augsburger A, et al. Multiple sclerosis symptom recrudescence at the end of the natalizumab dosing cycle. Int J MS Care 2014;16:92–98.
5. van Kempen ZLE, Doesburg D, Dekker I, et al. The natalizumab wearing-off effect: end of natalizumab cycle; recurrence of MS symptoms. Neurology 2019;93:e1579–e1586.
6. Punet-Ortiz J, Hervas-Garcia JV, Teniente-Serra A, et al. Monitoring CD49d receptor occupancy: a method to optimize and personalize natalizumab therapy in multiple sclerosis patients. Cytometry B Clin Cytom 2018;94:327–333.
7. Bandura DR, Baranov VI, Ornatsky OI, et al. Mass cytometry: technique for real time single cell multitarget immunoassay based on inductively coupled plasma time-of-flight mass spectrometry. Anal Chem 2009;81:6813–6822.
8. Smith A. Symbol digit modalities test: Manual. Los Angeles, CA: Western Psychological Services; 1982.
9. Kurtzke JF. Rating neurologic impairment in multiple sclerosis: an expanded disability status scale (EDSS). Neurology 1983;33:1444–1452.
10. Krupp LB, LaRocca NG, Muir-Nash J, Steinberg AD. The fatigue severity scale. Application to patients with multiple sclerosis and systemic lupus erythematosus. Arch Neurol 1989;46:1121–1123.
11. Rahman AH, Tordesillas L, Berin MC. Heparin reduces nonspecific eosinophil staining artifacts in mass cytometry experiments. Cytometry A 2016;89:601–607.
12. Bringeland GH, Bader L, Blaser N, et al. Optimization of receptor occupancy assays in mass cytometry: standardization across channels with QSC beads. Cytometry A 2019; 95:314–322.
13. Finak G, Perez JM, Weng A, Gottardo R. Optimizing transformations for automated, high throughput analysis of flow cytometry data. BMC Bioinformatics 2010;11:546.
14. Amir el AD, Davis KL, Tadmor MD, et al. viSNE enables visualization of high dimensional single-cell data and reveals phenotypic heterogeneity of leukemia. Nat Biotechnol 2013;31:545–552.
15. Bruggner RV, Bodenmiller B, Dill DL, Tibshirani RJ, Nolan GP. Automated identification of stratifying signatures in cellular subpopulations. P Natl Acad Sci USA 2014; 111:E2770–E2777.
16. R: A Language and Environment for Statistical Computing [computer program]. Vienna: R Foundation for Statistical Computing; 2017.
17. Iaffaldano P, Viterbo RG, Paolicelli D, et al. Impact of natalizumab on cognitive performances and fatigue in relapsing multiple sclerosis: a prospective, open-label, two years observational study. PLoS One 2012;7:e35843.
18. Morrow SA, O'Connor PW, Polman CH, et al. Evaluation of the symbol digit modalities test (SDMT) and MS neuropsychological screening questionnaire (MSNQ) in natalizumab-treated MS patients over 48 weeks. Mult Scler 2010;16:1385–1392.
19. Foley JF, Goelz S, Hoyt T, Christensen A, Metzger RR. Evaluation of natalizumab pharmacokinetics and pharmacodynamics with standard and extended interval dosing. Mult Scler Relat Dis 2019;31:65–71.
20. Tanaka M, Kinoshita M, Foley JF, Tanaka K, Kira J, Carroll WM. Body weight-based natalizumab treatment in adult patients with multiple sclerosis. J Neurol 2015;262:781–782.
21. Varhaug KN, Torkildsen O, Myhr KM, Vedeler CA. Neurofilament light chain as a biomarker in multiple sclerosis. Front Neurol 2019;10:338.
22. Muralidharan KK, Kuesters G, Plavina T, et al. Population pharmacokinetics and target engagement of natalizumab in patients with multiple sclerosis. J Clin Pharmacol 2017;57:1017–1030.
23. Mahnke YD, Brodie TM, Sallusto F, Roederer M, Lugli E. The who's who of T-cell differentiation: human memory T-cell subsets. Eur J Immunol 2013;43:2797–2809.
24. Sallusto F, Geginat J, Lanzavecchia A. Central memory and effector memory T cell subsets: function, generation, and maintenance. Annu Rev Immunol 2004;22: 745–763.
25. Bloomgren G, Richman S, Hotermans C, et al. Risk of natalizumab-associated progressive multifocal leukoencephalopathy. N Engl J Med 2012;366:1870–1880.
26. Bomprezzi R, Pawate S. Extended interval dosing of natalizumab: a two-center, 7-year experience. Ther Adv Neurol Disord 2014;7:227–231.
27. Zhovtis Ryerson L, Frohman TC, Foley J, et al. Extended interval dosing of natalizumab in multiple sclerosis. J Neurol Neurosurg Psychiatry 2016;87:885–889.
28. Ryerson LZ, Foley J, Chang I, et al. Risk of natalizumab-associated PML in patients with MS is reduced with extended interval dosing. Neurology 2019;93:e1452–e1462.

Supplementary Material

Table e-1: Antibody panel

Metal isotope tag	Target	Clone	Company
141Pr	CD49d	9F10	Fluidigm
142Nd	CD19	HIB19	Fluidigm
143Nd	HLA-DR	L243	Fluidigm
144Nd	CD146	P1H12	Biolegend
145Nd	CD4	RPA-T4	Fluidigm
146Nd	CD8a	RPA-T8	Fluidigm
147Sm	CD20	2H7	Fluidigm
148Nd	CD34	581	Fluidigm
149Sm	CD25 (IL-2R)	2A3	Fluidigm
150Nd	CD61	VI-PL2	Fluidigm
151Eu	CD278/ICOS	C398.4A	Biolegend
152Sm	CD66b	80H3	Fluidigm
153Eu	CD194 (CCR4)	205410	Fluidigm
154Sm	CD3	UCHT1	Fluidigm
155Gd	CD161	HP-3G10	Biolegend
156Gd	CD184 (CXCR4)	12G5	Fluidigm
158Gd	CD27	L128	Fluidigm
159Tb	CD45RO	UCHL1	Biolegend
160Gd	CD14	M5E2	Fluidigm
161Dy	CD183 (CXCR3)	G025H7	Biolegend
162Dy	CD11c	Bu15	Fluidigm
163Dy	CD33	WM53	Fluidigm
164Dy	CD15	W6D3	Fluidigm
165Ho	CD127 (IL7-Ra)	A019D5	Fluidigm
166Er	CD123 (IL-3R)	AO19D5	Biolegend
167Er	CD162	KPL-1	Fluidigm
168Er	CD185 (CXCR5)	51505	R&D Systems
169Tm	Human IgG4	HP6025	Abcam
170Er	CD45RA	HI100	Fluidigm
172Yb	CD38	HIT2	Fluidigm
173Yb	CD196/CCR6	G034E3	Biolegend
174Yb	CD279 (PD-1)	EH12.2H7	Fluidigm
175Lu	CD235ab (Glycophorin)	HIR2	Fluidigm
176Yb	CD56	NCAM16.2	Fluidigm
209Bi	CD16	3G8	Fluidigm
89Y	CD45	HI30	Fluidigm

Figure e-1. Data analysis of peripheral blood leukocyte (PBL) samples. **A)** Clean-up gating into single PBLs. RBC = red blood cells. **B)** Manual workflow: gating of 11 PBL subtypes, QSC bead standardization, and RO calculation. ABC = antibody binding capacity. **C)** Unsupervised workflow: dimensionality reduction for visualization with ViSNE, automated clustering and significance testing with SAM analysis in CITRUS, and visualization of clusters with significantly different median ROs in the three patient groups on the ViSNE map.

A.

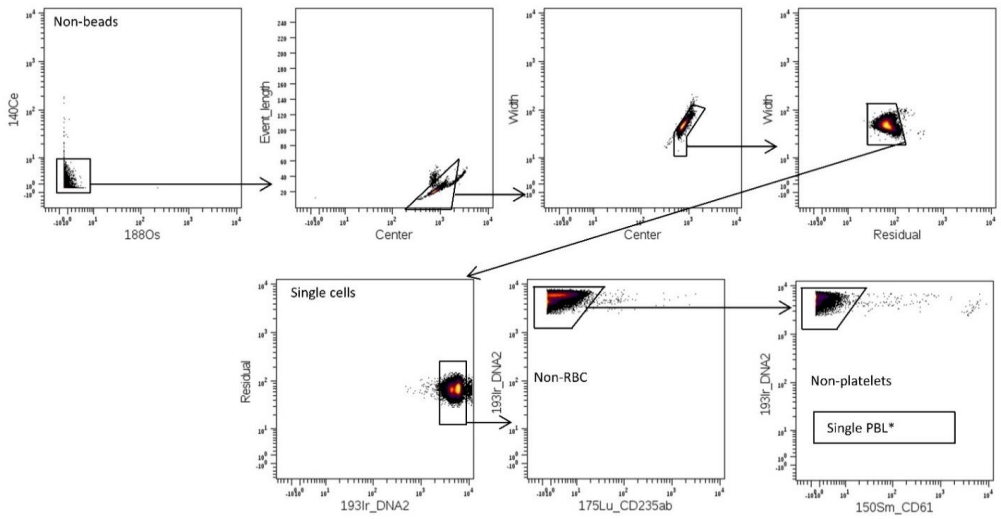

B.

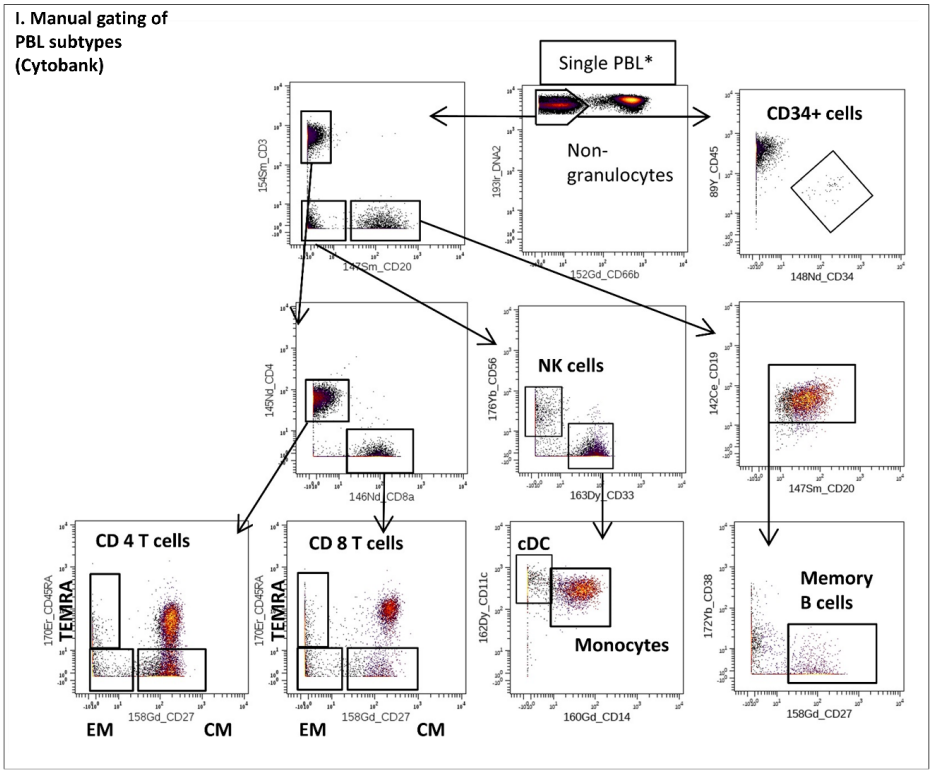
I. Manual gating of PBL subtypes (Cytobank)
Single PBL*
Non-granulocytes
CD34+ cells
NK cells
CD 4 T cells
CD 8 T cells
cDC
Monocytes
Memory B cells
EM
CM
EM
CM
II. QSC bead standardization of signal intensity (QuickCal, Bangs Laboratories)
PBL subtype
QSC beads with increasing ABC
Anti-IgG4
Anti-CD49d
Anti-CD49d
Anti-IgG4
Bead 1
Bead 2
Bead 3
Bead 4
Bead 5
Signal intensity
Standard curves
ABC
ABC
Signal intensity
III. RO calculation
%RO = 100X QSC bead standardized anti−IgG4 (169Tm) / QSC bead standardized anti−CD49d(141Pr)
IV. Comparison of ROs of leukocyte subtypes in different patient groups (Kruskal-Wallis test, R version 3.4.3)

C.

I. Dimensionality reduction (ViSNE, Cytobank)

- Samples: patient PBLs before and after infusion + healthy donor
- Population: Single PBL* (pre-gated as shown in previous figure)
- Clustering channels: 142Ce_CD19, 143Nd_HLA-DR, 145Nd_CD4, 146Nd_CD8a, 147Sm_CD20, 148Nd_CD34, 149Sm_CD25, 152Sm_CD66b, 154Sm_CD3, 158Gd_CD27, 159Tb_CD45RO, 160Gd_CD14, 162Dy_CD11c, 163Dy_CD33, 164Dy_CD15, 165Ho_CD127, 170Er_CD45RA, 172Yb_CD38, 176Yb_CD56, 209Bi_CD16, 89Y_CD45

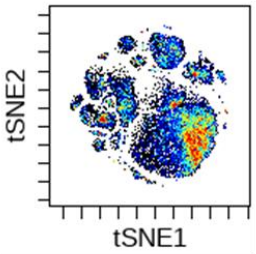

II. New RO variable (R version 3.4.3)

Adding a new column in FCS files using arcsign transformed signal intensity of IgG4 (natalizumab) and CD49d (α4 integrin) in each cell

$$RO = \frac{169Tm\_IgG\ 4 + 0.001}{141Pr\_CD49d + 0.001}$$

III. Median RO comparison between groups (Citrus, Cytobank)

- Samples: Before and after infusion in separate Citrus runs, each repeated for a total of 10 runs
- Population: All CD49 positive cells (CD49d dual count >10) from ViSNE
- Groups: Wearing-off never, sometimes, or regularly
- Clustering channels: Same as ViSNE
- Association model: SAM – correlative
- Cluster charachterisation: Median of channel "RO"
- Settings: Events sampled per file: 2061; mimimum cluster size: 5%; cross validation folds: 1; false discovery rate: 1%

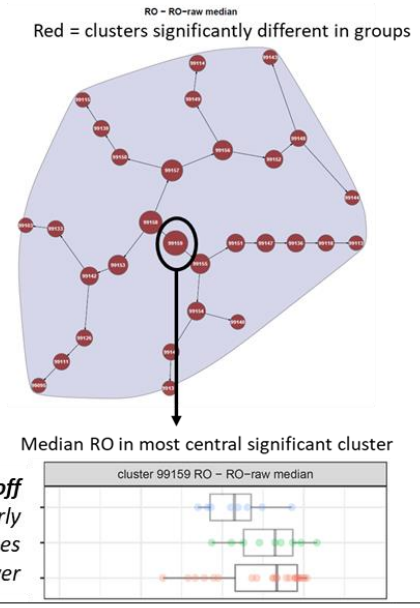

IV. Overlay significant clusters on the ViSNE map (Cytobank)

Export significant clusters to a new experiment for visualisation on the ViSNE map

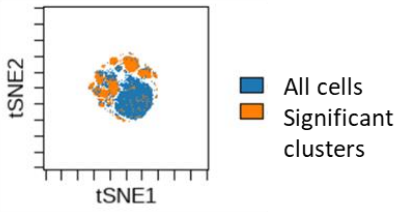

Figure e-2. Natalizumab RO in $CD8^+$ and $CD4^+$ T cells not stratified further into subtypes before (green) and after (orange) natalizumab infusion. P (based on Kruskal-Wallis test) comparing RO in patients reporting wearing-off symptoms never, sometimes, and regularly.

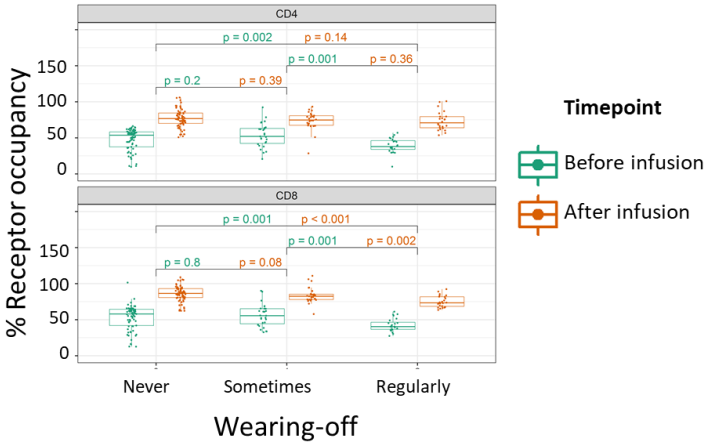

III

Wearing-off at the end of natalizumab dosing interval and risk of MS disease activity: a prospective 1-year follow-up study.

Gerd Haga Bringeland, M.D.[a, b], Kjell-Morten Myhr M.D., PhD [a, b], Christian Alexander Vedeler M.D., PhD [a, b], Sonia Gavasso, PhD [a, b]

[a]Neuro-SysMed, Department of Neurology, Haukeland University Hospital, Bergen, Norway, [b]Department of Clinical Medicine, University of Bergen, Bergen, Norway

Corresponding author:

Gerd Haga Bringeland,

Department of Neurology, Haukeland University Hospital, Jonas Lies Vei 65, 5021 Bergen, Norway

Phone: +47 55975045

gerd.haga.bringeland@helse-bergen.no

Co-authors:

Kjell-Morten Myhr: kjell-morten.myhr@uib.no

Christian Alexander Vedeler: christian.alexander.vedeler@helse-bergen.no

Sonia Gavasso: sonia.gavasso@helse-bergen.no

Abbrevations: RRMS (relapsing-remitting multiple sclerosis), RO (receptor occupancy), NF-L (neurofilament light chain), FSS (Fatigue Severity Scale), EDSS (Expanded Disability Status Scale), SDMT (Symbol Digit Modalities Test), NEDA (no evidence of disease activity).

Abstract

Natalizumab effectively prevents disease activity in relapsing-remitting multiple sclerosis by binding α4 integrin and inhibiting leukocyte migration to the central nervous system. We recently reported an association between low natalizumab receptor occupancy and subjective wearing-off symptoms at the end of the 4-week dosing interval. Here, we aimed to evaluate the short-term risk of disease activity in a 1-year prospective follow-up of the same patient cohort (n=40). We found that all patients available for follow-up after one year (n=35) fulfilled the criteria for no evidence of disease activity (NEDA). Thus, wearing-off symptoms were not associated with increased short-term risk of disease activity.

Key words

Relapsing-remitting multiple sclerosis, natalizumab, wearing-off, biomarkers, receptor occupancy, treatment response

1. Introduction

Natalizumab (Tysabri®, Biogen) administered intravenously at a standard dose of 300 mg every 4 weeks efficiently reduces disease activity in relapsing-remitting multiple sclerosis (RRMS).[1] By blocking α4 integrin on leukocytes, natalizumab inhibits leukocyte adhesion to and migration over the blood-brain barrier. Natalizumab receptor occupancy (RO) refers to the proportion of α4 integrins occupied by natalizumab on single cells, and has been suggested as a biomarker to monitor therapeutic efficacy and possibly patient-tailor therapy.[2] Neurofilament light chain (NF-L) is another emerging biomarker for disease activity and neuroaxonal damage in RRMS, and is reported to return to levels of healthy individuals following initiation of natalizumab therapy.[3]

Approximately 50% of patients treated with natalizumab report subjective wearing-off symptoms at the end of the 4-week interval between infusions.[4-6] The underlying mechanisms of this phenomenon are unknown, but we recently found that patients who regularly reported wearing-off symptoms had lower natalizumab RO than those reporting such symptoms occasionally or never.[6] Here, we aimed to investigate if the patients who regularly reported wearing-off symptoms had increased risk of disease activity during a 1-year follow-up.

2. Methods

2.1 Subjects

We invited all patients with a diagnosis of RRMS over 18 years of age who had received a minimum of six natalizumab infusions at the Department of Neurology, Haukeland University Hospital (n=45) to participate, of whom 40 (88.9%) participated after written informed consent. The study was approved by the Regional Ethics Committee (REK 2016/579).

2.2 Evaluation at inclusion and after one year

At inclusion, we obtained baseline demographic and clinical data from the patient's medical journal. Each patient filled in questionnaires on fatigue (Fatigue Severity Scale; FSS),[7] and on working status, smoking habits, weight, height, and whether they had wearing-off symptoms regularly (at the end of every dosing interval), sometimes (at the end of some dosing intervals), or never. Disability was evaluated with the Expanded Disability Status Scale (EDSS) and cognitive function was assessed by the Symbol Digit Modalities Test (SDMT)[8] at inclusion and after one year. T2 MRI lesions and number of clinical relapses were registered during a 1-year prospective follow-up. No evidence of disease activity (NEDA) was defined as freedom of relapses and EDSS worsening, and lack of new or enlarged T2 lesions on MRI. Serum collected at inclusion and after one year was stored at -80°C and NF-L was quantified with a single-molecule array (Simoa) assay (Quanterix).

2.3 Statistical analysis

For statistical analysis, patients were separated into two groups based on whether they reported wearing-off symptoms regularly (at the end of every dosing interval) or not (only sometimes or never). Patient characteristics, clinical and radiological signs of disease activity, and NF-L levels at baseline and after a 1-year follow-up were compared between the groups using a Kruskal-Wallis test. Statistical differences with $p < 0.05$ were considered significant using a two-sided comparison.

3. Results

Table 1 shows patient characteristics at inclusion and after a 1-year follow-up. After one year, five of the 40 included patients no longer received natalizumab therapy at our hospital; one had moved to another region and four had switched to other therapies due to antibodies against JC virus (n=2), side effects of natalizumab (n=1), or planned pregnancy (n=1). None of these five patients had reported wearing-off symptoms regularly.

None of the 35 remaining patients experienced clinical relapses, new or enlarged T2 lesions on MRI or EDSS score changes of >1 point during the 1-year follow-up period. Thus, all remaining patients fulfilled the criteria for NEDA.

At inclusion, patients reporting regular wearing-off symptoms had higher BMI and higher frequency of sick-leave than patients with wearing-off symptoms only sometimes or never.[6] Median EDSS was similar between the wearing-off groups both at baseline and after one year. Patients reporting wearing-off regularly had poorer median FSS (higher score) and SDMT (lower score) than patients reporting symptoms only sometimes or never both at inclusion and after one year, and these differences became statistically significant after 1-year follow-up. NF-L levels in serum were similar between the groups at inclusion and after 1-year follow-up.

4. Discussion

Subjective wearing-off symptoms at the end of the 4-week dosing interval are frequent among patients receiving natalizumab infusions, but the phenomenon remains poorly understood. Recently, we reported lower natalizumab RO in patients experiencing wearing-off symptoms regularly, possibly caused by high BMI.[6] In this study, we aimed to evaluate the risk of disease activity in a 1-year prospective follow-up of the same patient cohort.

We found that all patients available for follow-up after one year fulfilled the criteria for NEDA, and that subjective wearing-off symptoms were not associated with increased short-term risk of clinical or radiological signs of disease activity. The similar baseline and 1-year serum NF-L levels between the patient groups further supported this. Wearing-off symptoms were not associated with cessation of natalizumab therapy.

Patients reporting wearing-off regularly had more severe fatigue and cognitive impairment than patients with symptoms only sometimes or never. MS-related fatigue and cognitive impairment are common and affect quality of life independently of physical disability, and the

current criteria for NEDA have been criticized for not emphasizing fatigue and cognitive function in the evaluation of therapeutic efficacy.[9] Natalizumab has positive effects on fatigue and cognitive function[10] and more severe symptoms in the patient group with wearing-off regularly could thus represent a sub-optimal therapeutic effect. However, the differences in FSS and SDMT were small and need to be confirmed in larger populations.

In conclusion, although regular subjective wearing-off symptoms are associated with lower natalizumab RO,[6] they were not associated with increased short-term risk of breakthrough disease. Patients with wearing-off symptoms regularly had more severe fatigue and cognitive impairment in the 1-year follow-up. Longer prospective follow-up of a larger patient cohort is necessary to determine whether the therapeutic efficacy of natalizumab is maintained over time in patients reporting wearing-off symptoms regularly.

Table 1: Patient characteristics at inclusion and after a 1-year follow-up. *Patients reporting wearing-off symptoms at the end of natalizumab dosing intervals regularly (every dosing interval) or not (only sometimes or never). RRMS= relapsing-remitting multiple sclerosis, EDSS = Expanded Disability Status Scale, FSS = Fatigue Severity Scale, SDMT = Symbol Digit Modalities Test. S-NF-L = serum neurofilament light chain. P values of independent samples t test.*

		Wearing-off symptoms		
	Total	**Regularly**	**Not regularly**	**p**
RRMS patients, n (%)				
Baseline	40 (100)	8 (20)	32 (80)	
After 1 year	35 (87,5%)	8 (23)	27 (77)	
Patient characteristics at inclusion				
Age, y	43.0 (34.0-49.3)	43 (37-43.75)	44 (33.5-51)	0.531
Sex, females, n (%)	25 (62.5)	7 (87.5)	18 (51)	0.107
BMI	25.3 (22.6-27.2)	27.8 (26.5-31.2)	24.30 (22.34-26.11)	0.008
Current smoker, n (%)	7 (17.5)	1 (12.5)	6 (18.8)	0.681
Sick-leave, n (%)	9 (22.5)	4 (50.0)	5 (15.6)	0.040
Disease duration, y	13.0 (8.0-17.0)	12.5 (8.8-16.0)	13 (8-17.25)	0.747
Treatment duration, y	4.0 (3.0-7.3)	4.5 (2.0-8.0)	4 (3-7.25)	0.959
Dose number	56.5 (39.0-102.3)	63.5 (33.5-111.8)	56.5 (39-95.5)	0.933
Days since last dose	28.0 (28.0-28.0)	28.00 (27.0-28.0)	28 (28-28)	0.382
Markers of disease activity				
New or enlarged MRI T2 lesions during 1-year follow-up	0	0	0	-
Clinical relapses during 1-year follow-up	0	0	0	-
EDSS				
Baseline	2 (1.375-3.5)	2 (1.5-2.75)	2 (1-3.5)	0.681
After 1 year	2 (1.5-3.5)	2 (1.875-2.375)	2 (1-3.5)	1.000
FSS				
Baseline	4.78 (3.33-5.67)	5.33 (4.83-5.78)	4.44 (3.25-5.67)	0.119
After 1 year	4.89 (3.56-5.72)	5.89 (5.31-6.31)	4.11 (3.39-5.39)	0.005
SDMT				
Baseline	57 (50-67.25)	48.5 (45.5-56)	58 (52.75-68.25)	0.052
After 1 year	59 (50.5-69)	48.5 (47-55.75)	62 (56-70)	0.023
S-NF-L pg/ml				
Baseline	7.09 (5.27-9.38)	5.19 (5.03-6.09)	7.12 (5.55-9.64)	0.098
After 1 year	7.71 (5.57-10.82)	6.46 (5.89-7.89)	8.02 (5.45-11.59)	0.610

Acknowledgements

We thank Fritz og Ingrid Nilsens legat for financial research support, and Hanne Linda Nakkestad at the Neurological Research Laboratory at Haukeland University Hospital for performing SiMOA analyses. The mass cytometry was performed at the Flow Cytometry Core Facility, Department of Clinical Science, University of Bergen. The Helios mass cytometer was funded by Bergen Research Foundation. Neuro-SysMed is jointly hosted by Haukeland University Hospital and University of Bergen and supported as a Centre for Clinical Treatment Research (FKB) by grants from The Research Council of Norway, project number 288164.

Declaration of Conflicting Interests

The authors declared the following potential conflicts of interest with respect to the research, authorship, and/or publication of this article: C.A.V. and S.G. have nothing to disclose. G.H.B. has received research support from Novartis. K.M.M. has received grants and personal fees from Biogen and Novartis; personal fees from Genzyme, Roche, Almirall, and Merck; and personal fees and nonfinancial support from Teva.

References

1. Polman CH, O'Connor PW, Havrdova E, et al. A randomized, placebo-controlled trial of natalizumab for relapsing multiple sclerosis. *N Engl J Med* 2006; 354: 899-910. 2006/03/03. DOI: 10.1056/NEJMoa044397.
2. Punet-Ortiz J, Hervas-Garcia JV, Teniente-Serra A, et al. Monitoring CD49d receptor occupancy: A method to optimize and personalize natalizumab therapy in multiple sclerosis patients. *Cytometry B Clin Cytom* 2017 2017/04/06. DOI: 10.1002/cyto.b.21527.
3. Gunnarsson M, Malmestrom C, Axelsson M, et al. Axonal damage in relapsing multiple sclerosis is markedly reduced by natalizumab. *Ann Neurol* 2011; 69: 83-89. 2011/02/01. DOI: 10.1002/ana.22247.
4. Ratchford JN, Brock-Simmons R, Augsburger A, et al. Multiple sclerosis symptom recrudescence at the end of the natalizumab dosing cycle. *Int J MS Care* 2014; 16: 92-98. 2014/07/26. DOI: 10.7224/1537-2073.2013-017.
5. van Kempen ZLE, Doesburg D, Dekker I, et al. The natalizumab wearing-off effect: End of natalizumab cycle; recurrence of MS symptoms. *Neurology* 2019 2019/09/26. DOI: 10.1212/WNL.0000000000008357.
6. Bringeland GH, Blaser N, Myhr KM, et al. Wearing-off at the end of natalizumab dosing intervals is associated with low receptor occupancy. *Neurol Neuroimmunol Neuroinflamm* 2020; 7 2020/02/06. DOI: 10.1212/NXI.0000000000000678.

7. Krupp LB, LaRocca NG, Muir-Nash J, et al. The fatigue severity scale. Application to patients with multiple sclerosis and systemic lupus erythematosus. *Arch Neurol* 1989; 46: 1121-1123. 1989/10/01. DOI: 10.1001/archneur.1989.00520460115022.
8. Smith A. The Symbol Digit Modalities Test (SDMT) Symbol Digit Modalities Test: Manual. *Western Psychological Services* 1982.
9. Stangel M, Penner IK, Kallmann BA, et al. Towards the implementation of 'no evidence of disease activity' in multiple sclerosis treatment: the multiple sclerosis decision model. *Ther Adv Neurol Disord* 2015; 8: 3-13. 2015/01/15. DOI: 10.1177/1756285614560733.
10. Iaffaldano P, Viterbo RG, Paolicelli D, et al. Impact of natalizumab on cognitive performances and fatigue in relapsing multiple sclerosis: a prospective, open-label, two years observational study. *PLoS One* 2012; 7: e35843. 2012/05/05. DOI: 10.1371/journal.pone.0035843.

Graphic design: Communication Division, UiB / Print: Skipnes Kommunikasjon AS

uib.no

ISBN: 9788230842393 (print)
9788230849477 (PDF)